

**Contents**

Editorial ..... 1

**News**

Dr Anthony (Tony) Hollingsworth (1943 – 2007) ..... 2  
 ENSEMBLES public data dissemination ..... 4  
 New items on the ECMWF web site ..... 4  
 Changes to the operational forecasting system ..... 5  
 Third EUMETCAL Workshop at ECMWF ..... 5  
 Replacement of the Automated Tape Library for  
 the Disaster Recovery System ..... 6

**Meteorology**

Operational assimilation of surface wind data from the  
 MetOp ASCAT scatterometer at ECMWF ..... 6  
 Climate variability from the new  
 System 3 ocean reanalysis ..... 8  
 Evaluation of the impact of the space component of  
 the Global Observing System through  
 Observing System Experiments ..... 16  
 Impact of airborne Doppler lidar observations on  
 ECMWF forecasts ..... 28

**Computing**

New Automated Tape Library for  
 the Disaster Recovery System ..... 34  
 Improving the Regional Meteorological Data  
 Communications Network (RMDCN) ..... 36

**General information**

ECMWF publications ..... 40  
 Index of past newsletter articles ..... 40  
 Useful names and telephone numbers  
 within ECMWF ..... 43

**Publication policy**

The ECMWF Newsletter is published quarterly. Its purpose is to make users of ECMWF products, collaborators with ECMWF and the wider meteorological community aware of new developments at ECMWF and the use that can be made of ECMWF products. Most articles are prepared by staff at ECMWF, but articles are also welcome from people working elsewhere, especially those from Member States and Co-operating States. The ECMWF Newsletter is not peer-reviewed.

Editor: Bob Riddaway

Typesetting and Graphics: Rob Hine

Any queries about the content or distribution of the ECMWF Newsletter should be sent to  
 Bob.Riddaway@ecmwf.int

**Contacting ECMWF**

Shinfield Park, Reading, Berkshire RG2 9AX, UK  
 Fax: .....+44 118 986 9450  
 Telephone: National .....0118 949 9000  
 International .....+44 118 949 9000  
 ECMWF Web site .....http://www.ecmwf.int

**Front cover**

An illustration of the new data communications network described in the article starting on page 36.

EDITORIAL

**Optimizing the observing system**

ONE OF the goals stated in the ECMWF strategy is “to contribute towards the optimization of the Global Observing System”. The idea of Numerical Weather Prediction (NWP) contributing to the observing system started very early with the monitoring of radiosonde observations. It has now developed into a mature activity and is able to provide very useful information to the managers of the various observing systems.

An important development has been the reanalysis activity. The aim is to produce analyses from past decades which benefit from the most recent state of the art assimilation system and, wherever possible, include all possible observations, some of them unused at the time they were made. It is important to note that one of the initial goals of reanalysis was to quantify the contribution made by the new observing systems.

Another development has been the monitoring of satellite observations as soon as they become available and the provision of feedback to the space agencies. This is a win-win evolution as NWP benefits from an early availability of new satellite data whilst the space agencies get immediate feedback from the comparison with other systems through the assimilation process.

A crucial recent development has been the generalization of Observing System Experiments based on short reanalysis runs with or without some of the observing systems, where their impact is measured by the verification scores of the corresponding forecasts. A good example is provided in this newsletter with the article by Kelly & Thépaut (see page 16) concerning the evaluation of the various elements of the space component. Such studies are now important tools to evaluate the impact of various components of the Global Observing System and are required either by space agencies or in-situ network managers like those of EUCOS (EUMETNET Composite Observing System).

Similar techniques can also be used to measure the impact of experimental instruments used during specific campaigns and to evaluate whether it is worthwhile developing such measurements on an operational basis. The article by Weissmann & Cardinali (see page 28), evaluating the impact of airborne Doppler lidar observations, is particularly interesting as it supports the idea that such measurements could prove very beneficial as expected from the ESA ADM-Aeolus experiment.

The story does not stop here. There are also developments toward observation targeting whereby NWP centres indicate target areas where additional observations should improve the forecasts. ECMWF is currently developing such an automatic system for operational use. Later one should also consider the possibility of suspending observations (and saving accordingly) when they are not contributing positively to the forecast.

All these developments supporting the optimization of the Global Observing System are of direct interest to the NWP community as they will benefit the quality of the weather forecasts and, as such, are an integral part of THORPEX. But, keeping in mind the huge cost of the various observing systems, they also constitute a very beneficial side-development of NWP which would in itself justify the investment in NWP.

**Dominique Marbouty**

## Dr Anthony (Tony) Hollingsworth (1943 – 2007)

DAVID BURRIDGE

I KNEW Tony (Anthony) Hollingsworth for some thirty five years and for most of that time we worked together as colleagues at ECMWF. The shock, dismay and disbelief that I felt when I heard the message left for me by Dominique Marbouty (Director of ECMWF), “Tony died early this morning”, will stay with me for the rest of my days. Tony died on Sunday 29 July whilst on holiday in Galway where he had a second home. He was 64.

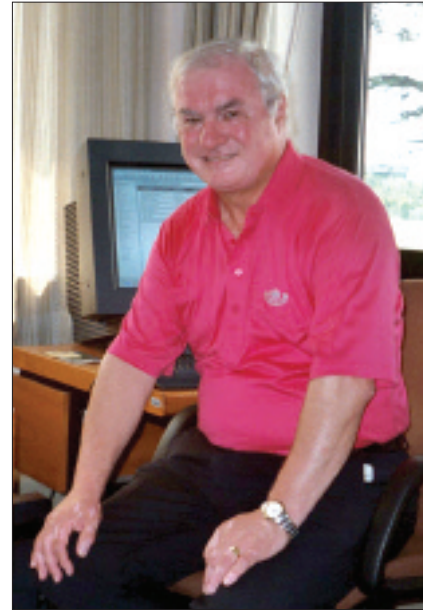
Tony was born in Dublin and for all his life he was immensely proud of his home town and his Irish background. He left his secondary school “on a high” when he became top of his year in the whole of Ireland. After graduating from University College Cork with a first class honours degree in mathematics Tony joined the Irish Meteorological Service in 1965 where he trained to become a certified meteorologist.

After training, Tony’s first “hands on” job was at Shannon Airport where he became an aviation and general forecaster. One of his more interesting summer tasks was to prepare regular route forecasts for a US team flying an old Catalina on round-trips from Shannon taking in Keflavik and Narssarsuaq (Greenland). The US team was testing a scatterometer. Tony often used this experience to remind me that he was “in at the start” in the satellite-based observing business. However, I was more impressed with his skill at hand-drawing weather charts which would prove very useful in the early days at ECMWF when the best computer graphical output we had were line-printer “zebra” charts! At Shannon, and in his “leisure time”, Tony followed the Masters Course in Pure Mathematics at the University of Cork.

After a few years in the Meteorological Service Tony joined the Massachusetts Institute of Technology (MIT) to study for a doctorate in meteorology. During his time at MIT he was a research assistant to two of the founding fathers of modern numerical prediction: Ed Lorenz and Norman Phillips who supervised his thesis on “*Effects of ocean and solid earth tides on the semi-diurnal lunar air tide*”. Tony received his PhD in 1970 and at the time was the third fastest to gain a doctorate in meteorology since the Second World War. Tony felt that the intellectually robust discussions that he had with “Norm” during his student days prepared him well for committee work at ECMWF and in other international milieu. I must say that he was right and I am glad that he was on my side – well most of the time he was!

After a spell at the Department of Atmospheric Sciences at Oregon State University, Tony returned to Europe in 1971. He joined the UK Universities Atmospheric Modelling Group at the University of Reading as a Research Fellow and founder member with Brian Hoskins (now Professor Sir Brian Hoskins FRS) and Eli Doron. Over the years, what was begun by the Reading Group has evolved into a major UK environmental research community spread over many universities. But despite the growing prestige of the “Reading Group” Tony wanted something different.

Tony applied for a post at ECMWF in November 1974 almost a year before the ECMWF convention was formally ratified. He, like me, had heard the talks given by Aksel Wiin-Nielsen and Lennart Bengtsson (subsequently, the first and third Directors of ECMWF) on the preparations being made to establish ECMWF. We both wanted to join the



Tony’s last day as Head of Research at ECMWF on 6 July 2003.

Centre as we were keen to see the day when weather forecasts would cease to be a joke for the public at large and we knew that improved global NWP was the key. The ECMWF plans looked realistic with the added advantage that there was no model or analysis system (data assimilation system) – the “slate was clean”. I think this was a big attraction for both of us.

We were both offered jobs starting on 1 March 1975 but in February 1975 we heard that there was delay in getting funds from “Europe” because the required “unanimity” was not achieved! The Civil Service would not release me but wisely Tony told Aksel Wiin-Nielsen he had resigned from the University of Reading and so a few “shillings” were scrapped together to employ Tony from the 1 March 1975. I joined two months later on 1 May but ever since then I have remained envious of Tony’s two additional months which made him the Centre’s longest serving employee – I doubt that many will break this record.

The first two years at ECMWF were hectic for both of us. I was building a variety of simple models and throwing them away on a monthly basis and Tony was posted for a few months to GFDL in Princeton to work with and “acquire” the GFDL global climate model which he transferred to the Centre’s first computer system, a CDC

David Burridge worked at ECMWF from 1975 to 2004 and was Director of ECMWF from January 1991 to June 2004.



Tony receiving the Jule G. Charney Award from the AMS in 1999.

6600. Tony and his small team eventually got this model to work on this very slow computer and produced a few global forecasts. This relaxed learning period came to an end in 1976 as the target to develop and implement a full operational forecasting system by mid-1979 became firmly embedded in the Centre's planning documents.

From 1976 to his sixtieth birthday in July 2003, Tony worked on virtually every aspect of NWP, heading in turn the Physical Aspects Section and the Data and Model Divisions of the Research Department. He was appointed Head of Research in 1991 and Deputy Director in 1995. In addition to his management role, during this time Tony made many personal contributions to the science of NWP that led to major improvements to the ECMWF global forecasts. For ECMWF, I believe that the two most important were as follows.

- ◆ His contribution to the identification of serious systematic model errors as a major component of the total error of the Centre's first forecasts. This work set the agenda; it provided the tools and even set the style for modelling work for the whole of the 1980s.

- ◆ His studies of the errors of the observing system and of short-range forecasts. This provided tools, which are in use today, to monitor the performance of the observing system and the basis for the improvement of data analysis and data assimilation, thereby increasing the accuracy of initial conditions.

Tony believed that the job was not complete until the paper was published and to his immense credit he was involved, often with others, in publishing more than 100 reports and papers – many young scientists learnt how to “write up” their work under Tony's guidance or example.

Tony stepped down as Head of Research and Deputy Director on reaching his sixtieth birthday, but real retirement was not what he had in mind. He was keen to run the Europe-wide GEMS project which is concerned with global and regional earth-system monitoring using satellite and in situ data. Tony saw GEMS as the grand finale of his career at ECMWF since GEMS promised to combine atmospheric chemistry and dynamics, and exploit the best available satellite and in-situ data. The aim is to provide real-time and retrospective analyses of greenhouse gases, reactive gases and aerosols in the troposphere and in the stratosphere on regional and global scales. This in turn should improve the regional forecasts that are used by air-quality authorities at city level across Europe and deliver valuable new data products for the Global Monitoring for Environment and Security (GMES) Service Elements. In addition, key information relevant to the Kyoto and Montreal protocols and to the UN Convention on Long-Range Trans-boundary Air Pollution could be provided. After the usual tough contract negotiations Tony stayed on at ECMWF and “took on” GEMS and led the project energy with vision and dedication to the end.

Tony was an important player also on a wider international stage, fostering extensive collaboration with EUMETSAT, the European Space Agency (ESA) and space agencies worldwide. Also he worked in support of the World Climate Research Programme, the Global Climate Observing System, the US National Academy of Sciences and the American Meteorological Society (AMS). He was a recipient of the Jule G. Charney Award from the AMS, and a D.Sc. from the University of Cork for his contributions to NWP.

It would be too rosy a picture if I made no mention of any professional flaws but there were few. Tony could at times be an overly rough manager and, initially, he was “blind” to the potential of four-dimensional variational data assimilation which is now the cornerstone of modern NWP systems. His roughness stemmed, I think, from a strong desire to succeed, but underneath there was a warmer and more supportive attitude that emerged quickly for those who were in personal difficulties. In the late 1980s he believed that the combination of Optimum Interpolation (OI) analysis and Normal-mode Initialization, which was being used for data assimilation at ECMWF, could be improved to extract all the meteorologically useful information from the observations. As a consequence he was not keen to develop four-dimensional variational methods for data assimilation in which the calculation of adjoints and the integration of adjoint equations were essential elements. However, when it became clear that the variational approach improved the use of satellite data he became an enthusiastic convert.

Tony and I worked together at ECMWF for almost thirty years and despite competing for the same post from time to time we maintained a strong friendship and with many others we were part of the successful team that revolutionised NWP. In this appreciation, I deliberately did not try to do full justice to Tony's contributions to meteorology in the full knowledge that meetings to celebrate Tony's achievements are currently being planned both for Europe and North America. All of us who knew Tony have lost an energetic and hospitable friend and colleague and the wider weather community has lost a great scientist. Although he was keen to continue contributing, what he has left behind is of immense value. Tony is survived by his dearly loved wife Breda and his wonderfully talented children Cormac and Deidre.

Tony was buried in the old Franciscan cemetery in Claregalway near to where the family has a second home.

## ENSEMBLES public data dissemination

FRANCISCO J. DOBLAS-REYES,  
CARLOS VALIENTE, MANUEL FUENTES

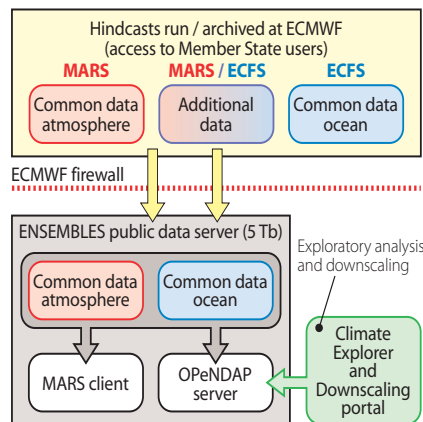
A NEW service for public data dissemination of the multi-model seasonal and interannual ensemble hindcasts generated as part of the EU-funded ENSEMBLES project is now available from:

[www.ecmwf.int/research/EU\\_projects/ENSEMBLES/data/data\\_dissemination.html](http://www.ecmwf.int/research/EU_projects/ENSEMBLES/data/data_dissemination.html)

This service disseminates the same data using two different systems: MARS-based and OPeNDAP-based tools. Each system is intended to best satisfy the requirement of different groups of users.

The MARS-based system uses the technology developed for the ECMWF public data server ([data.ecmwf.int/data/](http://data.ecmwf.int/data/)). It offers a view of the available data on a user-friendly front page. From that page the user can easily download daily and monthly mean data in both GRIB and NetCDF formats, as well as plot the required fields. This system is expected to be of use to scientists interested in relatively small samples or needing an interactive access to the dataset.

The OPeNDAP-based tool ([www.opendap.org](http://www.opendap.org)) allows remote application clients to access the ENSEMBLES data set. This is a powerful tool to provide automatic



access to clients for a variety of tasks, including the following.

- ◆ Exploratory analysis (e.g. the KNMI Climate Explorer, [climexp.knmi.nl/](http://climexp.knmi.nl/))
  - ◆ Statistical downscaling (e.g. with the tool developed at the Universidad of Santander, Spain, [grupos.unican.es/ai/meteo/ensembles/index.html](http://grupos.unican.es/ai/meteo/ensembles/index.html))
  - ◆ Fast download (e.g. with the NCO routines, [nco.sourceforge.net/](http://nco.sourceforge.net/))
- The OPeNDAP serves data in both ASCII and CF-compliant NetCDF formats.

The NetCDF format used in the OPeNDAP system is one of the main novelties of this service. An efficient dissemination requires a unified framework for product standardisation to provide a coherent service. However, a standardization of multi-forecast system ensemble predictions

does not exist outside the GRIB community. The standardisation in NetCDF has been achieved in ENSEMBLES by creating a new set of rules to encode multi-forecast system ensemble simulations in CF-compliant NetCDF files. This is the first time such an attempt has been undertaken. The rules define the structure of the metadata to be used to thoroughly describe the data, including the way the ensemble has been generated. Operational requirements have been taken into account at the time of designing the structure. Based on this combination (OPeNDAP dissemination and CF-compliant NetCDF format), the multi-model seasonal forecast experiment sponsored by the Working Group of Seasonal to Inter-annual Prediction (WGSIP) of CLIVAR will use a similar approach as an efficient method for data dissemination and exchange. It is expected that this set of rules will help to encode in a unified NetCDF format the multi-forecast system simulations carried out by short-term climate forecast systems and by models used for the assessment of anthropogenic climate change.

At present, the service disseminates daily and monthly mean hindcast atmospheric data, but it is expected to also serve ocean analyses and hindcasts in the near future.

## New items on the ECMWF web site

ANDY BRADY

### Presentations from the ECMWF Annual Seminar 2007

The ECMWF Annual Seminar on *Recent Developments in the Use of Satellite Observations in Numerical Weather Prediction* was held on 3 to 7 September 2007. The presentations for this Seminar are now available.

[www.ecmwf.int/newsevents/meetings/annual\\_seminar/2007/presentations/](http://www.ecmwf.int/newsevents/meetings/annual_seminar/2007/presentations/)

### Presentations from the 2007 EUMETCAL Workshop

The Third EUMETCAL Workshop was held at the Centre during 29 to 31 August. Presentations were given by delegates from ECMWF, Météo-France, SCHAPI, EUMETCAL, ZAMG and FMI covering the provision of meteorology training in Europe using advanced teaching strategies and technologies. The workshop also considered the meteorology training for hydrologists.

[www.ecmwf.int/newsevents/meetings/workshops/2007/EUMETCAL/](http://www.ecmwf.int/newsevents/meetings/workshops/2007/EUMETCAL/)

### IFS documentation of Cy31r1

The scientific and technical documentation for the Integrated Forecast System (IFS) has been updated from Cy28r1 to Cy31r1. Operational implementation of Cy31r1 took place on 12 September 2006.

[www.ecmwf.int/research/ifsdocs/CY31r1/](http://www.ecmwf.int/research/ifsdocs/CY31r1/)

## Changes to the operational forecasting system

DAVID RICHARDSON

### New cycle – Cy32r3

A new cycle of the ECMWF forecast and analysis system, Cy32r3, is ready for operational implementation. The new cycle includes significant changes to the model physics, including the convection scheme, that increase the

model activity in the tropics. The main changes included in this cycle are:

- ◆ New formulation of convective entrainment and relaxation timescale.
- ◆ Reduction in free atmosphere vertical diffusion.
- ◆ New soil hydrology scheme.
- ◆ New radiosonde temperature and

humidity bias correction.

- ◆ Increase in number of radio occultation data from COSMIC.
- ◆ Assimilation of AMSR-E, TMI, SSMIS window channels (clear sky).
- ◆ Assimilation of Solar Backscatter Ultraviolet (SBUV) (NOAA-17, NOAA-18) and monitoring of OMI ozone data.

## Third EUMETCAL Workshop at ECMWF

RENATE HAGEDORN

ECMWF hosted the Third EUMETCAL Workshop from 29 to 31 August 2007. Trainers from National Meteorological Services (NMSs), EUMETSAT, ECMWF and various other interested parties met to consider future developments in training.

EUMETCAL is a virtual training organisation established by EUMETNET in 2001 with the general goal of sharing training resources amongst its members. Meteorology is a specialised field that is heavily dependent on effective exploitation of modern information and

communication technologies. In addition, the ever-increasing budget restrictions on the NMSs have led to a situation in which it is often difficult to satisfy training needs without cooperation and the sharing of resources. Thus, the specific objectives of the EUMETCAL programme are to:

- ◆ Help instructors to prepare their lectures.
  - ◆ Minimise the number of sources they need to search.
  - ◆ Minimise development time by avoiding duplication.
- Sharing, reprocessing and exchanging training material and organising material into comprehensive online training modules can significantly

reduce development time for instructors. Also this approach provides NMSs with ready-made packages for students without excessive use of staff resources. It is found that e-learning methods provide a fast response to new technologies and can be used to reach a wide audience which potentially spans the whole world. However, the increasingly fast development of new e-learning programmes and methods demands dedicated personnel who are aware of the benefits of the various methods available and their potential applications. The current wealth of resources developed in the EUMETCAL programme along with



expertise in Computer Aided Learning (CAL) methods creates a natural platform on which to base a cooperative approach to meeting the training needs faced by the meteorological community.

The main topics discussed during the workshop at ECMWF were the advances in modern training strategies and technologies. In particular there was consideration of how new online learning tools, which enable highly interactive virtual classroom learning, can be incorpo-

rated into existing “face-to-face” training structures. In other words how to achieve the ultimate goal of delivering blended learning in an optimal way. During the workshop the opportunity was taken to inform participants about operational and research activities at ECMWF. All the presentations given at the workshop can be accessed from the following web address

[www.ecmwf.int/newsevents/meetings/workshops/2007/EUMETCAL/](http://www.ecmwf.int/newsevents/meetings/workshops/2007/EUMETCAL/).

ECMWF has a remit “to assist in advanced training for the scientific staff of the meteorological offices of the Member States in the field of numerical weather forecasting”. Consequently, ECMWF will provide teaching resources for a blended learning course on Numerical Weather Prediction which is run under the auspices of EUMETCAL. More information on this blended course in particular or EUMETCAL in general can be found at [www.eumetcal.org](http://www.eumetcal.org).

## Replacement of the Automated Tape Library for the Disaster Recovery System

NEIL STORER

In February 2007 a new Automated Tape Library (ATL) was installed in the Disaster Recovery System (DRS) Building. The new ATL consists of an IBM TS3500 linear robotic library containing twenty LTO-3 tape drives.

At 80 MB/s the performance of the drives is twice that of the LTO-2 drives in the old AML/J ATL. After a period of parallel running the old system was switched off and decommissioned. It is expected that the service provided by the new system will be as good as, if not better than, the old one.

The article about the “*New Automated Tape Library for the Disaster Recovery System*” starting on page 34 of this edition of the newsletter describes the history of the DRS and gives a comparison of the various tape drives and media technologies used at ECMWF.

## Operational assimilation of surface wind data from the MetOp ASCAT scatterometer at ECMWF

HANS HERSBACH, PETER JANSSEN

ASCAT (Advanced Scatterometer) is a new-generation C-band instrument on-board EUMETSAT’s MetOp satellite (launched on 19 October 2006). It is based on the successful AMI scatterometers on-board the ERS missions. Use is made of triplets of radar backscatter to estimate surface vector winds over the global oceans, soil moisture over land, and properties of sea ice in polar regions. Both AMI and ASCAT operate at C-band (5.3 GHz) and share antenna geometry. Two main differences are a different range of incidence angle (optimized for ASCAT to enhance performance in wind direction) and the fact that ASCAT carries two sets of antennas, providing two swaths of 550 km each. This doubles the coverage compared to the ERS-1 and ERS-2 scatterometers. For more details about geometry and design see *Figa-Saldaña et al. (2002, Can. J. Remote Sensing, 28, 404–412)*.

	Wind speed (m s <sup>-1</sup> )		Wind direction (degrees)	
	Bias	Standard Deviation	Bias	Standard Deviation
<b>ASCAT</b>	(2 ambiguities)			
<b>First guess</b>	0.00	1.29	0.8	14.6
<b>Analysis</b>	0.06	0.97	0.4	10.1
<b>QuikSCAT</b>	(2 ambiguities / 4 ambiguities)			
<b>First guess</b>	-0.09/-0.12	1.33/1.30	0.7/0.8	18.5/14.3
<b>Analysis</b>	0.06/0.04	1.11/1.08	0.6/0.7	15.6/11.1

**Table 1** Average bias and standard deviation of scatterometer data as assimilated compared to ECMWF first-guess at appropriate time and the associated analysis for wind speed and direction for the ASCAT assimilation experiment. At assimilation, neutral QuikSCAT winds are lowered by 4% to incorporate average stability effects, and two out of four possible wind ambiguities are used.

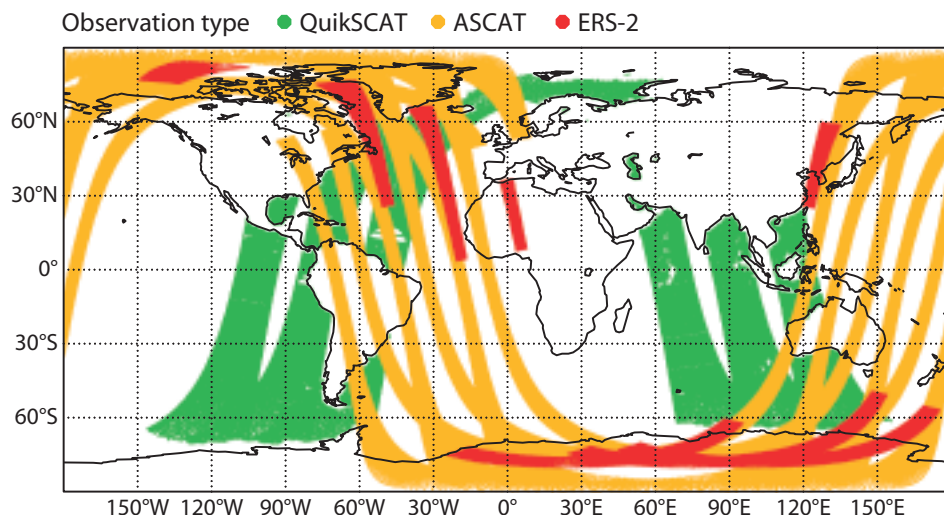


**Figure 1** Coverage of received scatterometer data for the six-hourly cycle starting at 00 UTC on 6 June 2007. The total number of observations is 279,253.

Data from ASCAT has been monitored at ECMWF since the start of dissemination via the EUMETCast system on 31 January 2007. Surface winds are inverted in-house from available (level 1B) backscatter triplets on the basis of a modified version of the geophysical model function CMOD5 (see *Hersbach et al., 2007, J. Geophys. Res., 112, C03006, doi: 10.1029/2006JC003743*) and compared to collocated ECMWF short-range forecast winds. This monitoring confirmed that the ASCAT instrument is working well. Due to the unavailability of two out of three in situ transponders, the absolute calibration performed at EUMETSAT has not been finalized. However, stable average levels have been observed from the start. After appropriate corrections in backscatter space prior to wind inversion, a homogeneous and stable wind product of high quality has been obtained at ECMWF throughout.

By using a similar set-up as for ERS-2 winds, assimilation experiments including ASCAT surface vector

winds in the ECMWF analysis and forecast system at full model resolution (T799) showed a positive effect on forecast skill over the southern hemisphere. For ocean waves, in addition, significant positive impact was observed in the tropics. The excellence of ASCAT data is illustrated in Table 1; this summarizes global statistics for actively assimilated ASCAT and QuikSCAT data accumulated over the period covered by the ASCAT experiment.

Following the promising results, surface winds from ASCAT were introduced into the operational suite on 12 June 2007 by a blacklist change, one week after the introduction of model cycle Cy32r2. Since this change, data from three scatterometers is assimilated simultaneously: ERS-2, QuikSCAT and now also ASCAT. ECMWF is the first operational institute to actively assimilate wind data from ASCAT. Since ascending nodes for ASCAT, QuikSCAT and ERS-2 are all different, large portions of the globe are now covered during a six-hour period.

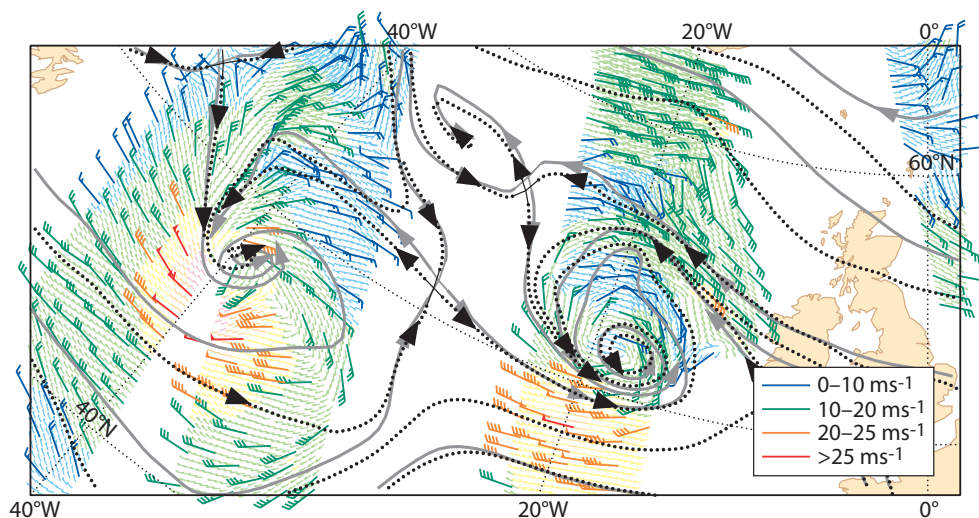


**Figure 2** ASCAT wind field at 00 UTC on 20 February 2007 in the North Atlantic. Large bars indicate actively assimilated winds and small bars indicate rejected (mostly thinned) winds within the ASCAT assimilation experiment. Black and grey lines represent streamlines for the ECMWF analysis and first-guess surface winds.

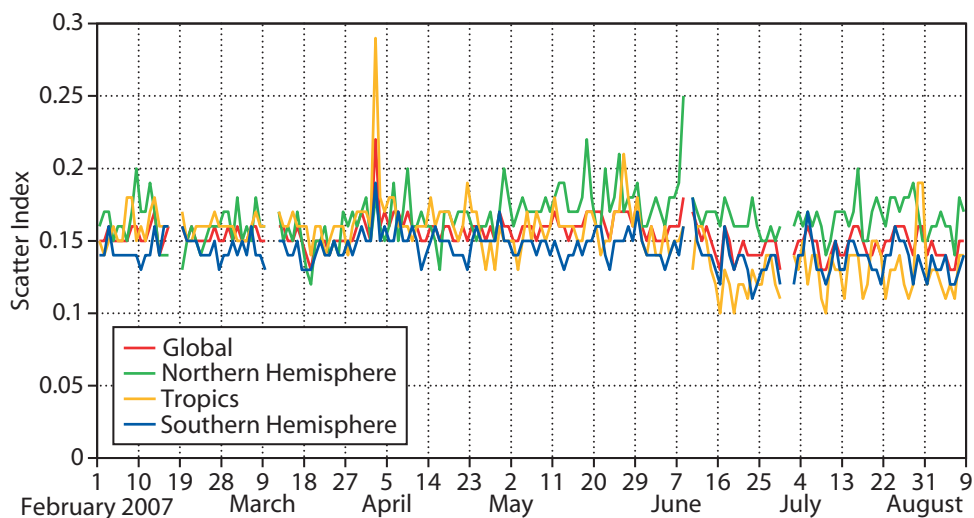


**Figure 3** Time series of the Scatter Index for ENVISAT Radar Altimeter wind speed versus ECMWF analysis surface wind speed for the globe, northern hemisphere, tropics and southern hemisphere.

Figure 1 shows a typical coverage plot. This coverage should allow to some extent a diurnal cycle in surface winds to be represented.

At EUMETSAT data is processed at 50 km and 25 km horizontal resolutions on grids of 25 km and 12.5 km. At ECMWF only the product at lower resolution is currently presented to the assimilation system. Like scatterometer wind from ERS, data is thinned to 100 km and use is made of the standard scatterometer observation operator (model vector wind at 10-metre height), 4D-Var cost function and variational quality control. The only difference is that ASCAT data is given a larger weight than that for ERS and QuikSCAT data (an observation error of  $1.5 \text{ m s}^{-1}$  is assumed instead of  $2 \text{ m s}^{-1}$ ). This reflects the higher accuracy in wind direction for

ASCAT data, and appears to result in a comparable contribution per datum to the 4D-Var cost function.

Since ASCAT operates at C-band, the data is hardly affected by rain; therefore it provides accurate winds in all weather conditions. An example of a system of two extreme storms in the North Atlantic is displayed in Figure 2. ASCAT winds up to 65 knots are observed, and show the full structure of the two weather systems. Assimilation of ASCAT winds resulted in small adjustments in position and intensity for both systems.

After the operational implementation of the ASCAT data an improved accuracy of the first-guess and analysis surface wind was revealed. This is illustrated by a comparison with ENVISAT altimeter wind data as given in Figure 3.

## Climate variability from the new System 3 ocean reanalysis

MAGDALENA ALONSO BALMASEDA, DAVID ANDERSON,  
FRANCO MOLteni

IN AUGUST 2006 a new ocean analysis (System 3 or S3) was implemented in operations at ECMWF. This is used to provide ocean initial conditions for the seasonal forecasts and, with some modifications, the monthly forecast system. Since both the seasonal and monthly forecast systems require an extensive set of hindcasts over many previous years, it is necessary to perform an ocean reanalysis as well. Currently a reanalysis has been performed back to 1959. Since the ocean reanalysis is an integral part of the operational system, the ocean model, resolution and assimilation procedure for the historical reanalysis are always the same as for the current operational analysis. Note that this is different

from the approach used for atmospheric reanalyses such as ERA-40 in which the assimilation/model system is not necessarily the same as in the current operational system.

In addition to providing initial conditions for forecasts, the ocean reanalysis is an important resource for climate variability studies. We show that as well as improving the skill of seasonal forecasts, the S3 ocean reanalysis (hereafter denoted by ORA-S3) offers an interesting perspective on the earth's climate. The 48-year reconstruction is used to explore the amplitude, vertical penetration and geographical distribution of the ocean warming. It is also possible to estimate the steric changes in global sea level (i.e. changes in volume due to changes in the water density), which can be compared with the estimation of global sea level provided by the altimeter data since 1993.

A major concern for the historical reconstruction of the climate is the non-uniform observation coverage in time and space. To assess the robustness of the climate signals found in ORA-S3, we compare with those from an equivalent ocean experiment that is forced by atmospheric fluxes, but without assimilating ocean data. The consistency between ORA-S3 and this later experiment, called ORA-nobs hereafter, not only consolidates the significance of the ocean signals, but also provides an assessment of the quality of the atmospheric fluxes used to drive the ocean model.

### The ORA-S3 system

The ORA-S3 system has several innovative features, including an on-line bias correction algorithm, the assimilation of salinity data on temperature surfaces, and assimilation of altimeter-derived sea level anomalies and global trends. A detailed description of the analysis system is provided in *Balmaseda et al. (2007a)*. A selection of historical and real-time ocean analysis products can be seen at

[www.ecmwf.int/products/forecasts/d/charts/ocean/](http://www.ecmwf.int/products/forecasts/d/charts/ocean/)

Figure 1 shows schematically the different data streams used in the production of ORA-S3.

- ◆ **Subsurface observations.** The subsurface observations come from the quality-controlled dataset prepared for the ENACT and ENSEMBLES projects until 2004 (*Ingleby & Huddleston, 2006*), and from the Global Telecommunication System thereafter (ENACT/GTS). Before the start of the Argo programme in 2002, the subsurface data consist mainly of profiles of temperature from XBTs (expandable bathythermographs), CTDs (conductivity-temperature-depth profiling floats) and moored arrays (TAO/TRITON and PIRATA), and a smaller number of salinity profiles from CTDs and TRITON moorings. The implementation of the Argo programme was largely completed in 2006, providing for the first time near global coverage of both temperature and salinity (*Gould, 2005*).
- ◆ **Altimeter data.** The altimeter data used are global gridded weekly maps from 1993 onwards (*Le Traon et al., 1998*).
- ◆ **Sea surface temperatures.** The model sea surface temperatures (SSTs) are strongly relaxed to analyzed daily SST maps from the OIv2 SST product (*Reynolds et al., 2002*)

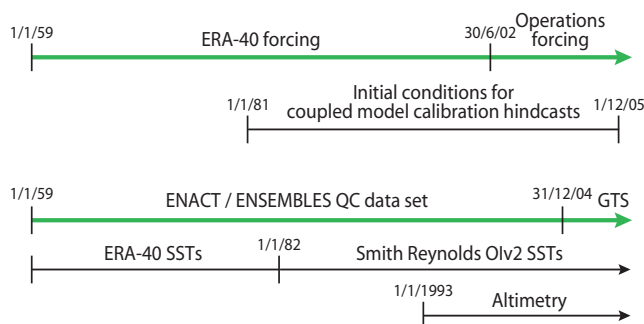


**Figure 1** Data streams used in the S3 ocean reanalysis.

from 1982 onwards. Prior to that date, the same SST product as in the ERA-40 reanalysis was used.

The ocean data assimilation system for ORA-S3 is based on the HOPE-OI scheme. The first guess is obtained by forcing the ocean model with daily fluxes of momentum, heat and fresh water from the ERA-40 reanalysis for January 1959 to June 2002 and from the NWP operational analysis thereafter; the fresh water flux in ERA-40 has been corrected according to *Troccoli & Källberg (2004)*.

Since a historical reanalysis is required to initialize the calibrating hindcasts for the seasonal and monthly forecasting systems, the quality of the reanalysis will influence the calibration process, and hence the quality of the forecasts. Ideally, the ocean reanalysis should provide a reliable representation of the inter-annual variability. Often, however, the variability can be contaminated by changes in the observing system, especially if these act to correct biases in the background. In ORA-S3, the introduction of a bias-correction algorithm with both prescribed and adaptive components has improved the representation of the inter-annual variability of the upper ocean heat content (*Balmaseda et al., 2007b*). However, there may still be problems with the representation of the variability in very poorly observed areas, such as the Southern Ocean (also known as the Antarctic Ocean or South Polar Ocean), and in the salinity field.

As for the previous operational analysis system (S2), ORA-S3 consists of an ensemble of five simultaneous reanalyses. The purpose of the multiple analyses is to sample uncertainty in the ocean initial conditions, and thereby contribute to the creation of the ensemble of forecasts for the probabilistic predictions at monthly and seasonal ranges. Five simultaneous ocean analyses are created by adding perturbations to the wind stress while the ocean model is being integrated forward in time. The perturbations are commensurate with the estimated uncertainty in the wind stress product, but the ensemble does not sample uncertainties in fresh water fluxes, heat fluxes or model formulation.

### Impact of the ocean analyses on the forecast skill

The ultimate goal of the ocean reanalysis is to improve the skill of the seasonal forecasts of SST. It is important to quantify the impact of improving the ocean initialization compared with the impact of improvements in the atmosphere model.

To this end, a coupled seasonal forecast experiment has been conducted with the atmospheric model used in S3 (*Anderson et al., 2007*), but with ocean initial conditions from the previous S2 ocean analysis. We call this experiment S2icS3m. The experiment consists of 76 ensemble forecasts, with initial conditions three months apart (January, April, July and October) spanning the period 1987–2005. For each date, an ensemble of five coupled forecasts (with perturbed initial conditions) is integrated with a lead-time of up to 7-months. The forecast SST anomalies are then computed with respect to the model climatology (which depends on the lead time).

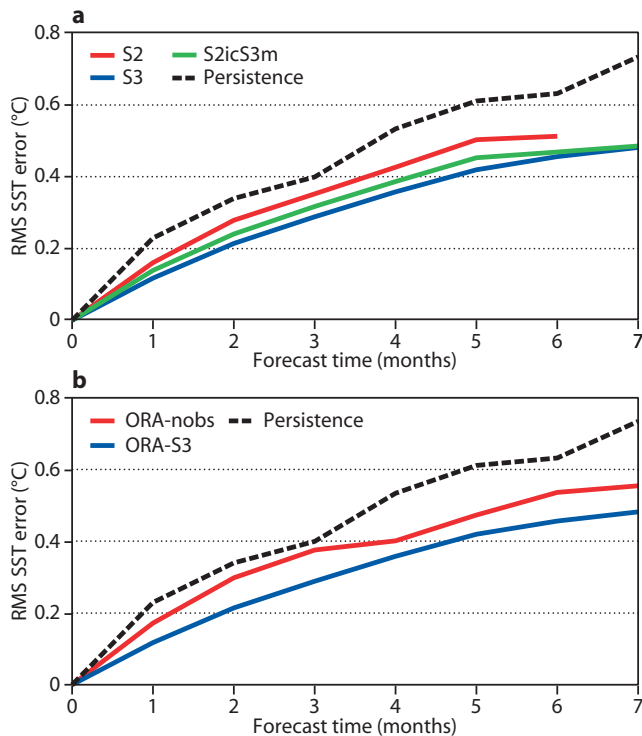


**Figure 2** RMS error in the seasonal forecast of SST in the region Niño 4 (5°N–5°S, 160°E–150°W) as a function of lead-time. (a) Results from S2 (red), S3 (blue) and the hybrid S2icS3m (green). (b) Results from ORA-S3 (blue) and ORA-nobs (red) for which no ocean data has been used in the preparation of the ocean initial conditions.

Figure 2(a) shows the RMS error in the forecast of SST anomalies as a function of lead-time in the Niño4 area for S2icS3m, together with the results from the S3 and S2 seasonal forecasting systems which have been subsampled to cover exactly the same set of 76 forecasts as for S2icS3m. The results indicate that the impact of the improved ocean initial conditions is comparable to the impact of changing the atmospheric cycle from Cy23r4, as used in S2, to Cy31r1, as used in S3.

It is also important to quantify the improvement in the forecast skill resulting from the assimilation of ocean data. To this end, another seasonal forecast experiment has been performed using ocean initial conditions from ORA-nobs, identical to the ORA-S3 ocean analysis where no ocean data, apart from SST, has been assimilated. Everything else (spin up, SST relaxation, forcing fields etc.) is the same as in ORA-S3. As before, the experiment consists of 76 different ensemble forecasts, with initial conditions from the period 1987–2005. The coupled model is that used by S3. Results displayed in Figure 2(b) show that data assimilation significantly improves the forecasts of SST: the RMS error from forecasts using ORA-S3 is substantially smaller than that of forecasts from ORA-nobs. The improvement, more noticeable in the western Pacific, is also apparent in the Indian Ocean, eastern Pacific and subtropics. However, in regions where the forecasting system has little skill, for example the equatorial Atlantic, the assimilation of data in the ocean initialization does not lead to any noticeable improvement.

**Changes in the ocean heat content**

Monitoring the changes in ocean heat content is important for understanding and predicting changes in the climate. *Levitus et al., 2005* (referred to as Levitus05 in what follows) estimate that about 84% of the increased heat stored by the Earth system during the past 50 years has been stored in the world’s oceans. Their work, describing the spatial distribution of the heat storage and time evolution of the warming trends over the period 1955–2003, is an important contribution of the IPCC AR4 (*Bindoff & Willebrand, 2007*).

We now describe the evolution of the ocean heat content from ORA-S3 for the period 1959–2006 and compare the results with Levitus05 as a demonstration of the value of the ORA-S3 reanalysis for climate studies. As the variability in both Levitus05 and ORA-S3 can be affected by changes in the observing system, we also make a comparison with ORA-nobs. This comparison allows a consistency check of the climate signals in both the ocean observations and in the atmospheric forcing fluxes, as well as demonstrating the impact of assimilating ocean data.

**Time evolution of the upper ocean heat content**

The time evolution of the upper ocean heat content of the World Ocean (i.e. all the oceans) for the five ensemble members of ORA-S3 and estimates from ORA-nobs, as measured by the average temperature in the upper 300 m (denoted T300), are shown in Figure 3(a). As well as a clear warming trend, captured by both ORA-S3 and ORA-nobs, there is significant decadal variability, though with smaller amplitude in ORA-nobs. The coherence between ORA-S3 and ORA-nobs indicates that the variability in ORA-S3 is not simply due to changes in the oceanic observing system but must come in part from the surface forcing.

The curve for ORA-S3 in Figure 3(a) shows several features in common with Figure 1 of Levitus05. Particularly noticeable are the minimum after 1965, the local maximum around 1980 and the local minimum around 1985, more pronounced in ORA-S3 than ORA-nobs. The cooling after 1980 occurs mainly in the Pacific, in agreement with Levitus05. ORA-S3 also shows a brief stabilization of the warming around 1992, and a cooling starting in 2002. This cooling was first reported by *Lynnman et al. (2003)*, and has been attributed to faulty sensors in some of the Argo floats (SOLO/FSI). We refute this latter point as an additional experiment was conducted, similar to ORA-S3 but with all the SOLO/FSI data blacklisted, the results of which show that the SOLO/FSI data are not responsible for the 2002 cooling and subsequent stabilization of the warming trend. In fact there is little difference between the two experiments, probably because the bad data were rejected by the ORA-S3 quality control system in first place. Besides, in our analysis the cooling takes place in the Southern Ocean, where there were no SOLO/FSI floats. The 2002 cooling is captured in ORA-nobs, indicating that it is not an artefact of the sampling.

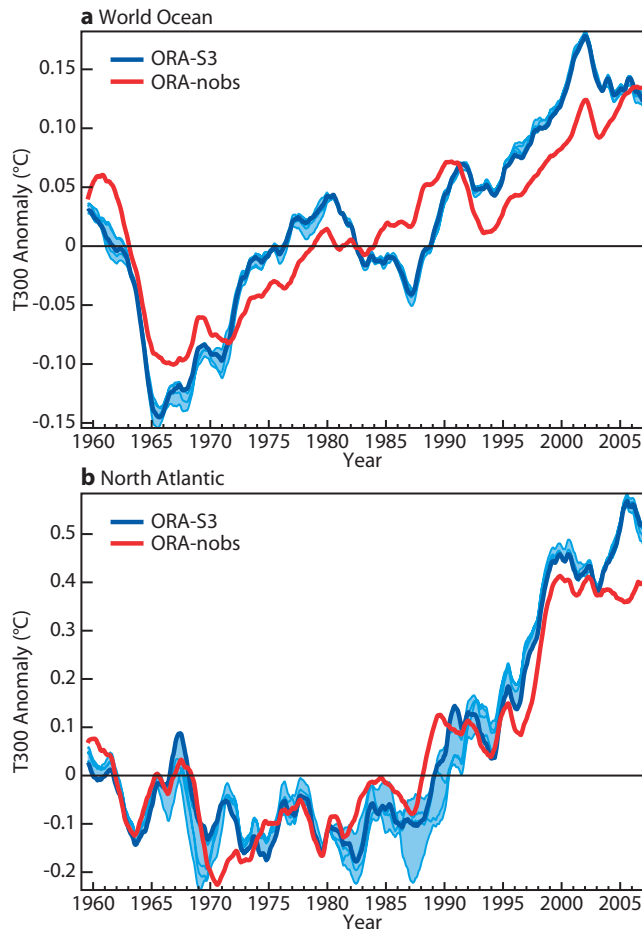


**Figure 3** Time evolution of the upper ocean heat content, as measured by the averaged temperature in the upper 300 m (T300) in (a) the World Ocean and (b) in the North Atlantic (30°N–60°N). The time series show the 12-month running average anomalies, relative to the 1960–2005 climatology. The blue curves are the five ensemble members in ORA-S3 with solid blue line indicating the unperturbed analysis and the shading indicating the spread. The red curve is from ORA-nobs.

The stabilization of the heat content post-2003 in ORA-S3 shown in Figure 3(a) is more debatable. It does not appear in ORA-nobs, where the 2002 cooling is short-lived and warming of the upper ocean soon recommences. Additional observing system experiments, in which the Argo floats are removed, show that the post-2003 stabilization of the heat content in ORA-S3 is affected by the Argo data, since it is the first time that there is good observational coverage of the Southern Ocean.

Figure 3(b) shows the time evolution of T300 for the North Atlantic region (30°N–60°N), which is quite different from the time evolution for the World Ocean, illustrating the regional variations in the warming trends. In the North Atlantic, the warming only starts in the late 1980s, in both ORA-S3 and ORA-nobs. The warming trend is interrupted for a few years after 2000. The warming then continues in ORA-S3, reaching a peak in 2005, but there is no such warming in ORA-nobs. From various observing system experiments we have conducted, we attribute the pronounced 2005 warming

in ORA-S3 to the Argo data. The evolution of sea level from altimeter data (see later) does not show any special rise during 2005 in the North Atlantic suggesting that the warming may be an artefact of nonuniform sampling.

#### *Spatial distribution of the changes*

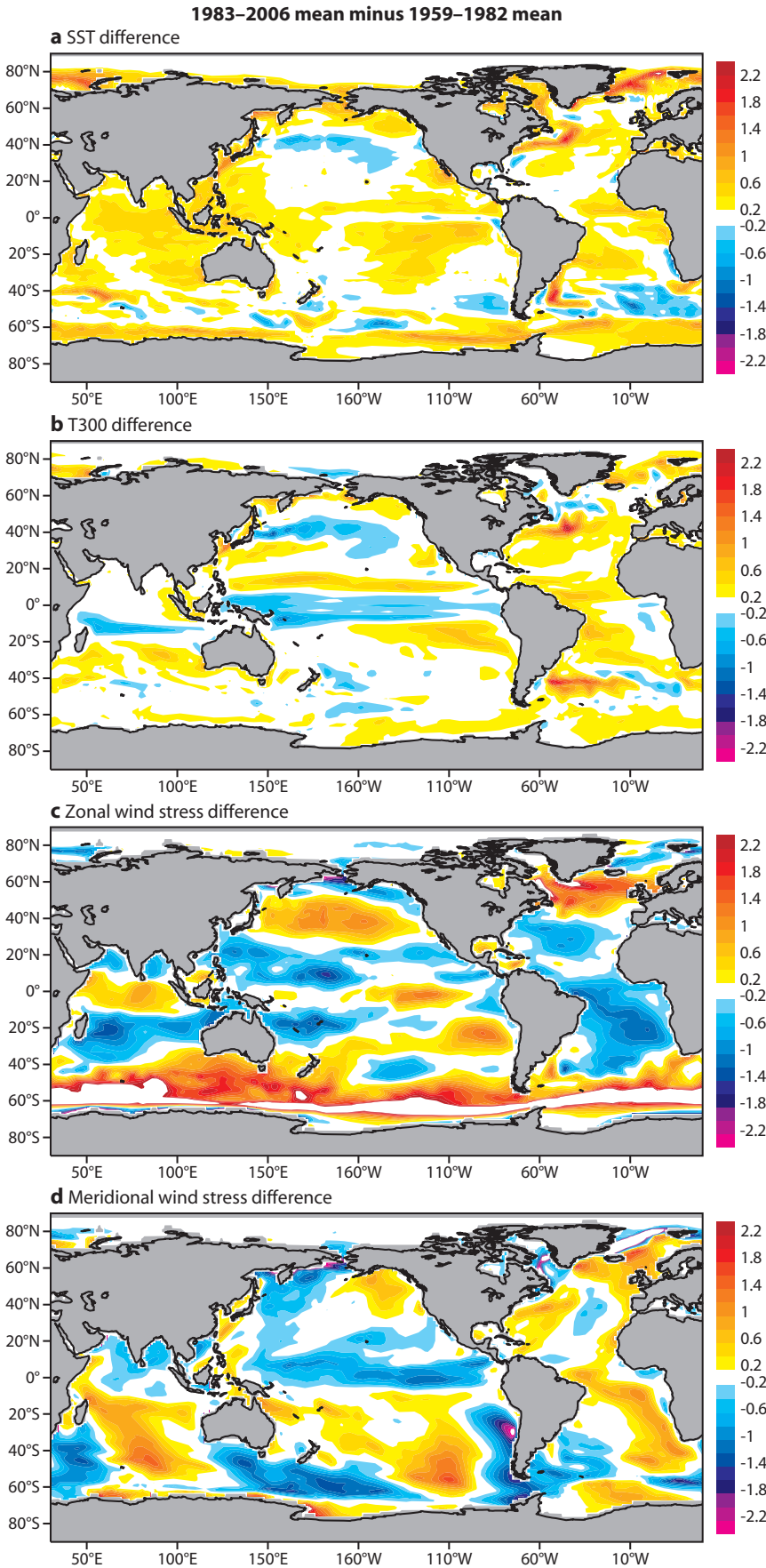
Differences between the 1983–2006 and the 1959–1982 climatologies shown in Figure 4 are used to explore the spatial distribution of the warming in SST and T300.

Figure 4(a) shows that the warming of the surface temperatures is widespread, except for a cooling in the Pacific at 40°N and a region in the Southern Ocean around 50°S. The surface warming is extensive in the Indian and Atlantic Oceans. The tropical Pacific gets warmer nearly everywhere, but not in an equatorially confined band in the eastern part of the basin. Peak values, which in places exceed 2 K, are reached in high latitudes, along the path of the Gulf Stream, the confluence of the Falkland and Brazil currents, in the Greenland-Norwegian Sea and in the southern part of the Antarctic Circumpolar Current.

The spatial patterns for T300 given in Figure 4(b) are quite different to those for SST. Below the surface, the equatorial Indian and Pacific Oceans are getting colder, especially south of the equator, a feature that does not reach the surface except for an equatorially confined band in the eastern Pacific. The warming of the SST in the tropical band is therefore quite shallow. The subsurface cooling within the 10°N–10°S latitudinal band in the Pacific and at around 10°S in the Indian Ocean is also observed in ORA-nobs, implying that it is the consequence of changes in the surface forcing, most likely in the wind stress.

Changes in the zonal and meridional wind stress are shown in Figures 4(c) and 4(d). In the Indian and Pacific basins, the equatorial easterlies are weaker in the later period, suggesting a reduction in the strength of the Walker circulation (Vechi *et al.*, 2006). The easterlies are stronger both sides of the equator, between latitudes of 5°–10°. There is a stronger convergence of the meridional component at the equator, suggestive of an intensified Hadley circulation. The weakening in the zonal winds along the equator leads to a reduced east-west slope of the equatorial thermocline and a weakening of the equatorial upwelling, mostly in the East Pacific.

The off-equatorial intensification of the trades increases the latitudinal extent of the meridional circulation cell in the ocean, with increased divergence either side of the equator and increased convergence at around 15°N/S. The net effect is an export of heat from the equator towards 15°N/S within the depth of the wind-driven meridional cell (~300 m). The cooling in the Indian Ocean south of the equator is produced by a similar mechanism. The changes in the wind stress lead to a weakening of the northern branch of the South Equatorial Current and the North Equatorial Countercurrent. That the 10°N–10°S cooling appears in



**Figure 4** Difference maps of the 1983–2006 mean minus the 1959–1982 mean for (a) SST (°C) and (b) T300 (°C). The differences in the zonal and meridional components of the wind stress ( $10^{-2} \text{ N m}^{-2}$ ) are given in (c) and (d).

ORA-nobs suggests that the signal is caused by the surface forcing. That the cooling appears in ORA-nobs and Levitus05 independently is indicative of a consistency between ocean observations and surface fluxes.

ORA-S3 also captures the cooling in the North Pacific around  $40^{\circ}\text{N}$  described in Levitus05. This cooling, apparent in both SST and T300, has been attributed to the positive phase of the Pacific Decadal Oscillation (PDO), which occurred after 1976 and led to a strengthening of the Kuroshio Extension. The cooling at  $40^{\circ}\text{N}$  is also reproduced in ORA-nobs, although with smaller amplitude. It may be related to the PDO through the intensification of the Aleutian Low. In the Southern Ocean, changes in ORA-S3 and ORA-nobs are found near the Antarctic Circumpolar Current also in agreement with the IPCC AR4. This warming has been linked to a southward shift and intensification of the westerly winds over this area. The warming is more pronounced in ORA-S3 than ORA-nobs. The largest degree of consistency between SST and T300 warming occurs in the Atlantic basin, where the warming signal occupies a large fraction of the basin. The cooling in the North Pacific is also consistent in SST and T300.

**Vertical structure**

A better insight into the vertical distribution of the changes in temperature is given in Figure 5. This shows a depth-latitude map of the zonally averaged temperature trends over the period 1959–2006 in ORA-S3 for the Atlantic, Pacific, Indian and World Oceans. The figure is directly comparable with Figure 5.3 of the IPCC AR4 (*Bindoff & Willebrand, 2007*), using the same contour interval and shading convention. The spatial patterns in ORA-S3, although largely consistent with Levitus05, exhibit sharper vertical and meridional structures probably because the resolution used in ORA-S3 is higher, and no smoothing has been

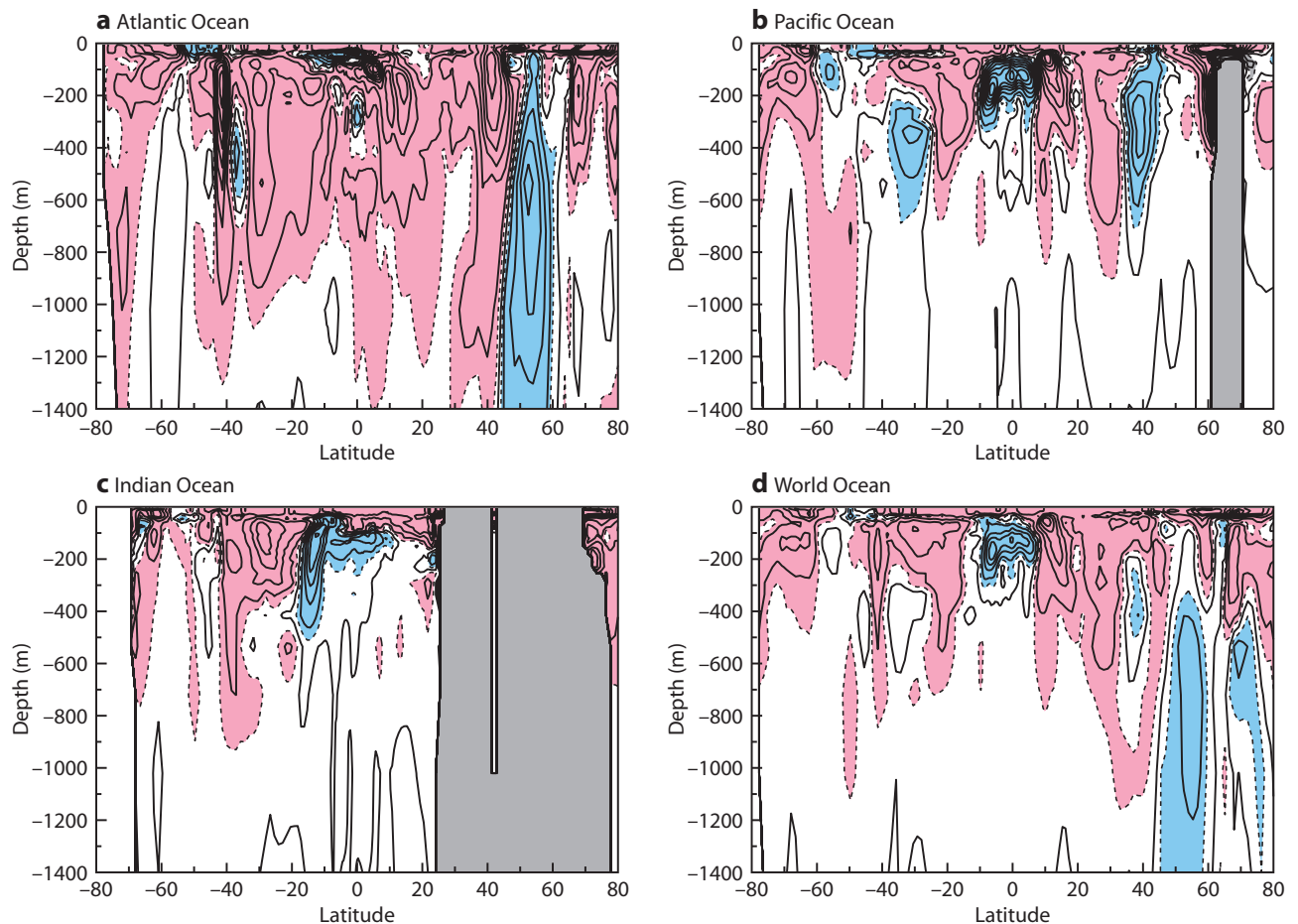


**Figure 5** Latitude-depth sections of the linear trends in temperature over the period 1959–2006 in ORA-S3 for the (a) Atlantic, (b) Pacific, (c) Indian Ocean and (d) World Ocean. The contour interval is 0.05 degrees/decade. Values above 0.025 degrees/decade are shaded in pink, and those below -0.025 degrees/decade are shaded in blue. The trends are the gradients obtained from the best root mean square fit of a straight line.

applied. Most of the changes in Figure 5 indicate warming, but interestingly there is also cooling occurring in the form of cold/warm dipoles, possibly associated with the displacement of the gyres, and also circulation changes in the equatorial Indian and Pacific Oceans.

The cooling of the equatorial cells in the Pacific and Indian Oceans is likely caused by changes in the ocean circulation. Poleward of the equatorial cooling, immediately adjacent to it and penetrating up to 400 m, there is warming, which in the Indian Ocean occurs only south of the equator. In the tropical Atlantic the cold equatorial cell is not so evident, but there is warming in the subtropics, similar to that in the Pacific. The changes in the North Pacific (40°N) may be circulation changes associated with the PDO and the strengthening of the Kuroshio Extension. The signal penetrates as deep as 600 m. Both the equatorial cells and the PDO signal in ORA-S3 are in agreement with Levitus05, although the amplitude is larger in ORA-S3. The equatorial cooling is also present in ORA-nobs, indicating that the signal is wind-driven. Curiously the signal in ORA-nobs is larger than in ORA-S3, suggesting that the wind changes are too strong or the model too sensitive.

Large changes are also apparent in the North Atlantic, with a deep and pronounced cooling around 50°N and a warming at around 40°N. Although the warming penetrates as far as 1000 m, the peak value occurs within the first 200 m. In Levitus05 the peak warming is deeper (~600 m), with a secondary maximum within the first 200 m. The cooling at 50°N is even deeper, and more intense in ORA-S3 than in Levitus05. The same dipolar structure also appears in ORA-nobs. The Atlantic is the ocean with the strongest warming and the deepest penetration.

In general, changes in the southern hemisphere are stronger in ORA-S3 than in Levitus05. Particularly noticeable is the large warming at around 40°S in the Atlantic observed in ORA-S3 but not in Levitus05. It is also much weaker in ORA-nobs. This warming is very noticeable in Figure 4(b) to the east of Argentina.

#### Sea level change and thermal expansion

Changes in the sea level can result from two major processes that alter the volume of the water in the global ocean: steric changes (due to variations in the density of water) and the exchange of water between the ocean and other water reservoirs such as glaciers and

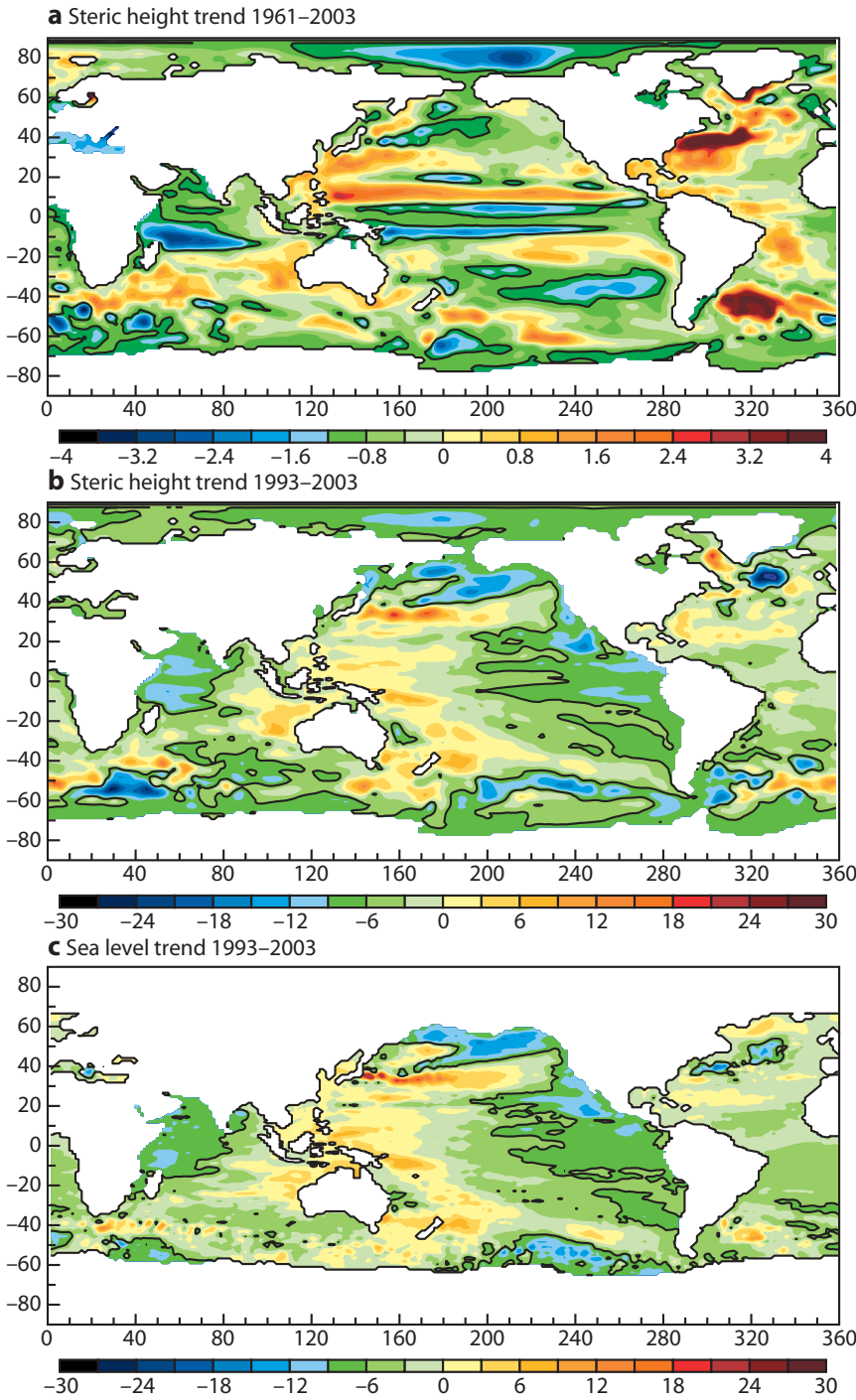


**Figure 6** Spatial pattern of the linear trends in steric height changes in ORA-S3 for (a) 1959–2003 and (b) 1993–2003. (c) This shows the spatial distribution of the linear trend in sea level from altimeter data for the period 1993–2003 (c). The colour interval is 0.4 mm/yr for (a) and 3 mm/yr for (b) and (c). The zero contours are shown.

ice sheets. Measurements of present-day sea level change rely on tide gauges and, since 1993, satellite altimetry. The steric changes can be diagnosed using analysis of temperature and salinity. The differences between global steric changes and global sea level can be used as an indication of mass variations. However, large uncertainties remain. Results summarized in the IPCC AR4 indicate that for the period 1961–2003 thermal expansion contributed only one-quarter of the estimated sea level rise, while melting of the land ice accounted for less than half. Thus, the full estimate of sea level rise cannot be accounted for. During recent years the observ-

ing system has improved, and for the period 1993–2003 it is possible to close the budget in sea level change, albeit with large uncertainties.

Here we present steric height estimations from ORA-S3 and compare them with the results in the IPCC-AR4. The geographical distribution of the linear trends in steric height for the periods 1961–2003, and 1993–2003 are shown in Figures 6(a) and 6(b). Both of them show large geographical variations but the spatial patterns differ substantially between the two periods. For the longer period, the pattern of steric height is very similar to the pattern of changes in the upper ocean heat content (Figure 4(b)). For the shorter period (Figure 6(b)), the trends in steric height in the Pacific and Indian Oceans show more zonal variability (rather than the meridional structure shown in Figure 6(a)). This is in good agreement with trends in sea level from altimeter (Figure 6(c)), and resembles the negative phase of ENSO and Indian Dipole patterns. The trends are for higher sea level in the western Pacific and eastern Indian Ocean, and lower sea level in the eastern Pacific and western Indian Ocean. The trends in the Atlantic Ocean are for higher sea level almost everywhere except for the pronounced negative trend southeast of Greenland. The altimeter data also shows a region of reduced sea level in the North Atlantic although not in exactly the same location.

Figure 7 shows the evolution in global steric height from the ORA-S3 ocean analysis and for ORA-nobs. The global sea level from altimeter data is also shown starting in 1993. The time evolution of the global steric height is similar to the evolution of the global upper ocean heat content as shown in Figure 3(a): there are local minima in the mid 1960s and 1980s, followed by a rapid rise and then a sharp decrease starting in 2002. For the period 1993–2002 the sea level evolution and the steric height exhibit similar trends, except for the period around 1998 when there is a large increase in sea level

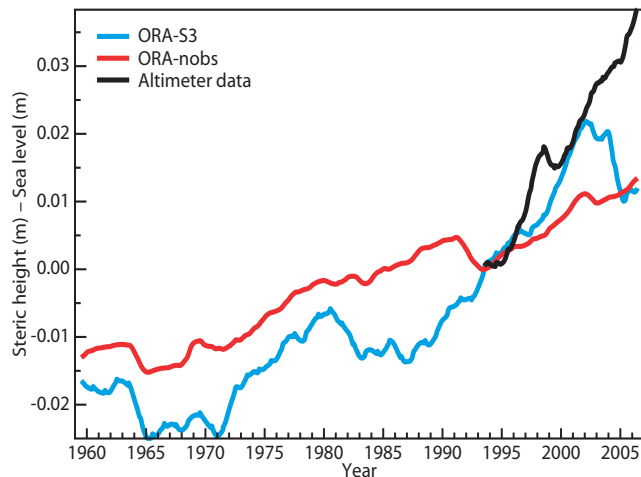


**Figure 7** Time evolution of the global steric height in ORA-S3 (blue) and ORA-nobs (red) for the period 1960–2007, and the global sea level from the altimeter data (black) for the period 1993–2007. The time series are 12-month running mean, relative to the 1993 average, so the three curves have the same origin in 1993.

not matched by the steric height. After 2002, the altimeter sea level and ORA-S3 steric height diverge considerably. In comparison, the steric height for ORA-nobs does not have the minimum in the 1980s, the increase in the period 1993–2003 is weaker and, as for T300, the post-2002 decrease in steric height is weak and short-lived. The trend for the period 1961–2003 is 0.9 mm/yr in ORA-S3, twice as large as previous estimates reported in the IPCC-AR4. It is only 0.55 mm/yr in ORA-nobs. Both ORA-S3 and ORA-nobs exhibit higher values in the steric height trends for the period 1993–2003 (2.1 and 1.1 mm/yr respectively) in agreement with the acceleration in sea level rise reported by *Church & White* (2006). The acceleration rate is stronger in ORA-S3.

The widening gap between the evolution of sea level and steric height after 2002 is worrying. The difference is even larger after 2004. The origin of this mismatch is unknown. One possibility is the underestimation of the volume increase by the ocean analysis. This could be a consequence of the changing observing system: the advent of Argo implies that for the first time there is a uniform distribution of temperature and salinity observations in the oceans of the southern hemisphere, but observing system experiments indicate that the widening gap occurs even without Argo. The mismatch could be real reflecting an increase in the mass of the oceans from the melting of glaciers and continental ice sheets. Understanding the origin of the widening gap between sea level trends and steric height trends is of paramount importance for the monitoring of the earth system and its response to global warming.

### Summary and conclusions

We have shown that the initial conditions from the ORA-S3 ocean reanalysis produce better forecasts of SST than those from the previous operational system (S2).

It is found that the effect of better ocean initialization in the forecasts of SST is of comparable magnitude to the effect of changing the atmospheric model cycle in the coupled system from that used in S2 to that used in S3. It has also been shown that assimilating ocean observations not only improves significantly the skill of the seasonal forecasts of SST, but also improves the estimation of climate signals (e.g. the distribution of warming trends in the ocean heat content and the trends in steric height).

The ORA-S3 provides a historical reconstruction of the ocean since 1959. The 48-year record has been used to investigate the distribution of the warming trends in the oceans and attribution of sea level changes due to changes in density and by inference mass. Comparisons between ORA-S3, ORA-nobs which has no assimilation of ocean data, and the Levitus05 analysis based solely on ocean observations, have been used as tests for the robustness of the climate signals. In some cases the trends in ORA-S3 have larger amplitude than either the estimates based solely on ocean observations or on ORA-nobs. This is indicative of the constructive synergy between the information provided by the ocean observations and atmospheric fluxes.

The changes in the ocean heat content are mostly shallow, occurring within the mixed layer and usually involving warming but they can penetrate deeper, up to 1000 m and involve both warming and cooling possibly associated with changes in the ocean circulation. Several important changes in the ocean circulation have taken place during the past 48 years. The equatorial meridional cell has intensified in the Pacific and Indian Oceans; apparently a consequence of changes in the winds, leading to a net cooling of the equatorial ocean in the upper 300 m and substantial changes in the equatorial current system. In the North Pacific, there is a cooling at around 40°N resulting from the intensification of the PDO. Also there is a deep meridional dipole (warming at around 40°N and cooling at 50°N) in the North Atlantic reaching depths of 1000 m. The circulation changes appear to be wind driven, and appear in ORA-nobs with smaller magnitude. The Atlantic Ocean is the basin most affected by warming trends in terms of amplitude, relative horizontal coverage and vertical penetration.

The analysis of the warming trends in the ocean has several implications for predictability studies. The time series of the upper ocean heat content shows that the warming trend is not uniform but exhibits large decadal variations with important regional variations. Understanding the origin and predictability of these decadal variations is important for future climate projections. The ocean heat content and circulation from the ocean reanalysis can also provide a metric for evaluating the quality of the climate models used for climate change predictions. Furthermore, the correct initialization of the ocean component may be important for the quality of climate predictions.

The attribution of sea level change is still an open issue: for the period 1961–2003, the rates of sea level rise given by historical reconstructions based on tide gauge and altimeter data are higher than the estimates of the steric effect from ocean temperature and salinity observations. The difference appears to be too large to be accounted for by an increase in mass due to melting of the continental ice. The steric height trends from ORA-S3 for the period 1961–2003 are 0.9 mm/yr, higher than existing reconstructions based on ocean and salinity observations, higher than in the experiment with no data assimilation, and closer to the trends in sea level from tide-gauges. ORA-S3 also captures the increase in steric height from 1993 to 2003. After 2002, the gap between sea level and steric height widens considerably for reasons that are not understood.

---

**FURTHER READING**

**Anderson, D., T. Stockdale, M. Balmaseda, L. Ferranti, F. Vitart, F. Molteni, F. Doblas-Reyes, K. Mogensen & A. Vidard, 2007:** Development of the ECMWF Seasonal Forecast System-3. *ECMWF Tech. Memo. No. 503*.

**Balmaseda, M., A. Vidard & D. Anderson, 2007a:** The ECMWF System-3 ocean analysis system. *ECMWF Tech. Memo. No. 508*.

**Balmaseda, M., D. Dee, A. Vidard & D.L.T. Anderson, 2007b:** A multivariate treatment of bias for sequential data assimilation: Application to the tropical oceans. *Q. J. R. Meteorol. Soc.*, **133**, 167–179.

**Bindoff, N. & J. Willebrand (and many others) 2007:** Observations: Oceanic climate change and sea level. *Chapter 5 of the*

*IPCC 4<sup>th</sup> Assessment*. Available from <http://ipcc-wg1.ucar.edu/wg1/wg1-report.html>

**Church, J. & N.J. White, 2006:** A 20<sup>th</sup> century acceleration in global sea level rise *Geophys. Res. Lett.*, **33**, L01602, doi:10.1029/2005GL024826.

**Gould, J., 2005:** From Swallow floats to Argo – the development of neutrally buoyant floats. *Deep-Sea Research II*, **52/3–4**, 529–543.

**Ingleby, B. & M. Huddleston, 2006:** Quality control of ocean temperature and salinity profiles – historical and real-time data. *J. Mar. Sys.*, **65**, 158–175.

**Le Traon, P.-Y., F. Nadal & N. Ducet, 1998:** An improved mapping method of multisatellite altimeter data. *Atmos. Oceanic Technol.*, **15**, 522–534.

**Levitus, S., J.I. Antonov & T.P. Boyer, 2005a:** Warming of the World Ocean, 1955–2003. *Geophys. Res. Lett.*, **32**, L02604, doi:10.1029/2004GL021592.

**Lyman, J.M., J.K. Willis & G.C. Johnson, 2006:** Recent cooling of the upper ocean. *Geophys. Res. Lett.*, **33**, L18604, doi:10.1029/2006GL027033.

**Troccoli, A. & P. Kållberg, 2004:** Precipitation correction in the ERA-40 reanalysis. *ERA-40 Project Report Series, No. 13*.

**Reynolds, R., N. Rayner, T. Smith, D. Stokes & W. Wang, 2002:** An improved in situ and satellite SST analysis for climate. *J. Clim.*, **15**, 1609–1625.

**Vecchi, G.A., B.J. Soden, A.T. Wittenberg, I.M. Held, A. Leetmaa & M.J. Harrison, 2006:** Weakening of tropical Pacific atmospheric circulation due to anthropogenic forcing, *Nature*, **441**, 73–76.

---

## Evaluation of the impact of the space component of the Global Observing System through Observing System Experiments

---

GRAEME KELLY, JEAN-NOËL THÉPAUT

---

AS MANY more satellite instruments (both active and passive) became operational the challenge was, and still is, how to assimilate these space measurements together with all the conventional measurements. Figure 1 shows most of the current and near future satellite sensors used or soon to be used. Since 2001 the number of satellite sensors being used has increased by a factor of four and now is in excess of forty sensors. A recent example of the number of observations, mostly satellite radiances, used in the operational data assimilation at ECMWF during a 12-hour period is given in Table 1. Complex data processing techniques are employed to assimilate all these observations in a timely manner

A study, sponsored by EUMETSAT, has been carried out to evaluate the impact of the space component of the Global Observing System through Observing System Experiments. In this study the relative contributions of the various space observing systems have been assessed within the context of the ECMWF data assimilation system. It is found that all the space based sensors generally contribute in a positive way to the overall improvement of the ECMWF forecast system.

### Requirement for Observing System Studies

At its meeting at ECMWF on 3 May 2003, the EUCOS Scientific Advisory Team discussed the need to investigate the interdependencies between the space-based and terrestrial components of the observing system. It was suggested that such an investigation could be based on

	Screening		Used in Analysis	
<b>SYNOP</b>	421,000	0.43%	64,000	1.94%
<b>Aircraft reports</b>	519,000	0.53%	247,000	7.53%
<b>DRIBU</b>	24,000	0.02%	6,000	0.18%
<b>TEMP</b>	152,000	0.16%	75,000	2.28%
<b>PILOT</b>	119,000	0.12%	57,000	1.75%
<b>AMVs</b>	4,272,000	4.37%	131,000	3.99%
<b>Radiance data</b>	91,786,000	93.91%	2,508,000	76.46%
<b>Scatterometer winds</b>	274,000	0.28%	118,000	3.61%
<b>GPS radio occultation</b>	167,000	0.17%	73,000	2.24%
<b>TOTAL</b>	97,734,000	100.00%	3,280,000	100.00%

**Table 1** Observation data count for one 12 hour 4D-Var cycle for 0900–2100 UTC on 24 April 2007. ‘Screening’ refers to the actual amount of data presented to 4D-Var and the ‘Used in Analysis’ indicates the amount of data used during the analysis minimization.

a set of carefully designed Observing System Experiments (OSEs). These studies would be designed to provide guidance on the future development of the terrestrial observing system in view of the increasing capabilities of the satellite observing systems provided by the meteorological space agencies.

In recent years, several NWP centres have demonstrated substantial benefit from the assimilation of, for example, ATOVS radiances and scatterometer winds (referred to hereafter as SCAT). Since 2003 data has become available from second-generation radiometers (AIRS on Aqua in 2003 and IASI on MetOp in 2007) providing significantly enhanced temperature and humidity sounding capabilities – to be followed (in the

five to ten year time frame) by similar instruments on the operational NPOESS series of satellites.

It was agreed that, as far as EUCOS is concerned, the primary issues were:

- ◆ What are the relative contributions of various components of the terrestrial observing system within the current overall composite observing system?
- ◆ How should the terrestrial systems evolve over the next five to ten years and beyond to complement the projected evolution of the space-based observing systems?

This led to a proposal from *Andersson et al.* (2004) to carry out a set of OSEs specifically designed to evaluate the role of the terrestrial component of the Global Observing System.

Following a number of discussions between EUMETSAT, ECMWF and EUCOS, it was agreed that specific OSEs dedicated to examining the various contributions of the different components of the space observing system were necessary to complement the original proposal about the terrestrial components. Taking this approach would provide a comprehensive assessment of the space/terrestrial links. It was also agreed that the robustness of this combined assessment would be strengthened by the adoption of similar strategies for experimentation and validation of the two studies.

These studies also take onboard one of the outcomes of the Third WMO Workshop on the Impact of Various Observing Systems on NWP. This suggested that, due to a large degree of redundancy of the Global Observing System (GOS), performing impact studies by removing one element of the GOS can show very limited impact and does not necessarily highlight the intrinsic benefit of the element in question. It was therefore decided that the scenarios in which the contributions of different elements of the GOS are investigated would be based on adding datasets or combination of datasets to a reference.

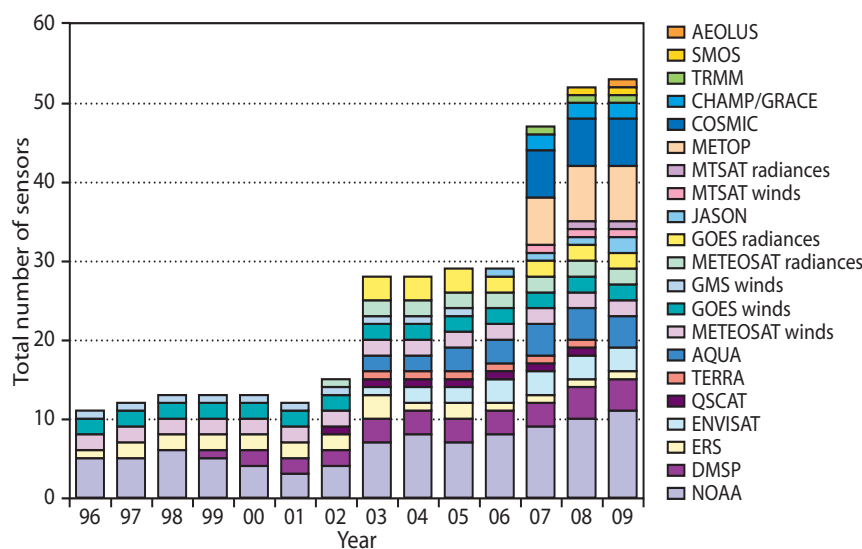


**Figure 1** Number of satellite sensors that are or will be soon assimilated in the ECMWF operational data assimilation.

This article will deal with the relative contributions of the various space observing systems which have been assessed within the context of the ECMWF data assimilation system. The results of the complementary study concerning the contributions from various terrestrial observing systems are summarised in Box A.

**Past OSEs (1996–2003) with satellite data**

Three sets of OSEs were run at ECMWF soon after the introduction of 3D-Var in 1996 (*Kelly, 1997*), after the operational implementation of 4D-Var in 2000 (*Bouttier & Kelly, 2001*), and later in 2003 (*Kelly et al., 2004*). For each set of OSEs there were four scenarios considered.

**Box A**

**Terrestrial observing system studies (EUCOS)**

The set of terrestrial observing system studies coordinated by EUCOS has been completed following the guidelines indicated in *Andersson et al. (2004)*. These impact studies aimed to examine the various components of the terrestrial observing system, in the presence of the current satellite-based observing system. The experiments have been run using the same first winter and summer period used for the space observing system studies with the identical assimilation setup to enable a direct comparison with the space studies. The total number of cases remains probably too short to provide statistical robustness to the findings (especially over small areas such as Europe), but it is reassuring that the impact of the various components of the terrestrial observing system remains similar to the first order between the two assessed periods.

The main findings of the winter impact studies indicate a large impact of the radiosondes (wind and temperature) and aircrafts (wind and temperature), a marginal impact of radiosonde humidity information, and a neutral impact from the wind profilers. Sole wind or temperature information from radiosondes is not sufficient to impact noticeably on the forecast skill. In contrast, coupled temperature/wind information from radiosondes seems to provide a large and significant improvement in the forecasts well into the medium-range. The experiments demonstrate that observations from aircraft and radiosondes are complementary: each observing system improves the forecast skill even in the presence of the other.

The summer impact studies confirm most of the findings from the winter experiments, although the impact of the various assessed components of the GOS is smaller, both in absolute and relative terms (*Thépaut & Kelly, 2007*).

- ◆ **CONTROL:** For each set of OSEs the model cycle closest to the operational system at that time was used.
  - ◆ **NOAIREP:** All aircraft measurements (wind and temperature) removed.
  - ◆ **NOUPPER:** All TEMP, PILOT and PROFILER reports removed.
  - ◆ **NOSAT:** All satellite data removed (the terrestrial network used in operations).
- As well as conventional observations (TEMP, PILOT, PROFILER, AIREPS, SYNOP, PAOBS and BUOY reports), the 2003 OSEs included data from:
- ◆ Three AMSU-A/B and two HIRS instruments from the NOAA satellites.
  - ◆ Five geostationary satellites and one polar orbiter (Terra) providing Atmospheric Motion Vectors.

- ◆ Three geostationary satellites providing clear-sky water-vapour radiances (CSRs).
- ◆ Three SSMI instruments from the DMSP platforms.
- ◆ Seawinds instrument from Quikscat.

The results from the three sets of OSEs are summarized in Figures 2 and 3. In a nutshell, they show that satellite data has progressively become the most important data source in both hemispheres, transcending even the conventional upper-air network in the northern hemisphere in the last set of OSEs.

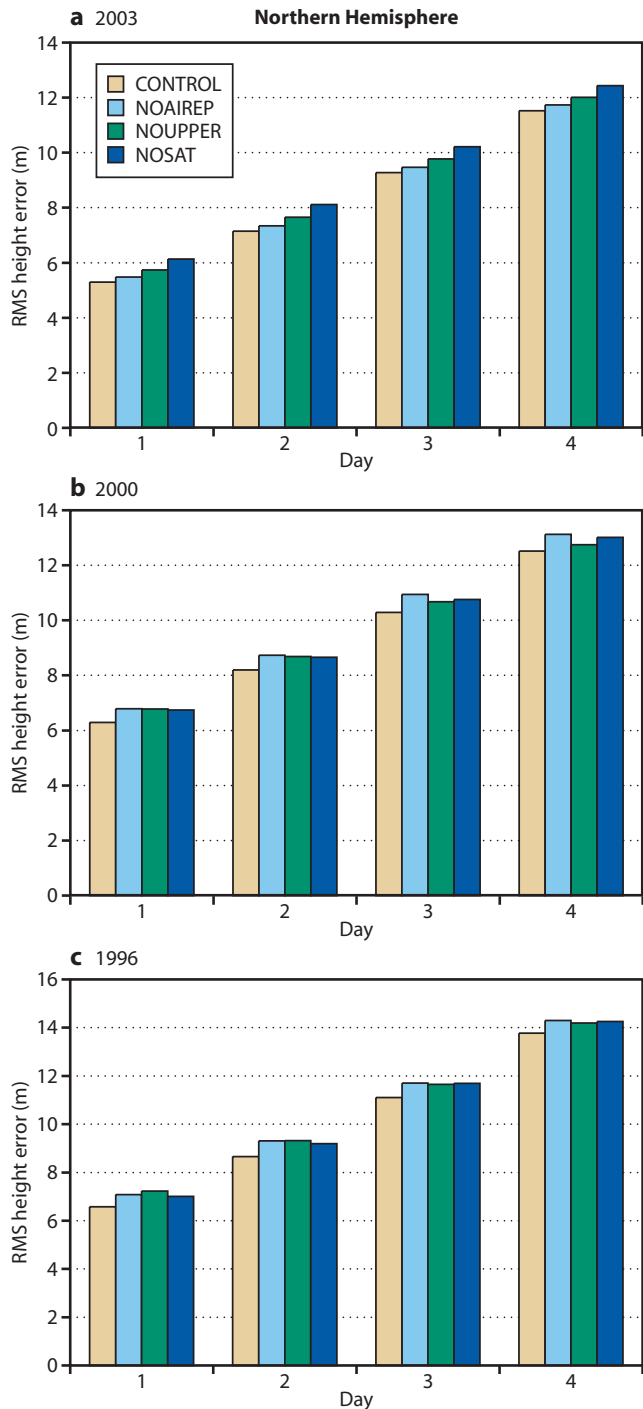


**Figure 2** Comparison of three OSEs in the northern hemisphere for the rms error of the 500 hPa geopotential height for (a) 2003, (b) 2000 and (c) 1996.

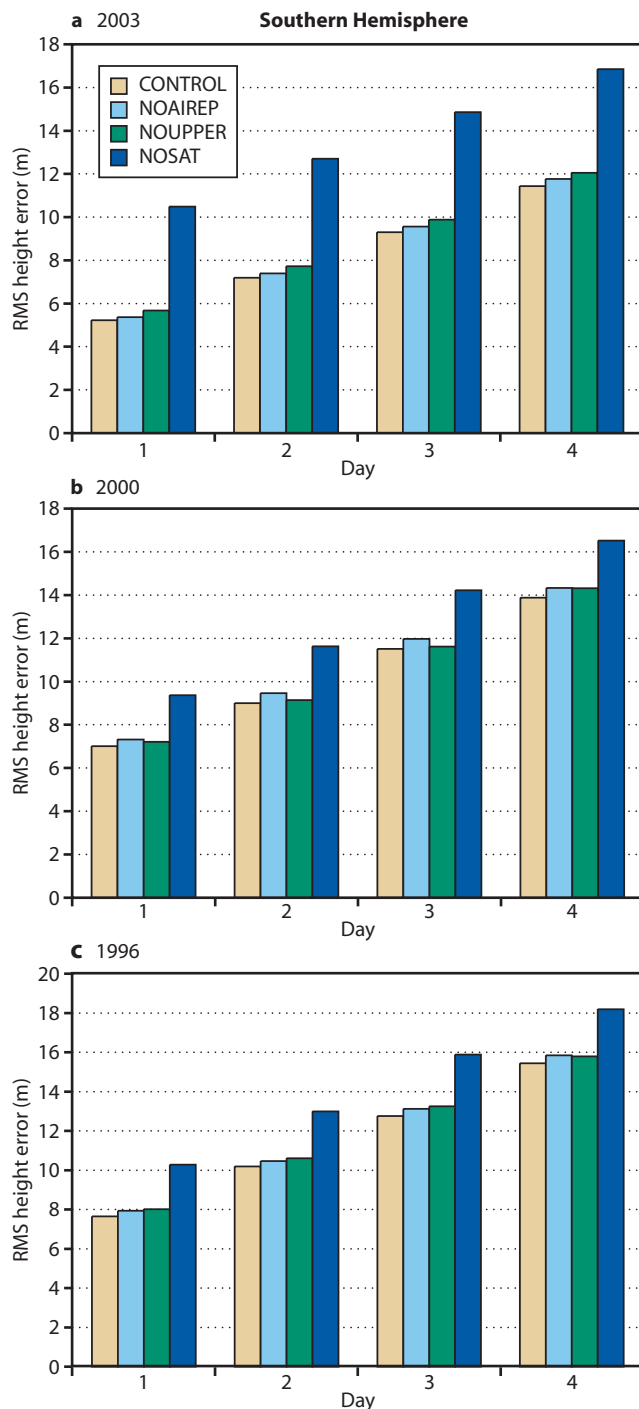


**Figure 3** Comparison of three OSEs in the southern hemisphere for the rms error of 500 hPa geopotential height for (a) 2003, (b) 2000 and (c) 1996.

### Studies of the various space observing systems

We now consider the relative contributions of the various space observing systems (infrared temperature soundings, microwave temperature soundings, imagers, scatterometers, etc.) within the context of a more recent ECMWF data assimilation system.

### Reference systems

We have assumed in this study that the current conventional observing system is maintained (thereafter called

the *BASELINE* system), and the main focus is to evaluate how specific satellite systems contribute individually to the robustness of the GOS, in addition to this degraded observing network.

The evaluation of satellite sensors is best done in the tropics and southern hemisphere, but the quality of the *BASELINE* system (equivalent to *NOSAT* referred to earlier) is so poor outside the northern hemisphere that it was not considered suitable as a reference by itself. Instead, two special reference systems have been designed to ensure a reasonable quality of the atmospheric analyses and forecasts in the tropics and southern hemisphere. These special reference systems are:

- ◆ *AMV(REF)*: *BASELINE* plus the Atmospheric Motion Vectors (AMVs).
- ◆ *AMSUA(REF)*: *BASELINE* plus data from one AMSU-A instrument.

### Experimental setup

The data assimilation framework used for all the OSEs corresponds to the system that was used in operations close to the time of the periods under investigation. The main characteristics of the data assimilation system are given in Box B.

The experiments were carried out for two periods, each covering a winter and summer.

- ◆ **Period 1.** Winter from 4 December 2004 until 25 January 2005 and summer from 17 July to 15 September 2005 using IFS Cy29r1 and Cy29r2 respectively. For this period, the OSEs were based on *AMV(REF)* as a reference.

- ◆ **Period 2.** Winter from 5 December 2006 to 14 February 2007 and summer from 1 June to 18 August 2006 using IFS Cy31r1. For this period, the OSEs were based on *AMSUA(REF)* as a reference.

All forecasts were run from 00 UTC.

### Standard experiments

Two sets of assimilation were performed.

- ◆ ***AMV(REF)* as reference for Period 1.** The observational scenarios tested with AMVs as reference (i.e. *AMV(REF)*) are described in Table 2. These experiments are based on the winter and summer forming Period 1. The first ten days of each assimilation scenario are excluded from the verification to ensure a reasonable warm-up phase. No real difference in the impact was found between summer and winter so the mean scores are combined to give a sample of 89 days for each experiment. All experiments are validated using the operational analysis.

- ◆ ***AMSUA(REF)* as reference for Period 2.** The observational scenarios tested with one AMSU-A as reference (i.e. *AMSUA(REF)*) are described in Table 3. These experiments are based on the winter and summer forming Period 2. These experiments were delayed as long as possible in order to make use of the AMSU-A and MHS instruments from the EUMETSAT MetOp satellite. The first two weeks are excluded

**Box B**

**Main characteristics of the data assimilation system**

- ◆ T511L60 forecast model resolution
- ◆ 4D-Var assimilation with a 12-hour window and the analysis inner and out loop resolutions being T95/T159L60 and T511L60 respectively
- ◆ Conventional observations currently assimilated in the system include:
  - TEMP, PILOT and PROFILER reports
  - SYNOP, SHIP, METAR and BUOY (moored and drifters) reports
  - Aircrafts (AMDAR, AIREP, ACARS) including ascent/descent reports
- ◆ Satellite observations assimilated in the system for the atmospheric analysis were at that time for the winter run:
  - Atmospheric Motion Vectors from GEO (Meteosat-5/7, GOES-9/10/12) and LEO (MODIS Terra and Aqua) platforms
  - Clear-sky water vapour radiances from GEO (Meteosat-5/8, GOES-9/10/12)
  - Level 1c infrared radiances from NOAA-14/17 (HIRS) and Aqua (AIRS)
  - Level 1c microwave radiances from NOAA-15 (AMSU-A), NOAA-16 (AMSU-A and AMSU-B), NOAA-17 (AMSU-B), Aqua (AMSU-A) and DMSP 13/14/15 (SSM/I)
  - Sea surface winds from scatterometers QuikScat and ERS-2
  - Ozone products from NOAA-16 (SBUV) and ENVISAT (SCIAMACHY).

As this study has been spread over two years, different model cycles have been used for the two scenarios.

- ◆ **Period 1.** IFS model cycles Cy29r1 (winter) and Cy29r2 (summer) have been used, differing mainly by the inclusion of NOAA-18 level-1c radiances from AMSU-A and MHS and the blacklisting of NOAA-14 HIRS radiances that had become too noisy. *AMV(REF)* was used as a reference for Period 1.
- ◆ **Period 2.** IFS model cycle Cy31r1 has been used for both winter and summer. *AMSUA(REF)* was used as a reference for Period 2.

from the verification to ensure a reasonable warm-up phase for each assimilation scenario. For Period 2, the Variational Bias Correction for satellite radiances was operational and therefore activated during the warm-up phase of the experiments (bias correction coefficients are then kept constant for the remaining of the assimilation period). No real difference in the impact was found between summer and winter so the mean scores are combined to give a sample of 117 days for each experiment. All experiments are validated using the operational analysis.

Experiment	Datasets
<i>BASELINE</i>	All conventional observations used in NWP (radiosonde + aircraft + profiler network + surface land data + buoy observations + ship data)
<i>AMV(REF)</i>	<i>BASELINE</i> + AMVs from GEO & MODIS
<i>AMV(REF)+HIRS</i>	<i>AMV(REF)</i> + HIRS radiances
<i>AMV(REF)+AMSUA</i>	<i>AMV(REF)</i> + AMSU-A radiances
<i>AMV(REF)+AMSUB</i>	<i>AMV(REF)</i> + AMSU-B radiances
<i>AMV(REF)+SSMI</i>	<i>AMV(REF)</i> + SSMI radiances
<i>AMV(REF)+CSRs</i>	<i>AMV(REF)</i> + CSRs (Clear Sky Radiances) from GEO
<i>AMV(REF)+AIRS</i>	<i>AMV(REF)</i> + AIRS radiances
<i>AMV(REF)+SCAT</i>	<i>AMV(REF)</i> + SCAT winds
<i>AMV(REF)+AMVs</i>	<i>AMV(REF)</i> + AMVs from GEO
<i>CONTROL</i>	Full operational system (all the observations)

**Table 2** Observational scenarios tested with *AMV(REF)* (*BASELINE* plus AMVs from GEO and MODIS) as reference for Period 1.

Experiment	Datasets
<i>BASELINE</i>	All conventional observations used in NWP (radiosonde + aircraft + profiler network + surface land data + buoy observations + ship data)
<i>AMSUA(REF)</i>	<i>BASELINE</i> + AMSU-A radiances from NOAA-16
<i>AMSUA(REF)+AMVs</i>	<i>AMSUA(REF)</i> + AMVs from GEO & MODIS
<i>AMSUA(REF)+AMSUA</i>	<i>AMSUA(REF)</i> + AMSU-A radiances
<i>AMSUA(REF)+AMSUB</i>	<i>AMSUA(REF)</i> + AMSU-B radiances
<i>AMSUA(REF)+CSRs</i>	<i>AMSUA(REF)</i> + CSRs (Clear Sky Radiances) from GEO
<i>AMSUA(REF)+AIRS</i>	<i>AMSUA(REF)</i> + AIRS radiances
<i>AMSUA(REF)+SCAT</i>	<i>AMSUA(REF)</i> + SCAT winds
<i>CONTROL</i>	Full operational system (all the observations)

**Table 3** Observational scenarios tested with *AMSUA(REF)* (*BASELINE* plus AMSU-A from NOAA-16) as reference for Period 2.

**Additional experiments**

During the course of the study two additional sets of experiments using *AMV(REF)* and *AMSUA(REF)* have been carried out to specifically assess the impact of MODIS and AVHRR AMVs, the impact of various AIRS channel combinations (as a scientific preparation for the assimilation of IASI), and finally the respective contribution of clear and cloud/rain effected SSMI radiances.

The experiments using *AMV(REF)* are as follows.

- ◆ **Polar wind impact:** An experiment evaluating the impact of the MODIS winds by removing those winds from *AMV(REF)*.
- ◆ **Temperature and humidity impact:** An experiment adding AMSU-A and AMSU-B data to *AMV(REF)* to assess their impact compared to that of AIRS data. The following additional experiments have been conducted using *AMSUA(REF)* as a reference.
- ◆ **Impact of various AIRS channel combinations:** Four experiments (summer only) adding various combinations of AIRS channels. A data denial experiment has also been run by removing AIRS data from *CONTROL*.
- ◆ **SSMI impact:** Three experiments (summer only) adding SSMI (clear sky), SSMI(rainy) and SSMI (clear sky + rainy) data to the *AMSUA(REF)*. In addition, two data denial experiment have also been run: removing SSMI (clear sky) and SSMI (rainy) data from *CONTROL*.
  - SSMI (clear sky) are those SSMI radiances considered to be not affected by cloud or rain using a regression based cloud liquid check.
  - SSMI (rainy) are those radiances that fail the previous cloud liquid test and pass the convergence test in the SSMI 1D-Var (Bauer et al., 2002, 2005a and 2005b).
- ◆ **Polar wind impact:** An experiment (winter only) adding each wind set to *AMSUA(REF)* to evaluate the impact of the MODIS and AVHRR winds.

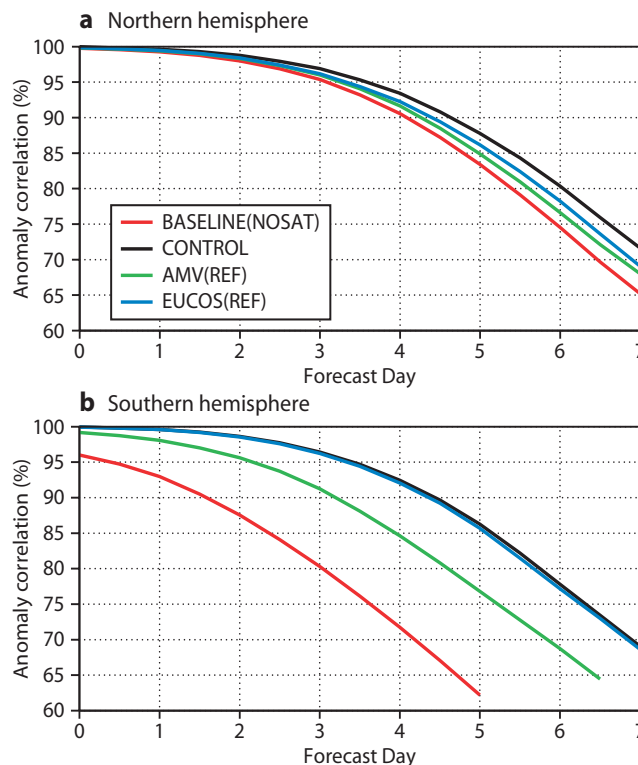
**Assimilation assessment**

In order to assess the impact of each OSE several statistical quantities have been calculated for temperature, humidity and wind at various levels. These include anomaly correlations, mean rms errors, geographical maps of rms error differences and mean rms error differences along with statistical significance. All these quantities have been computed but only a small selection is shown here; the remainder will be contained in a comprehensive report to be delivered to EUMETSAT. Most results shown are for the southern hemisphere or tropics where the impact is largest. In the northern hemisphere the impact is generally similar but reduced.

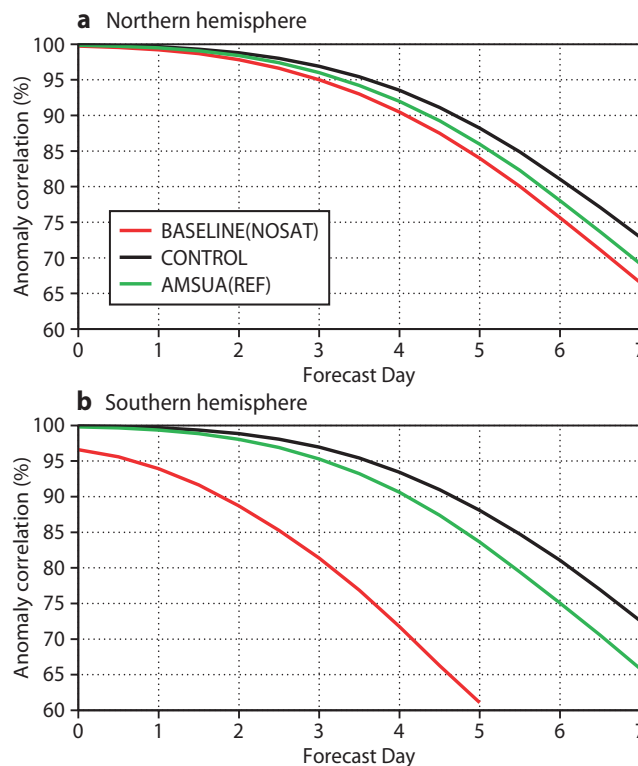
As stated above, in the southern hemisphere and tropics the *BASELINE* assimilation (terrestrial observations only) is poor and not suitable as a reference. The addition to the *BASELINE* of either AMVs (geostationary and polar) or data from one AMSU-A instrument considerably improves the quality of the assimilation with the southern hemispheric forecast skill increasing by about two days at day 4.

Figure 4 shows the mean anomaly correlation at 500 hPa for the combined summer and winter assimilation sets of Period 1. The experiments are:

- ◆ *BASELINE (NOSAT)*, *AMV(REF)* and *CONTROL* as described in Table 2.



**Figure 4** Comparison of *EUCOS(REF)* and *AMV(REF)* with *BASELINE (NOSAT)* and *CONTROL* for (a) northern hemisphere (20°–90°N) and (b) southern hemisphere (20°–90°S).



**Figure 5** Comparison of *AMSUA(REF)* with *BASELINE (NOSAT)* and *CONTROL* for (a) northern hemisphere (20°–90°N) and (b) southern hemisphere (20°–90°S).

◆ *EUCOS(REF)* which uses all satellite data and a reduced terrestrial network, i.e. the GCOS Upper Air Network (GUAN), GCOS Surface Network (GSN), and the buoys' network.

Figure 5 is similar to Figure 4 but for Period 2 and using *AMSUA(REF)* in place of *AMV(REF)*. The *EUCOS* experiments have not been run for this period.

For the northern hemisphere all experiments reach day 6 before the anomaly correlation drops to 0.75; this indicates the forecasts are of general good quality. When the anomaly correlation drops below 0.6 the forecasts are considered poor. In the southern hemisphere the *BASELINE* assimilations for both Period 1 and Period 2 are poor; their anomaly correlations reach 0.6 soon after day 5.

*EUCOS(REF)* is also shown for comparison with the satellite references (see Box B). With the addition of the remaining terrestrial observations the forecast improves by 8 hours at day 6 in the northern hemisphere. On the other hand, in the southern hemisphere, as expected, *EUCOS(REF)* is close to *CONTROL*.

**Impact of sensors**

To present the results of eleven sets of data assimilation experiment in a concise way is a somewhat daunting task. There are two sets of OSEs based on *AMV(REF)* and *AMSUA(REF)*. There is also a variety of variables and levels used for evaluation: 500 hPa geopotential height, relative humidity at 850, 500 and 200 hPa, and wind at 1000 and 200 hPa.

The results have been condensed into a series of bar graphs containing all experiments. Generally the sensors are ranked in order of increasing rms error for the first verified forecast range. Usually this ranking is maintained throughout the forecast, though there are some exceptions.

Generally all sensors impact in a positive way on some parameters but some sensors have a neutral or slightly negative impact on other parameters. The small negative impact, mostly noticed on the 500 hPa geopotential height parameter and when using *AMV(REF)* as a reference, may be due to the fact that the accuracy of the *AMV(REF)* temperature field is still not quite good enough to assimilate radiances that are mostly sensitive to moisture. This negative impact of some sensors is not generally found when *AMSUA(REF)* is used as a reference instead.

**500 hPa geopotential height**

The accuracy of the 500 hPa geopotential height forecast is an important and classical measure of forecast skill.

◆ *OSEs based on AMV(REF)*. Figure 6 shows the performance of all the OSEs as described in Tables 2 at days 2, 5 and 7. The largest impact can be seen in the southern hemisphere and is maintained throughout the full forecast range. Clearly the most important sensors are AMSU-A and AIRS followed by

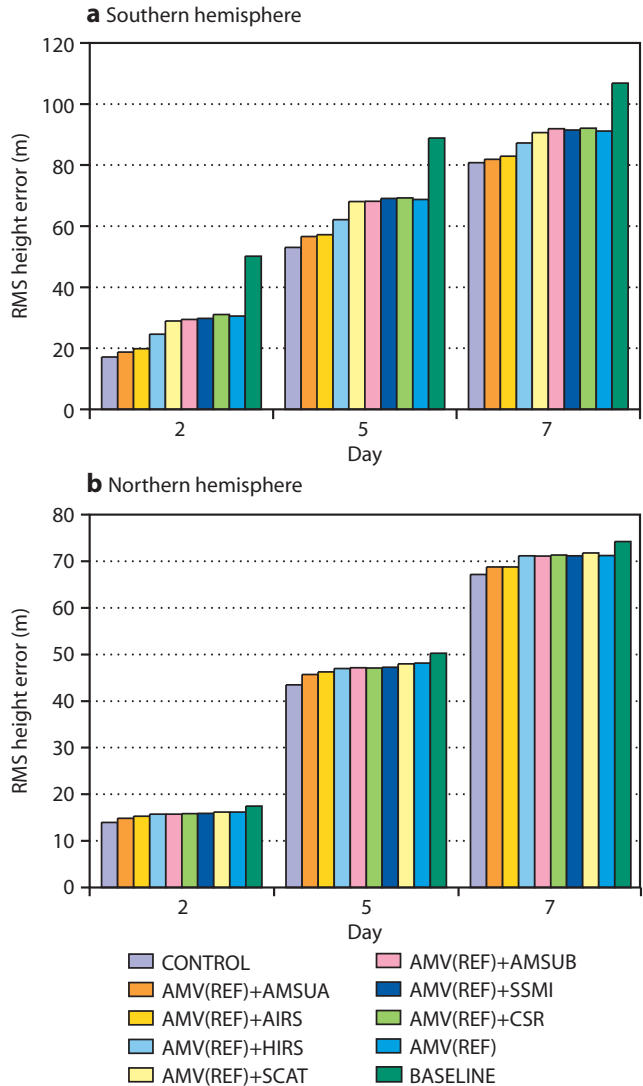


**Figure 6** Impact of all sensors (based on *AMV(REF)*) on 500 hPa geopotential height for (a) southern hemisphere (20°–90°S) and (b) northern hemisphere (20°–90°N).

HIRS. All other sensors have a relatively small impact; some sensors even show a small negative impact relative to *AMV(REF)* for this particular parameter. However, other scores are improved by these sensors (this is for example the case for the CSRs which improve the humidity scores). The impact in the northern hemisphere is similar to that in the southern hemisphere but smaller in magnitude.

◆ *OSEs based on AMSUA(REF)*. The performance of all the OSE experiments as described in Table 3 at days 2, 5 and 7 is shown in Figure 7. First of all, it is worth noticing that the relative difference for 500 hPa geopotential height between *AMSUA(REF)* and *CONTROL* compared to the relative difference between and *AMV(REF)* and its *CONTROL* is smaller, and therefore gives less margin to measure quantitatively the impact of individual sensors. However, the largest sensor impacts can still be seen in the southern hemisphere and these are maintained throughout the full forecast range. Clearly the most important sensors

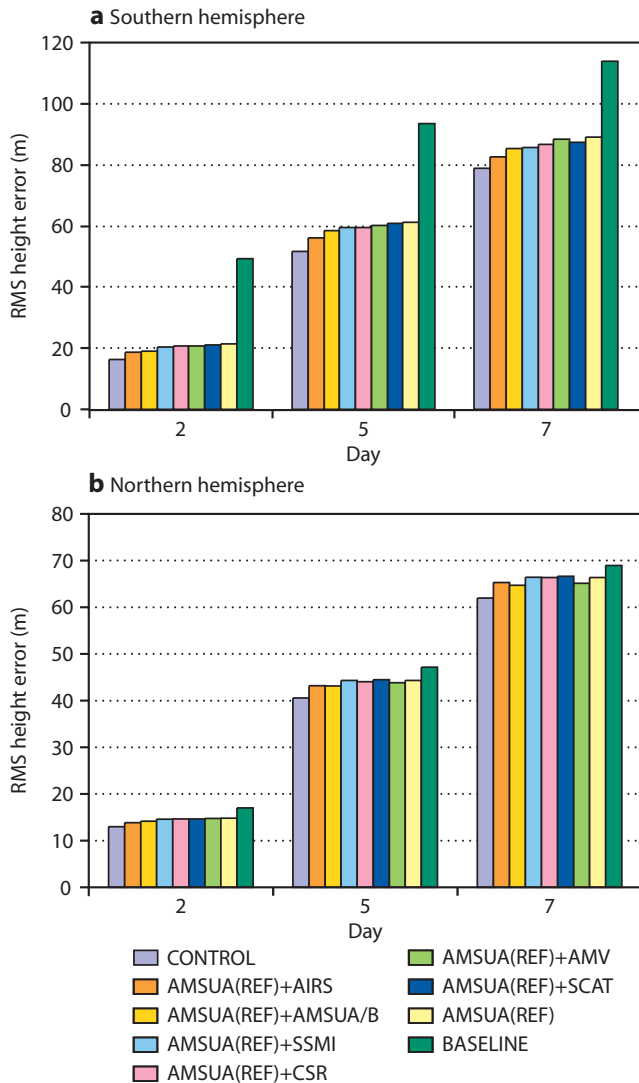


**Figure 7** Impact of all sensors (based on *AMSUA(REF)*) on 500 hPa geopotential height for (a) southern hemisphere (20°–90°S) and (b) northern hemisphere (20°–90°N).

are AIRS and the AMSU-A/B combination. All other sensors have a relatively small impact. In the northern hemisphere the impact of the sensors is similar but smaller in magnitude.

**850 hPa relative humidity**

Moisture forecasts, particularly in the tropics, tend to be less accurate than forecasts of mid-latitude geopotential height. After day 4, the moisture forecast becomes less dependent on the initial moisture conditions and the model moisture processes dominate. For this reason all the moisture validations are presented for days 1 to 3.

◆ **OSEs based on *AMV(REF)***. Figure 8(a) shows the performance of all the OSEs as described in Table 2 for the tropics. SSMI is the most important sensor at day 1 but by day 3 the impact is reduced and overtaken by that of AIRS. However the gap between the *CONTROL* and the *AMV(REF)+SSMI* at day 1 is much larger than the difference between *AMV(REF)+SSMI* and *AMV(REF)* suggesting it is the combination of all

sensors that is important rather than a single sensor. The impact in the northern hemisphere and southern hemisphere is similar to that in the tropics but smaller.

◆ **OSEs based on *AMSUA(REF)***. Figure 8(b) shows the performance of all the OSEs as described in Table 3 for the tropics where the impacts are the largest. In this set, *AMSUA(REF)+SSMI* now includes both clear-sky and rain/cloud affected radiances and SSMI is the most important sensor for low level humidity. However there is still a gap between the *CONTROL* and *AMSUA(REF)+SSMI*, which again suggests that it is the combination of all sensors that is important for improving the moisture analysis and forecasts rather than a single sensor. The impact in the northern hemisphere and southern hemisphere is similar but smaller in magnitude than in the tropics.

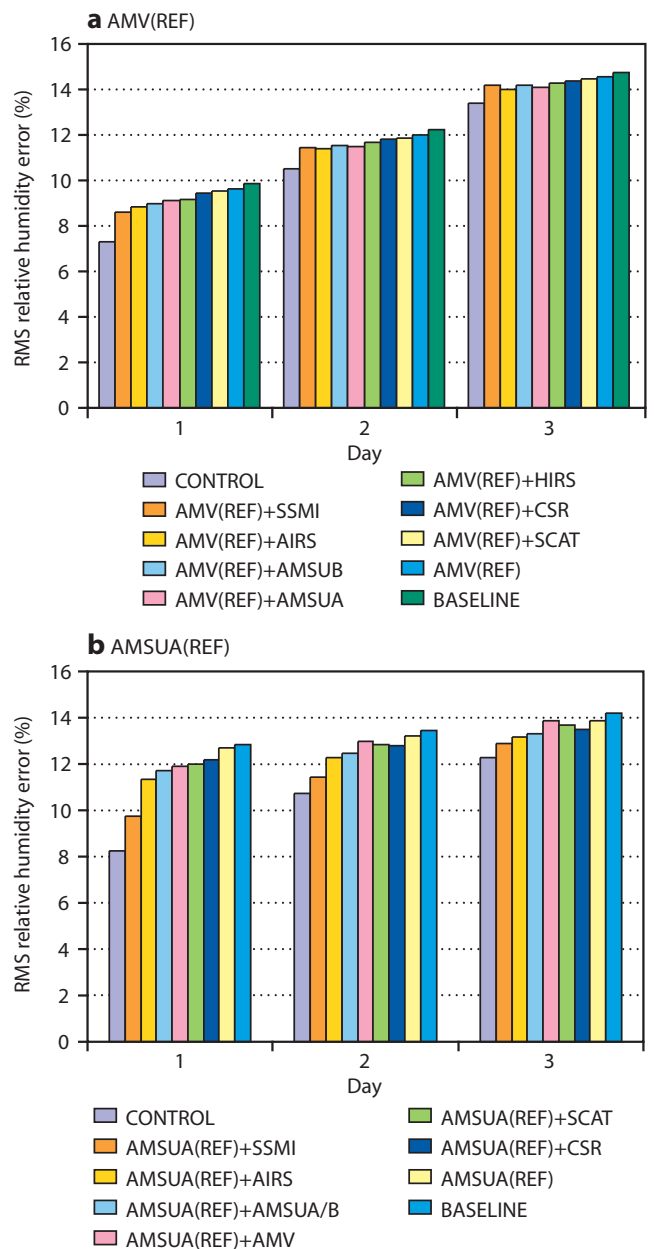


**Figure 8** Impact of all sensors on 850 hPa relative humidity for the tropics based on (a) *AMV(REF)* and (b) *AMSUA(REF)*.

1000 hPa wind

Wind forecasts in the tropics tend to be less accurate than in mid latitudes. In the tropics after day 4 the model wind forecast becomes less dependent on the initial conditions. Therefore all the wind validations presented here are for days 1, 2 and 3.

◆ **OSEs based on AMV(REF).** Figure 9(a) shows the performance of all the OSEs as described in Table 2. In the tropics SSMI is the most important sensor. However, at day 1 the gap between CONTROL and AMV(REF)+SSMI is much larger than the difference between AMV(REF)+SSMI and AMV(REF) suggesting again that it is the combination of all sensors that is important. The impact in the northern hemisphere and southern hemisphere is similar to that in the tropics but smaller in magnitude.

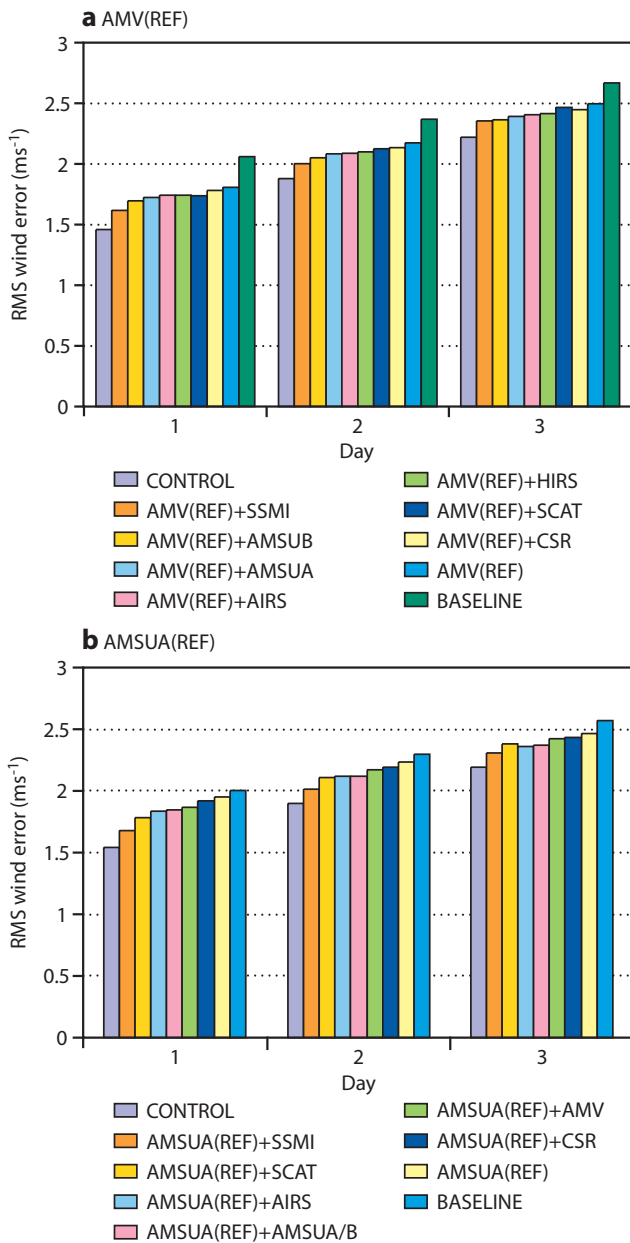


Figure 9 Impact of all sensors on 1000 hPa vector wind for the tropics based on (a) AMV(REF) and (b) AMSUA(REF).

◆ **OSEs based on AMSUA(REF).** Figure 9(b) shows the performance all the OSEs as described in Table 3. In the tropics SSMI is the most important sensor, though SCAT winds are also important in the early part of the forecast. However the gap between the CONTROL and AMSUA(REF)+SSMI suggests it is the combination of all sensors that is important. The impact in the northern hemisphere and southern hemisphere is similar but smaller in magnitude to that in the tropics.

Additional studies with AMV(REF)

Impact of MODIS AMVs

An experiment was run to evaluate the impact of the MODIS AMVs. This experiment is identical to AMV(REF) but with the MODIS AMVs removed. One can see that the impact of these AMVs on the 500 hPa geopotential height is very positive in the southern hemisphere (Figure 10(a)) and northern hemisphere (Figure 10(b)). The AMVs are clearly very important for observing the polar flow.

Comparison of AIRS with a combination of AMSUA-A and AMSUA-B

In the standard set of impact experiments using AMV(REF), Table 2, the AMV(REF)+AMSUA assimilation used all four AMSUA-A instruments. This is a somewhat unfair comparison if one wants to directly compare the impact

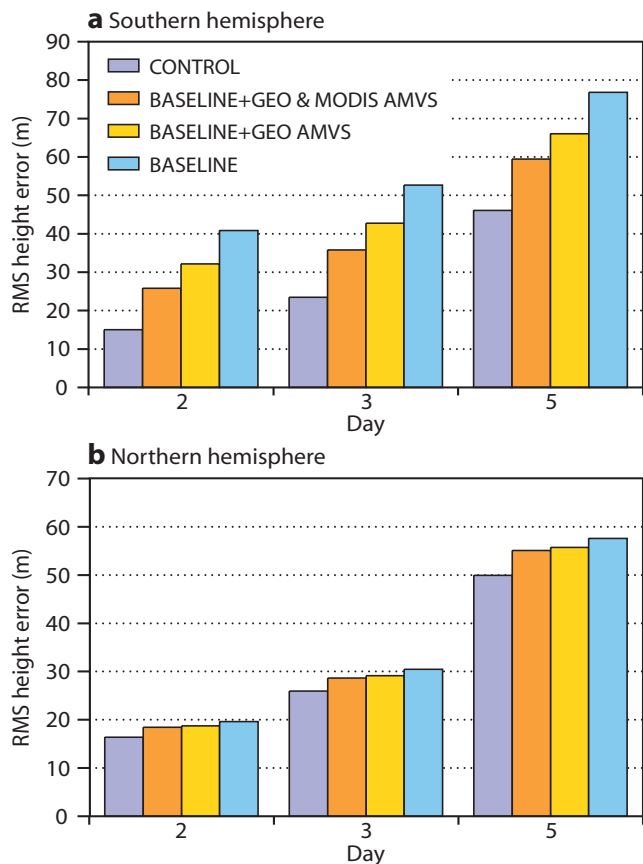
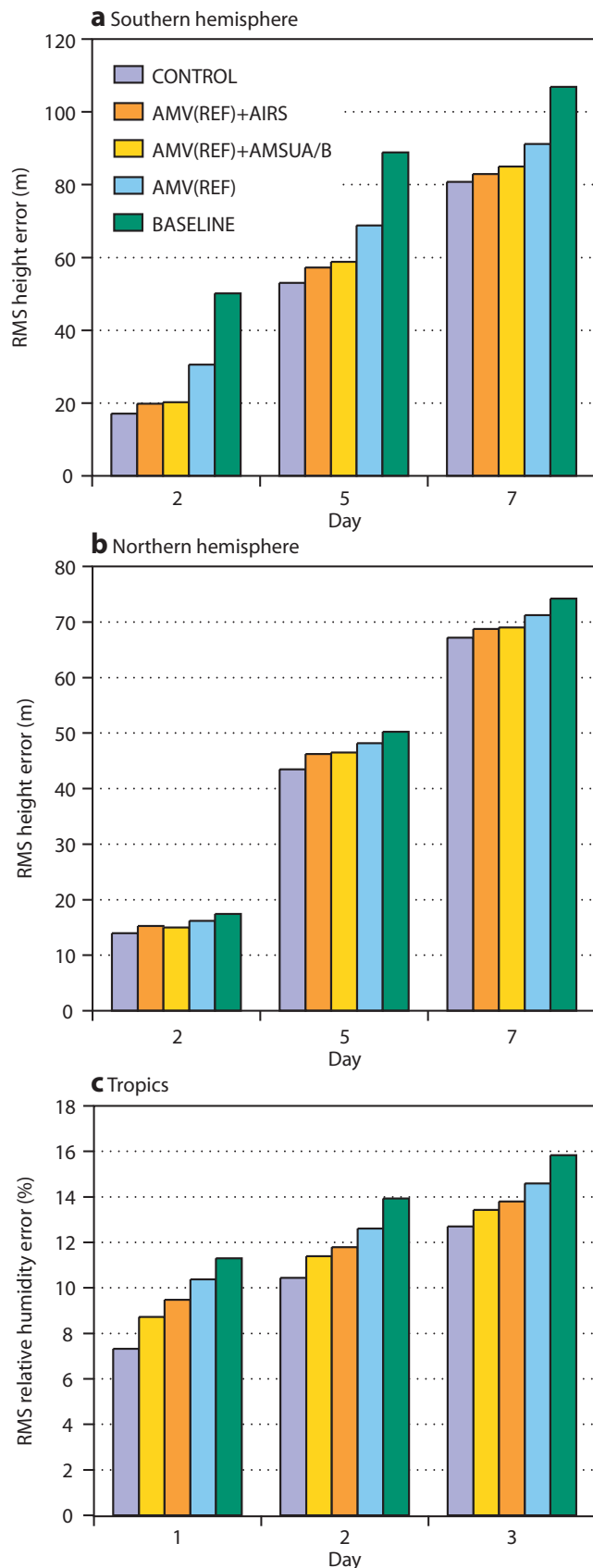


Figure 10 Impact of MODIS AMVs on 500 hPa geopotential height for (a) southern hemisphere (20°–90°S) and (b) northern hemisphere (20°–90°N).



**Figure 11** Comparison of AIRS with the two microwave instruments (AMSU-A and AMSU-B) on NOAA-16 for (a) 500 hPa geopotential height in the southern hemisphere, (b) 500 hPa geopotential height in the northern hemisphere and (c) 500 hPa relative humidity in the tropics.

of AIRS data with that of AMSU-A. The AIRS channels used in the operational assimilation are mostly sensitive to temperature and moisture (McNally et al., 2004). A microwave assimilation experiment was therefore run adding one AMSU-A/B combination to the *AMV(REF)*. This OSE was then compared with the *AMV(REF)+AIRS* assimilation referred to in Table 2. The results are shown in Figures 11(a) and 11(b).

In the southern hemisphere at day 2 the impact of AIRS and AMSU-A/B data on the geopotential height scores is similar but at days 5 and 7 the impact of the AIRS data becomes larger. However, the impact on tropical moisture, Figure 11(c), shows that AMSU-A/B data has a larger impact than AIRS in terms of the short-range forecast of tropical moisture.

**Additional studies with AMSUA(REF)**

*AIRS channel combinations*

For a number of reasons (including CPU time, memory size and file space constraints) the current operational system uses a reduced channel set for AIRS (and more recently IASI) radiances. The aim of this study was to explore which AIRS channels are the most important. Experiments have been run (summer only) by adding various AIRS channel combinations to the *AMSUA(REF)*, and also denying AIRS data from *CONTROL*. The results are shown in Figure 12 for 500 hPa geopotential height in the southern hemisphere. The respective performance of each scenario is consistent throughout the forecast range up to day 5.

When looking at the day 3 impact on the geopotential height at 500 hPa, one notices that:

- ◆ The positive impact of AIRS data can be seen from the differences between the data denial experiment and *CONTROL*. There is also a clear separation between *AMSUA(REF)* and *AMSUA(REF)+AIRS*.

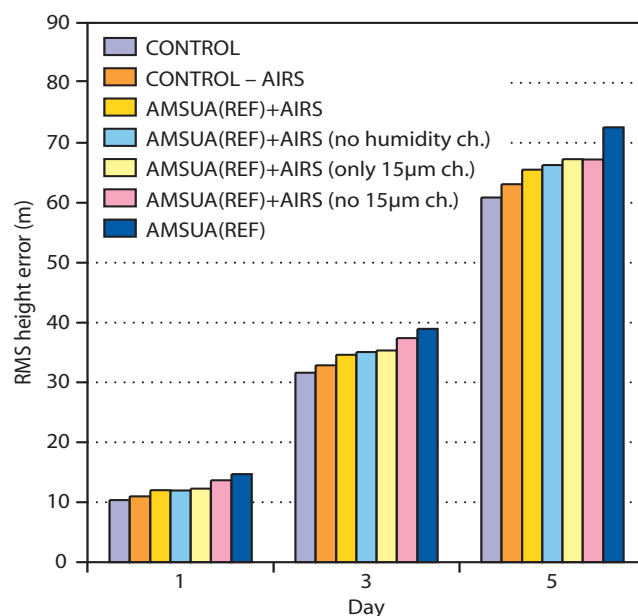


**Figure 12** Comparison of the impact of various AIRS channel combinations on 500 hPa geopotential height based on *AMSUA(REF)*.

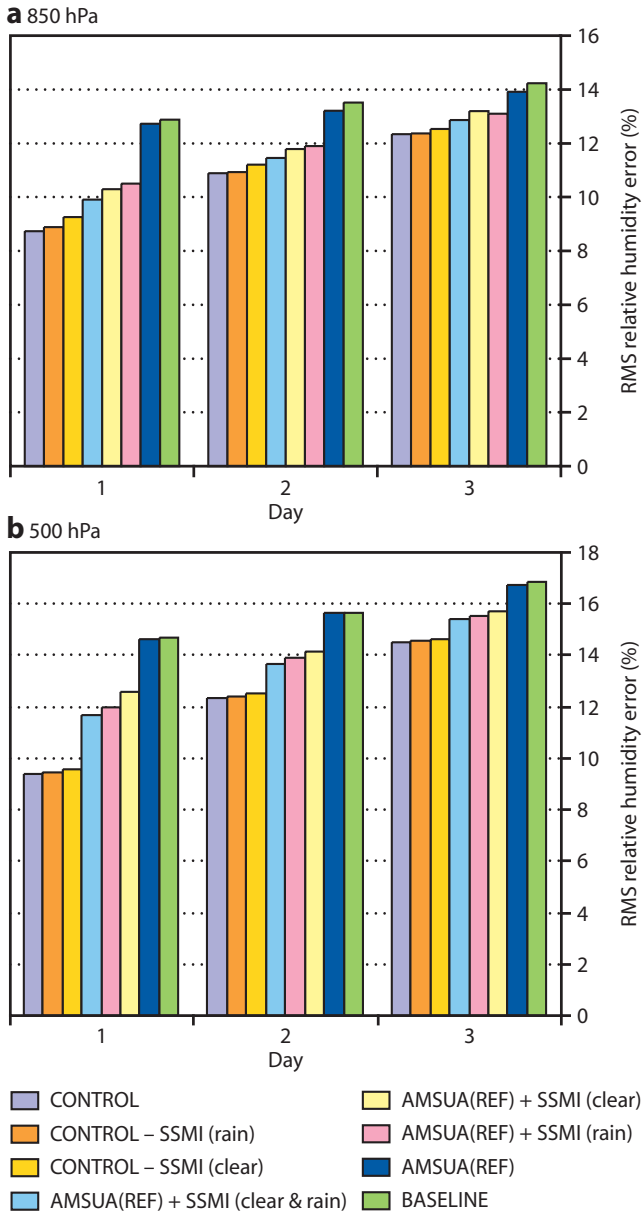


**Figure 13** Comparison of the impact of various SSMI usage configurations based on *AMSUA(REF)* for (a) 850 hPa relative humidity and (b) 500 hPa relative humidity.

- ◆ *AMSUA(REF)+AIRS* is close to the *AIRS* experiment not using humidity channels, indicating that *AIRS* humidity channels do not have a large effect on the geopotential height at 500 hPa.
- ◆ The fact that *AMSUA(REF)+AIRS* is close to the experiment using only the 15 micron channels from *AIRS* suggests that these channels contribute most to the impact of this instrument.

**Impact of the SSMI clear-sky and rain-affected radiances**

In addition to the *AMSUA(REF)* plus all SSMI data (clear-sky and rain affected observations, *Bauer et al., 2002, 2006a and 2006b*), *CONTROL* (all data) and *AMSUA(REF)* the following experiments have been performed to separate the effects of clear-sky and rain-affected SSMI radiances:

- ◆ *AMSUA(REF)* plus SSMI rain affected radiances.
- ◆ *AMSUA(REF)* plus SSMI clear-sky radiance radiances.
- ◆ *CONTROL* minus all SSMI (clear-sky and rain-affected) radiances.

Figure 13 shows the impact of denying and adding SSMI radiances (in the various configurations explained above) on the 850 and 500 hPa relative humidity forecast scores. The rain-affected radiances contribute more to the moisture forecast skill at 500 hPa whereas the clear-sky radiances are more important at 850 hPa. The experiment that combines both SSMI radiance types further improves the forecast. It is therefore clear that both types for SSMI radiances are important for the global moisture analysis.

**Impact of AVHRR AMVs**

During the study, a new experimental AMV product became available from CIMSS and it was decided to evaluate them in this OSE framework. These AMVs are produced from overlapping orbits from the AVHRR imager onboard the NOAA polar satellite series. Unfortunately this instrument does not have a water vapour channel like MODIS and this greatly reduces the amount of AMVs produced, particularly over the polar ice. The impact on mean scores is small but positive and can be best seen on the mean geographical rms forecast error difference with *AMSUA(REF)* for the 500 hPa geopotential height (Figure 14(a)). Very little impact is found in the northern hemisphere. For comparison a similar plot is shown when MODIS AMVs are assimilated instead (Figure 14(b)). The impact from the MODIS AMVs is similar to that of AVHRR AMVs over the Southern Ocean but extends further to the south over the polar ice.

**Overall assessment and further prospects**

All the space based sensors contribute in a positive way to the overall improvement of the ECMWF forecast system. Sensors like AMSU-A, AIRS and HIRS are clearly the most important for mass and wind forecasts. However the accuracy of the humidity forecast relies on AMSU-B/MHS, GEO CSRs and SSMI. The positive impact of AMVs (GEO and MODIS) and SCAT on the forecast is also clearly demonstrated.

At present, there are no plans to fly an instrument with MODIS-like water vapour channels on future polar satellites. This is a concern as the positive impact of MODIS AMVs in polar regions and mid-latitudes has clearly been demonstrated. The experiment using AVHRR derived AMVs show that their quality is similar to MODIS AMVs but the coverage is and will remain much poorer over the frozen regions due to a lack of water vapour channel on the instrument.

The studies also show that AIRS is the sensor that has the most impact on the mass field and experiments indicate that most of the impact comes from its 15 micron spectral band. Otherwise SSMI is vital for humidity analysis and the newly introduced cloud/rain effected SSMI radiances further improve the humidity analysis.

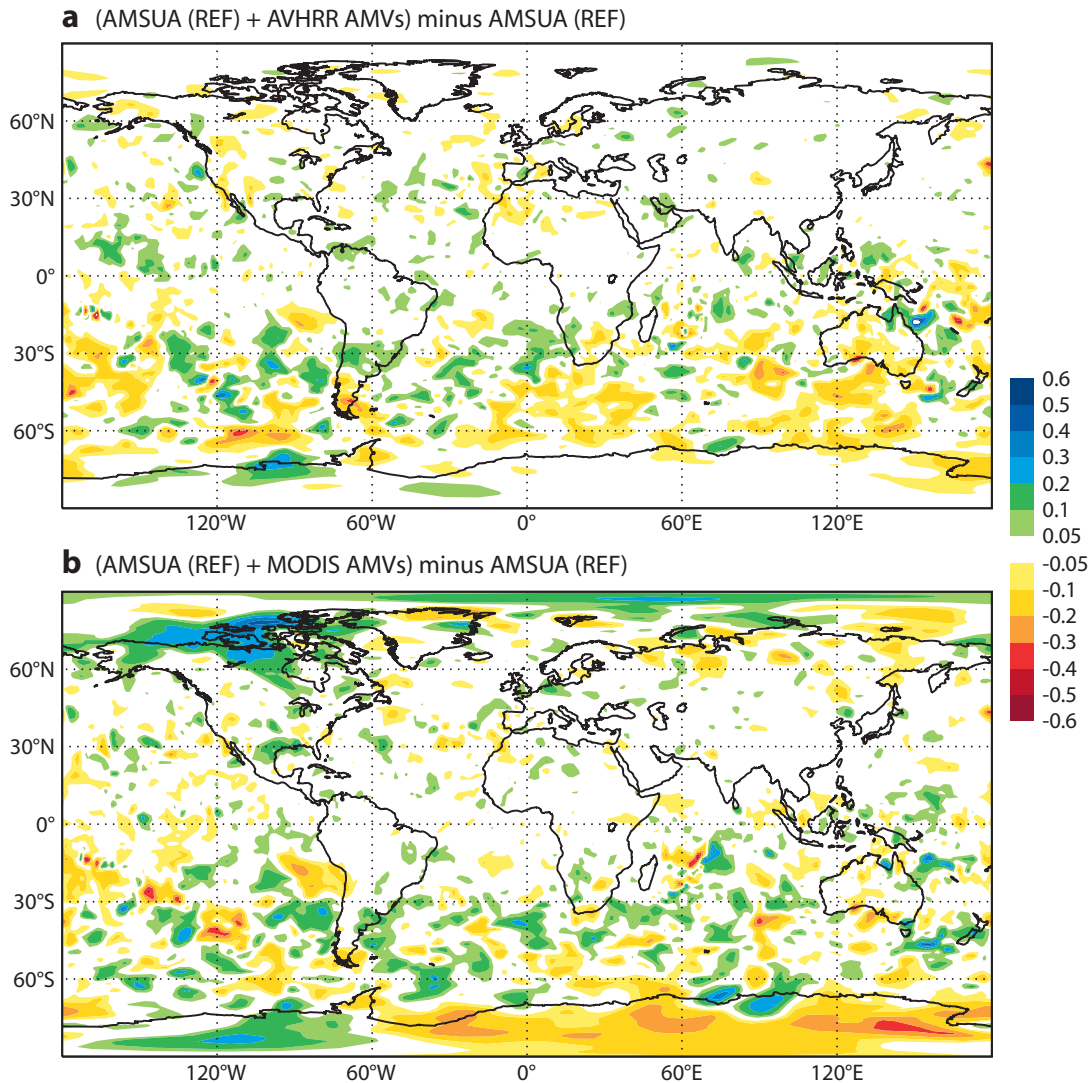


**Figure 14** Mean normalized 48-hour forecast error difference between (a) AVHRR AMVs and *AMSUA(REF)*, and (b) MODIS AMVs and *AMSUA(REF)* for the 500 hPa geopotential height.

These experiments confirm the crucial impact of satellite data on the performance of the ECMWF NWP system. Since the completion of the OSEs, the importance of satellite data has further increased with, for example, the implementation of GPS radio-occultation observations or more recently the introduction of IASI. On the scientific side, further changes are expected in the near future that include the use of more infrared and microwave radiances in cloudy and rainy conditions, and an improved use of all types of satellite radiances over land and sea-ice.

#### FURTHER READING

Andersson, E., R. Dumelow, H. Huang, J.-N. Thépaut & A. Simmons, 2004: *Space/Terrestrial Link – Outline study proposal for consideration by EUCOS Management* (available from EUCOS Secretariat).

Andersson, E., J. Pailleux, J.-N. Thépaut, J.R. Eyre, A.P. McNally, G.A. Kelly & P. Courtier, 1994. Use of cloud-cleared radiances in three/four-dimensional variational data assimilation. *Q.J.R. Meteorol. Soc.*, **120**, 627–654.

Bauer, P., G. Kelly & E. Andersson, 2002: SSM/I radiance assimilation at ECMWF. In *Proc. ECMWF/GEWEX Workshop on Humidity Analysis*, Reading, United Kingdom, ECMWF, 167–175. Available from European Centre for Medium-Range Weather Forecasts, Shinfield Park, Reading RG2 9AX, UK.

Bauer, P., P. Lopez, A. Benedetti, D. Salmond & E. Moreau, 2006a: Implementation of 1D+4D-Var assimilation of precipitation affected microwave radiances at ECMWF, Part I: 1D-Var. *Q.J.R. Meteorol. Soc.*, **132**, 2277–2306.

Bauer, P., P. Lopez, A. Benedetti, D. Salmond, S. Saarinen & M. Bonazzola, 2006b: Implementation of 1D+4D-Var assimilation of precipitation affected microwave radiances at ECMWF, Part II: 4D-Var. *Q.J.R. Meteorol. Soc.*, **132**, 2307–2332.

Bouttier, F. & G. Kelly, 2001: Observing-system experiments in the ECMWF 4D-Var data assimilation system. *Q.J.R. Meteorol. Soc.*, **127**, 1469–1488.

Kelly, G. 1997: Influence of observations on the operational ECMWF system. *Bulletin of WMO*, **46**, 336–341.

Kelly, G., A. McNally, J.-N. Thépaut & M. Szyndel, 2004. Observing System Experiments of all main data types in the ECMWF operational system. In Proc. of the Third WMO Workshop on the Impact of Various Observing Systems on NWP, Alpbach, Austria, 9–12 March 2004.

McNally, A.P., P.D. Watts, J.A. Smith, R. Engelen, G. Kelly, J.-N. Thépaut & M. Matricardi, 2004: The assimilation of AIRS

radiance data at ECMW. In *Workshop on Assimilation of High Spectral Resolution Sounders in NWP*, 28 June–1 July 2004, Shinfield Park, Reading 73–88.

Thépaut, J.-N. & G.A. Kelly, 2007. Relative contributions from various terrestrial observing systems in the ECMWF NWP system. *Final Report EUCOS*, 23 June 2007 (available from EUCOS Secretariat).

## Impact of airborne Doppler lidar observations on ECMWF forecasts

MARTIN WEISSMANN, CARLA CARDINALI

THE WIND field over oceans is still poorly observed. Single-level wind measurements are provided at the surface by buoys, ships and satellite scatterometers, while aircraft observe wind mainly at the cruise level along the air traffic corridors. Wind profiles are only provided by a small number of radiosondes launched from ships. Satellite cloud-drift winds are numerous, but they have fairly large errors due to inaccurate height assignment. In such a framework, Doppler wind lidar offers a great opportunity to measure the wind field either globally with a polar-orbiting satellite or regionally when mounted on aircraft.

During the Atlantic THORPEX Regional Campaign (A-TReC) in autumn 2003, the airborne Doppler lidar of the Deutsches Zentrum für Luft- und Raumfahrt (DLR) was used to observe wind profiles over the Atlantic Ocean. In eight flights, the system measured a total of 1,600 profiles that were used experimentally in the global assimilation system at ECMWF. These lidar observations had a significant impact on the analyses as well as on forecasts due to their high accuracy and spatial resolution. On average, the measurements reduced the forecast error of geopotential height for days 2–4 over Europe by 3%. Furthermore, forecast errors of wind, temperature and humidity fields over Europe were reduced. This is a promising result, considering that observations have been gathered from only 28.5 flight hours in a two-week period. Dropsondes released in the same area where the Doppler lidar was operating showed good agreement in terms of measured winds, but smaller analysis impact and less reduction of the forecast error. A detailed assessment of the experiments can be found in *Weissmann & Cardinali (2007)*.

### AFFILIATIONS

**Martin Weissmann:** Institut für Physik der Atmosphäre, DLR Oberpfaffenhofen, Postfach 1116, 82230 Weßling, Germany  
**Carla Cardinali:** ECMWF, Shinfield Park, Reading, RG12 9AX, UK

### The airborne Doppler lidar system

The principle of Doppler lidar is in many ways similar to that of Doppler radar except that a lidar emits pulses of laser light instead of radio waves. The airborne DLR Doppler lidar system measures wind profiles beneath the aircraft using the velocity-azimuth display (VAD) technique. The instrument performs a conical step-and-stare scan around the vertical axis at 20° off nadir. At 24 different azimuth angles, the lidar emits 500 or 1,000 laser pulses at a wavelength of ~2.02 µm and measures the backscatter signal from atmospheric aerosols. The Doppler shift of the backscatter signal is proportional to the velocity component in the pointing direction; this is the line-of-sight (LOS) velocity. Wind profiles are usually derived from 24 or 96 LOS profiles. The vertical resolution of the profiles is 100 m.

Combined with the movement of the aircraft the conical scanning leads to a cycloid scan pattern beneath the aircraft and the derived winds are averaged along this scan. This horizontal averaging is the main advantage of airborne Doppler lidar observations compared to in-situ observations as it makes the data more representative of the wind in a model grid box. The horizontal width of the scan pattern is up to ~7 km. During A-TReC, the horizontal length of one scanner revolution was usually ~10 km.

### Lidar observations during A-TReC

The airborne Doppler Lidar operated from the DLR Falcon aircraft during eight flights between 14 and 28 November 2003 (Figure 1). Four of these flights were part of targeted campaigns. These observations were guided by sensitive area calculations carried out at ECMWF and other meteorological services using singular vectors and ensemble methods. The other four flights were designed for other objectives, but were also used for the impact study. Several people from DLR made a vital contribution to the collection of data: Andreas Dörnbrack organized the field campaign, and Stephan Rahm and Rudolf Simmet were responsible for the unique lidar measurements. Milan Dragosavac (ECMWF) converted the lidar data to BUFR format so that it could be assimilated in the ECMWF system.

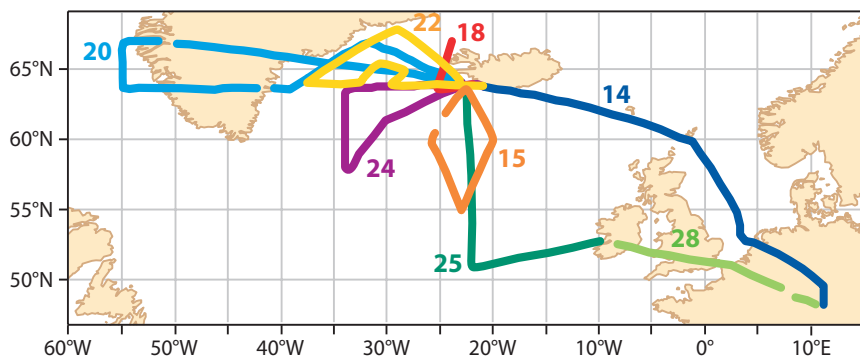


**Figure 1** Flight tracks of all flights during A-TReC. Numbers indicate the date of the flights in November 2003.

The data was processed with a horizontal resolution of ~10 km (one scanner revolution) and in parallel also with ~40 km (four scanner revolutions) to increase the measurement coverage and to reduce representativeness errors. The 10 km dataset consists of ~1,600 vertical profiles (~40,000 observations) and the 40-km dataset contains ~400 profiles (~15,000 observations). The vertical cross-section along the aircraft flight track accounts for 36% and 54% data coverage for the 10 km and 40 km resolution, respectively. Missing values in the data are either due to clear air with low aerosol content or to optically thick clouds that cannot be penetrated by the lidar. The number of measurements during the two weeks was fairly evenly distributed between the ground and 10.5 km altitude, the maximum aircraft flight level.

The standard deviation of the instrumental error was determined to be in the range of 0.75–1.0 ms<sup>-1</sup> through an intercomparison of collocated dropsonde and lidar measurements. The total error for the assimilation of such measurements (instrumental and representativeness errors) was estimated to be 1.0–1.5 ms<sup>-1</sup> for all model levels. This is smaller than the errors of all current routine observations: at ECMWF the error standard deviation of 1.8–3.0 ms<sup>-1</sup> is assigned to radiosonde and dropsonde wind observations, 2.5–3.4 ms<sup>-1</sup> to aircraft measurements, and 2.0–5.7 ms<sup>-1</sup> to satellite cloud-drift winds.

A detailed description of the intercomparison of lidar and dropsonde measurements can be found in Weissmann et al. (2005) or online at [www.pa.op.dlr.de/natrec/](http://www.pa.op.dlr.de/natrec/). These sources of information also provide a comprehensive overview of the lidar measurements during A-TReC and a full explanation of the airborne Doppler lidar system.

**Experimental setup**

Experiments were performed using the ECMWF Model at T511L60 resolution with a 12-hour window 4D-Var. The lidar observations were assimilated as aircraft in-situ observations, but with reduced observation errors. The assimilation of aircraft observations includes a first-guess check eliminating values whose background departures exceed five times that expected. The meas-

urements are thinned to the model resolution to avoid potential imbalances. After the first-guess check, a variational quality control (VarQC) is performed in the minimization procedure to decrease the weight of remaining doubtful observations.

Six experiments were conducted as outlined in Table 1. The control run (*Control*) used all routine observations. All other experiments assimilated either lidar or dropsonde observations in addition to the routine observations. The exper-

iment *1Rev* assimilated lidar wind profiles at a horizontal resolution of ~10 km (the standard resolution of the lidar measurements). Two experiments (*Median* and *4Rev*) were performed with lidar observations horizontally averaged to ~40 km. The purpose of *Median* and *4Rev* was to investigate how much the representativeness of the measurements increases by averaging the data horizontally to the model resolution.

In all these experiments an error standard deviation of 1 ms<sup>-1</sup> was assigned to the lidar data at all vertical levels. This error was derived by an intercomparison of collocated lidar and dropsonde measurements, which showed that there is no significant correlation of accuracy and height (Weissmann et al., 2005). The derived error assumes a continuous lidar measurement through a grid box, whereas in reality there were gaps in the measurements due to low aerosol concentrations or clouds. Therefore, the experiment *4RStd* was performed using the same pre-processed lidar data as *4Rev*, but with an error of 1.5 ms<sup>-1</sup> to take gaps in the observations into account.

Experiment	Period	Measurements and characteristics of experiments
<b>Control</b>	17 October–15 December	All measurements of the operational analysis without special A-TReC data (dropsondes, AMDAR, etc.)
<b>1Rev</b>	14–30 November	Lidar wind from one scan revolution, horizontal resolution ~10 km, lidar STD = 1 ms <sup>-1</sup>
<b>Median</b>	14–30 November	Median of lidar winds from one scan revolution, horizontal resolution ~40 km, lidar STD = 1 ms <sup>-1</sup>
<b>4Rev</b>	14–30 November	Lidar wind from four scan revolutions, horizontal resolution ~40 km, lidar STD = 1 ms <sup>-1</sup>
<b>4RStd</b>	14–30 November	Same lidar measurements as in 4Rev, but higher measurement error with lidar STD = 1.5 ms <sup>-1</sup>
<b>Drops</b>	14–30 November	Dropsonde wind and temperature measurements, 97 sondes, dropsonde STD = 2–3 ms <sup>-1</sup>

**Table 1** Overview of experiments. The STD refers to the assigned standard deviation of the wind error.

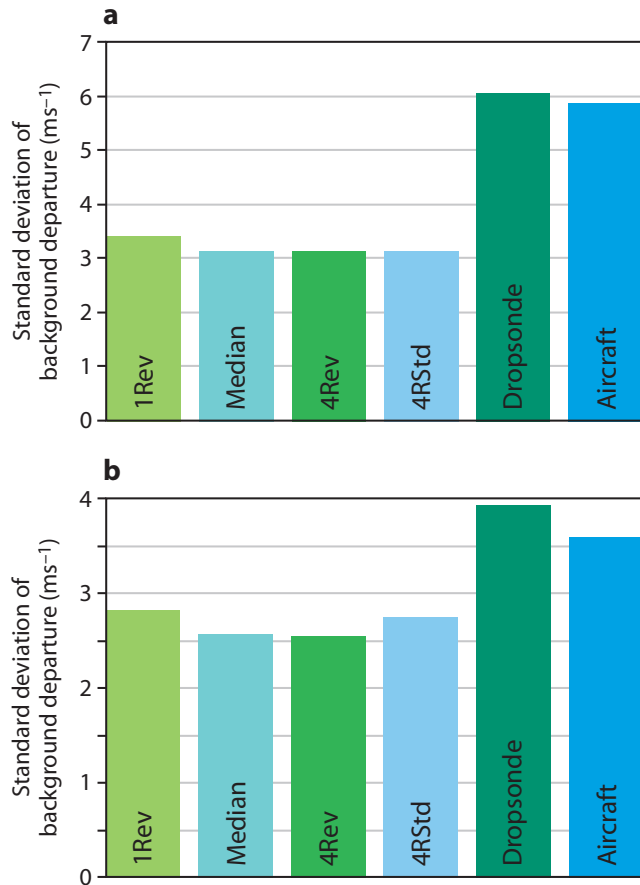


**Figure 2** Standard deviations of (a) background departures of all measurements and (b) background departures of observations that are not discarded by the first-guess check or VarQC. The statistics for aircraft and dropsonde measurements are shown for 4RStd and for the area 50°N–70°N, 40°W–15°W (main lidar operating area).

The experiment *Drops* assimilated 97 dropsondes (wind and temperature profiles) released on ten flights in the same period. About half of the dropsondes coincided with lidar measurements. The flight time for the dropsonde observations was similar to that for the lidar measurements. This makes the lidar and dropsonde experiments comparable in terms of observational costs. All experiments were run from 14 to 30 November 2003.

**Analysis impact**

**Assimilation statistics**

To investigate the performance of Doppler lidar measurements in the analysis, their background departures from the eight analyses with lidar measurements are sampled and compared to the background departures of aircraft and dropsonde measurements in the same area and at the same time (Figure 2). The variability of lidar background departures is smaller than that of aircraft and dropsonde measurements in the same region. This confirms that lidar winds are more representative of the wind for each model grid box.

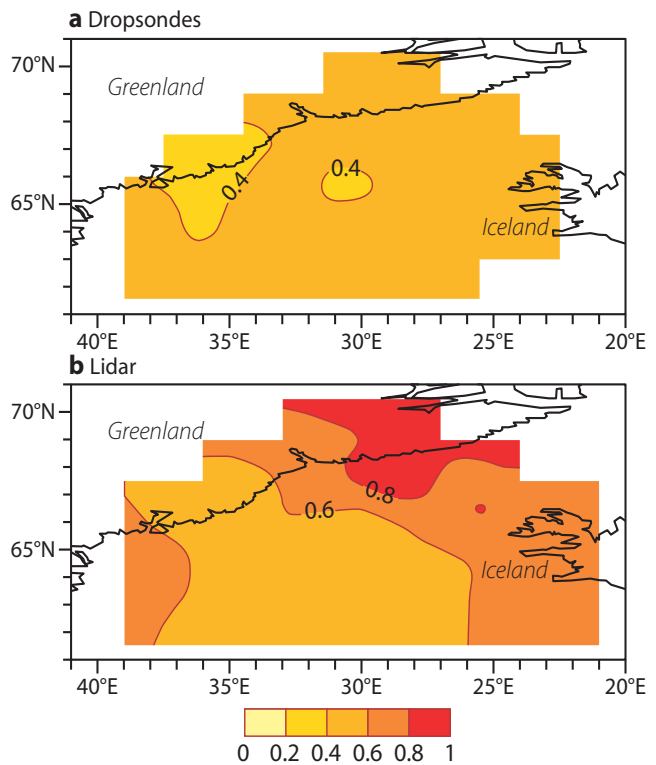
The statistics show an improved representativeness of the observations by averaging the measurements

towards the model resolution: on average, the standard deviation of the lidar background departures is about 0.3 ms<sup>-1</sup> smaller in the experiments with averaged data (*Median*, *4Rev*) than in the experiment with a 10 km resolution (*1Rev*). There are no significant differences between *Median* and *4Rev*, and at this stage it is not possible to determine which averaging method is best.

**Influence of observations**

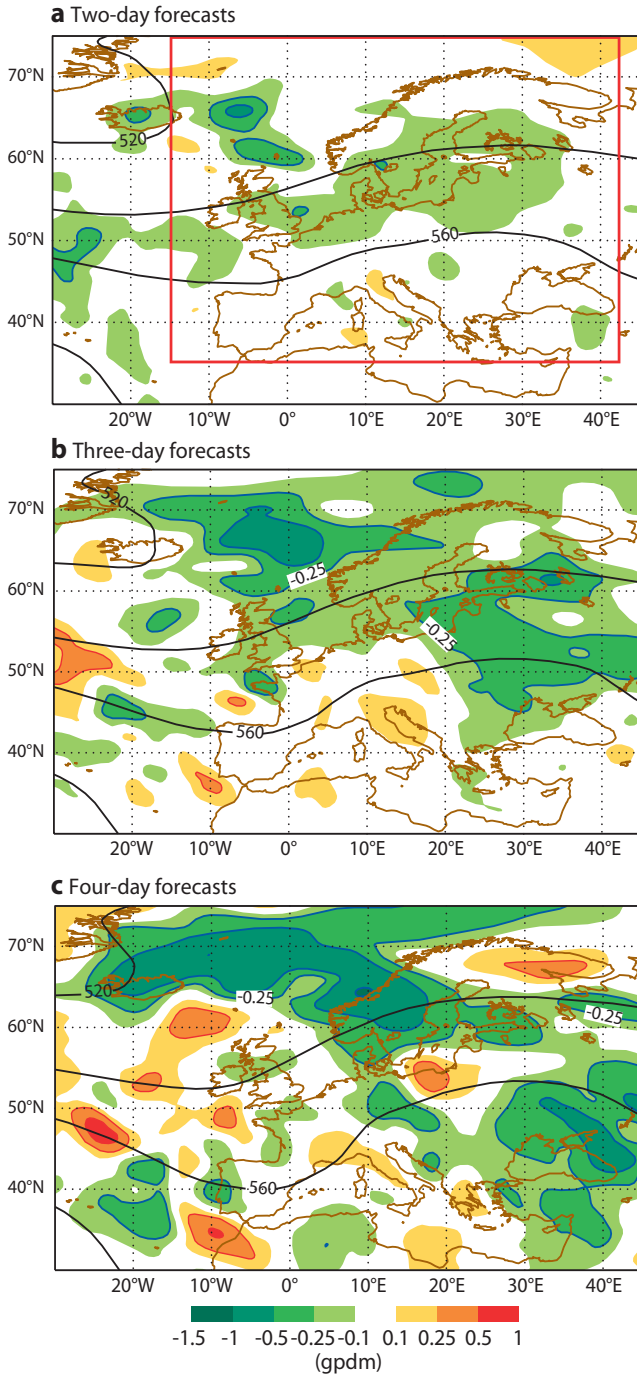
The influence of observations in the analysis can be calculated during the minimization by finding the diagonal elements of the influence matrix (*Cardinali et al.*, 2004). When the influence is 0, the analysis at the observation location is affected only by the background value (or pseudo-observation), while 1 means that only the observation counts in the final estimation at that location.

Figure 3 shows the vertically averaged influence of dropsonde and lidar observations on 22 November 2003. The influence of both observation types is high because the measurements were taken in a data-sparse sensitive region. The mean influence of dropsonde and lidar wind observations is 0.45 and 0.63, respectively. In comparison, the mean observation influence of operational radiosondes in the northern hemisphere extratropics is ~0.3, and the mean influence of aircraft measurements and cloud-drift winds is 0.15 (*Cardinali et al.*, 2004).



**Figure 3** Vertically averaged observation influence on 22 November 2003 for (a) dropsonde wind measurements from *Drops* and (b) lidar wind measurements from 4RStd. Numbers close to one indicate that the analysis is primarily based on the measurements, whereas numbers close to zero mean that the analysis is close to the background field.

The mean lidar observation influence is 40% larger than the mean influence of dropsonde wind measurements. Additionally, the number of lidar observations is about twice as large as the number of dropsonde observations because the horizontal resolution is higher for the lidar. This leads to an information content that is nearly three times higher for the lidar than for the dropsonde observations.



**Figure 4** Difference of the root mean square errors of the geopotential height at 500 hPa (gpdm) between *4RStd* and *Control* for (a) two-day forecasts, (b) three-day forecasts and (c) four-day forecasts between 15 and 28 November 2003 (28 forecasts). Negative values indicate a reduction of the forecast error. The box in (a) shows the verification area “Europe” used in this study.

**Forecast impact**

Figure 4 shows the difference in terms of root mean square forecast error of 500 hPa geopotential height (*Z*) between *4RStd* and *Control* for the period 15–28 November 2003. There is a clear reduction of the two-day forecast error over the Atlantic Ocean and Northern Europe. At day 3 the reduction increases and propagates further to the east. The four-day forecast error also decreases with the lidar measurements and the main reduction of forecast errors is located over the Middle East, and Northern and Eastern Europe. The improvement of one-day forecasts (not shown) was fairly small and mostly restricted to the Atlantic Ocean.

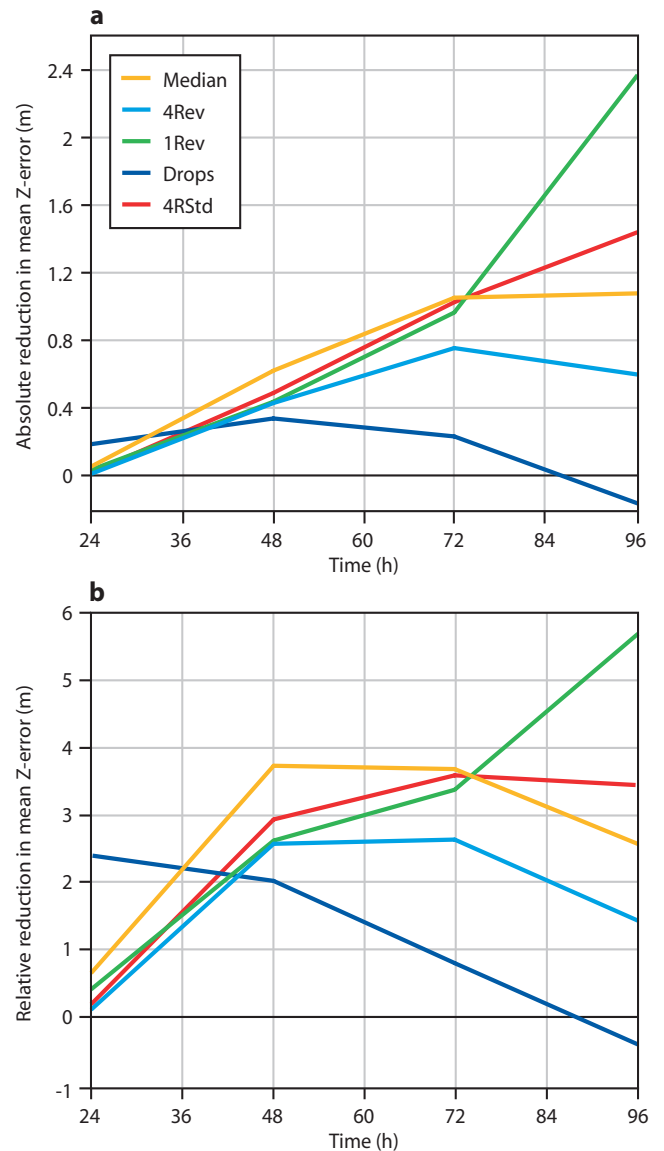


**Figure 5** Mean reduction of errors of the geopotential height at 500 hPa over Europe in different experiments compared to *Control*: (a) absolute reduction in metres and (b) relative reduction as a percentage of the mean error of *Control*. Positive values correspond to a smaller error in the experiment than in *Control*. The forecast error is averaged over all forecasts between 12 UTC on 14 November and 12 UTC on 28 November 2003 (29 forecasts). The verification area (“Europe”) is shown in Figure 4(a).

In order to quantify the impact, the forecast error is averaged for Z, wind and humidity for all levels over a box 35°N–75°N and 15°W–42.5°E (see Figure 4) and over 29 forecasts in the period of the lidar deployment. All experiments with lidar data show a Z-error reduction of the forecasts for days 1–4 over Europe compared to *Control* (Figure 5). The experiments *Median* and *4Rev* do not have smaller forecast errors than *1Rev*, although they show better departure statistics. At this stage it is not possible to explain why *1Rev* shows the largest improvement of all experiments at day 4.

The Z-error reduction increases with forecast time up to ~2 m for the four-day forecast. The increase is roughly proportional to the increase of forecast errors, and consequently the relative reduction of Z-errors remains fairly steady around 3% for the forecasts for days 2–4. On average about 60% of the 29 forecasts improved. The spread between the different lidar experiments increases with time indicating the uncertainty due to the small sample of 29 forecasts. The impact after five days is not significant. A larger data sample would be necessary to investigate the long-term impact.

In many experiments the reduction of the Z-error in the forecast is largest in the upper troposphere (Figure 6). The maximum reduction of all experiments is 3 m at 300 hPa for the four-day forecast. The impact extended vertically up to 100 hPa by the background covariance matrix, which is well above the highest lidar measurements at ~250 hPa. The maximum relative reduction of the Z-error for days 2–4 was up to 6%.

The experiment *Drops* also shows a reduction of the Z-error over Europe, mainly at days 1 and 2. At day 3 the reduction is fairly low and at day 4 some degradation above 700 hPa is observed. In general, experiments with lidar data show a larger and more sustained reduction of the forecast error than *Drops*, which is consistent with their larger impact on the analysis.

Wind errors decrease in a similar way as the Z-errors (Figure 7(a)). The relative reduction of wind errors in the troposphere is in the range 0.4–3.3%, which is slightly smaller than the reduction of Z-errors. Furthermore, the lidar wind measurements improve the accuracy of the humidity forecasts (Figure 7(b)) as an improved forecast of the wind and Z-field also leads to a more accurate forecast of humidity structures. The magnitude of the reduction is in the range 0–2%. The reduction of forecast errors of humidity for days 3–4 show maxima at 700 and 850 hPa that are presumably related to an improved prediction of frontal systems.

**To sum up**

Despite recent advances in the use of satellite observations, there is a drastic shortage of wind measurements over the oceans. This is a major deficiency in NWP as wind information has been shown to be of particular importance for representing dynamical fields in the forecast (*Cress & Wergen, 2001*). Thus, Doppler lidar measurements with their high accuracy and high resolution are a promising source of information to reduce errors in NWP models.

For the first time, airborne Doppler wind lidar observations were assimilated in a global model in the framework of A-TReC. The experiments confirmed that airborne lidar observations are more representative of the wind in a model grid box. Thus the resulting assigned observation error variability (instrumental and representativeness error) is about half that of most conventional observations. The mean lidar observation influence (i.e. the impact on the analysis) is found to be 40% higher than the influence of dropsonde wind measurements. Furthermore, it is shown that lidar wind observations have a significant impact on analysis and forecast errors.

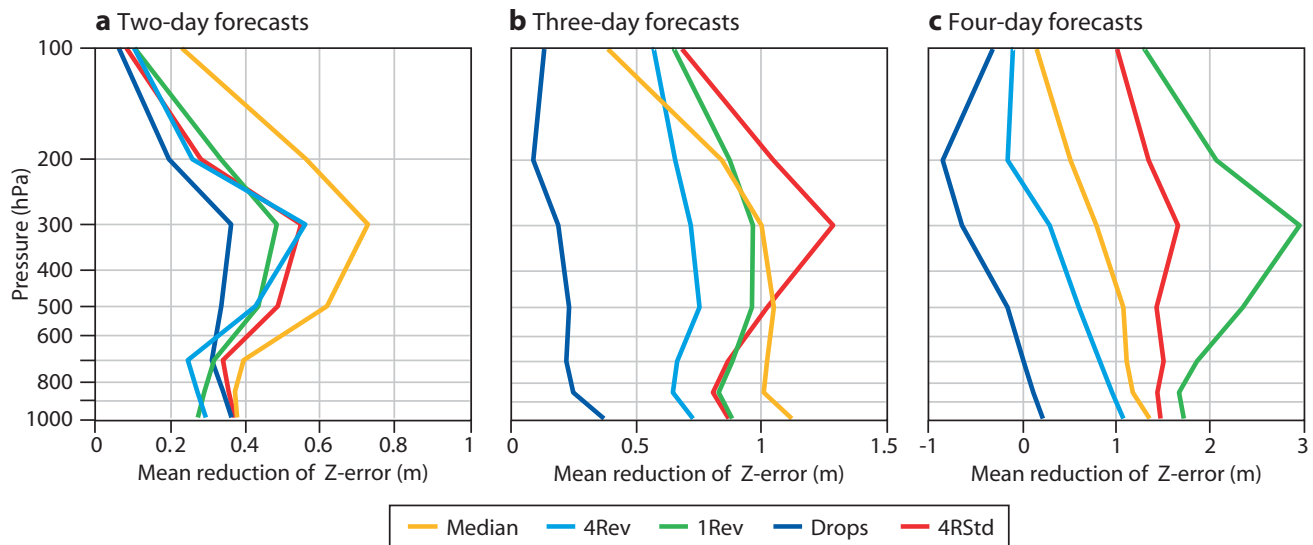


**Figure 6** Vertical profile of the mean reduction of the errors of the geopotential height over Europe for (a) two-day forecasts, (b) three-day forecasts and (c) four-day forecasts. The mean reduction was calculated in the same way as in Figure 5 for all 29 forecasts between 14 and 28 November 2003.

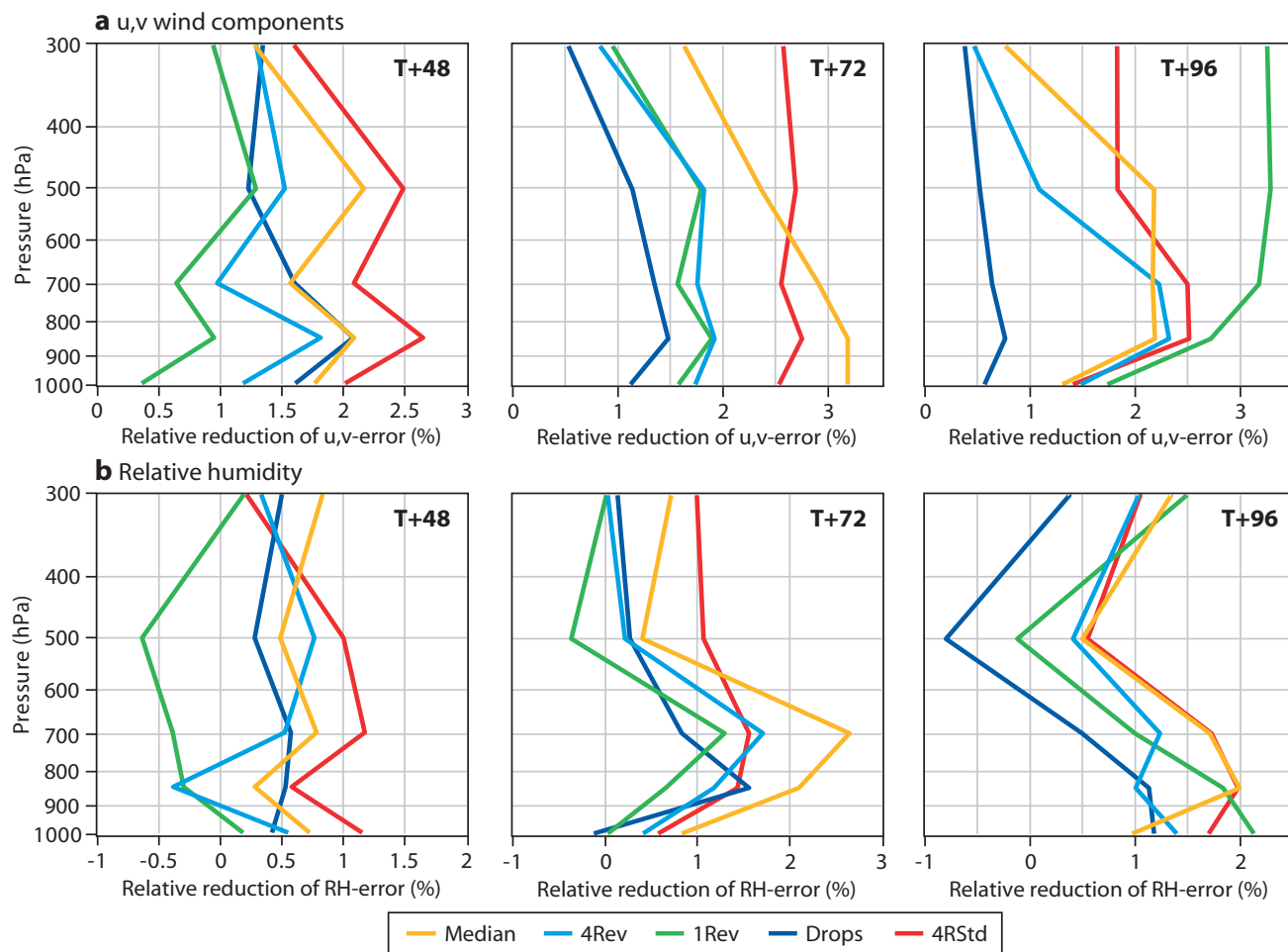


**Figure 7** Mean relative reduction of forecast error for (a) u, v wind components and (b) relative humidity over Europe: (left) two-day forecasts, (middle) three-day forecasts and (right) four-day forecasts. All values are in percent of the mean forecast error in the period of 14 to 28 November 2003. The relative reduction was calculated in the same way as in Figure 5, but for humidity and the wind components instead of geopotential height.

The experiment assimilating vertical profiles of wind and temperature from dropsondes for the same period shows only a mean reduction of ~1%, which is consistent with the smaller analysis impact of these observations compared to lidar data. Keeping in mind that the cost of lidar observations is comparable to the cost of dropsondes for the same flight time, the results given here show the potential of the airborne Doppler lidar for future observational campaigns.

**Future outlook**

Our results underline the importance of additional wind measurements over the oceans and demonstrate the potential of Doppler lidars. These findings support the high expectations for the satellite-based Doppler lidar ADM-Aeolus, which is planned to be launched in 2008 by the European Space Agency (ESA) (Stoffelen et al., 2005). ADM-Aeolus will provide a global coverage (3,000 profiles of LOS velocity per day), but the accuracy of ADM-Aeolus will only be half that of the airborne lidar and the vertical resolution is 500–1,000 m instead of 100 m. Given these differences, mounting Doppler lidars on commercial aircraft to provide wind profiles

over oceans with high accuracy and high resolution should be investigated.

Specific investigations of the impact of lidar data in the verification regions established by the targeting techniques will be carried out in subsequent studies. Furthermore, sensitivity studies are planned that investigate the impact of data accuracy, horizontal and vertical resolution, and data thinning. Experiments on the impact of differential absorption lidar (DIAL) water vapour measurements from different campaigns started recently in collaboration between DLR and ECMWF.

In the summer of 2007 the wind and the water vapour lidar system of DLR operated simultaneously on one aircraft for the first time. This configuration will be deployed during several field campaigns and is expected to provide a large dataset of collocated wind and water vapour observations for investigating the potential of lidars for the future observing system. In the near future research activities with airborne lidars will primarily focus on the THORPEX Pacific Asian Regional Campaign (T-PARC) in the second half of 2008, but a European THORPEX campaign is coming up in the time-frame of 2010/2011.

FURTHER READING

Cardinali, C., S. Pezzulli & E. Andersson, 2004: Influence-matrix diagnostic of a data assimilation system. *Q.J.R. Meteorol. Soc.*, **130**, 2767–2786.

Cress, A. & W. Wergen, 2001: Impact of profile observations on the German Weather Service’s NWP system. *Meteorol. Zeitschrift*, **10**, 91–101.

Stoffelen, A., J., Pailleux, E. Källén, J.M. Vaughan, L. Isaksen, P. Flamant, W. Wergen, E. Andersson, H. Schyberg, A. Culoma, R. Meynart, M. Endemann, M. & P. Ingmann: 2005: The Atmos-

pheric Dynamics Mission for global wind field measurement. *Bull. Am. Meteorol. Soc.*, **86**, 73–87.

Weissmann, M., R. Busen, A. Dörnbrack, S. Rahm & O. Reitebuch, 2005: Targeted observations with an airborne wind lidar. *J. Atmos. Ocean. Technol.*, **22**, 1706–1719.

Weissmann, M. & C. Cardinali, 2007: The impact of airborne Doppler lidar measurements on ECMWF forecasts. *Q.J.R. Meteorol. Soc.*, **133**, 107–116.

## New Automated Tape Library for the Disaster Recovery System

NEIL STORER

ECMWF recently replaced the Automated Tape Library (ATL) in the Disaster Recovery System (DRS) Building. In doing so it maintained the requirement that the specific tape media used by the DRS to hold secondary copies of the data should be different from that used by the Data Handling System (DHS) to hold the primary data. Here the history of the DRS will now be described followed by a comparison of the various tape drives and media technologies used at ECMWF.

In 1998 ECMWF procured its first ATL for the DRS with the specific purpose of providing storage space and magnetic tape drives to take secondary copies of important data in case the primary copy of the data was ever destroyed. Prior to then secondary copies were made using the same tape drives and media (IBM Magstar) as the primary copies.

Earlier experiences had shown the importance of having a secondary copy.

- ◆ Once some shelving holding magnetic tapes collapsed and although the data was not lost, all of the tapes had to be re-tensioned before they could be used again.
- ◆ In the early days of the DHS we had several instances of tapes holding primary data being damaged, or becoming unreadable.
- ◆ Many years ago ECMWF experienced several instances of stiction (static friction) on reel-to-reel magnetic tapes. Within certain batches of tapes the bonding between the various layers of the tape would weaken causing the magnetic oxide to flake off and stick to the tape drive heads as the tape passed over them. There was concern about the possibility of the secondary copy being written to a tape from the same batch as the primary copy, and both tapes exhibiting the same problem.

The need for more secure arrangements for making secondary copies led to an Invitation to Tender in 1998



Figure 1 The different cartridges are shown: Magstar on the left, AIT in the middle and LTO-3 on the right.

for a new DRS (ECMWF/1998/168). The type of medium chosen was Sony’s AIT (Advanced Intelligent Tape) 8-mm tape cartridges (see [www.aittape.com](http://www.aittape.com) for more information). Data is written onto AIT media using helical scan technology, where the tape is wrapped at an angle around a cylindrical drum with drive heads that are mounted flush with the drum’s surface so that the tracks are striped at an angle across the width of the tape. The drum rotates quite quickly while the tape passes across it at a relatively slow pace. This is the way a VHS recorder works and it enables four to five more data to be packed onto a tape than using the linear recording method, such as was employed by the IBM Magstar tapes that were used for writing the primary data at the time. The AIT-1 cassettes could hold 25 GB of data in a very small 8-mm cassette, while the IBM Magstars could only hold 10 GB in a much larger ½-inch cassette. However, the AIT-1 drive could only transfer data at 3 MB/s, quite a bit less than the 10 MB/s of the Magstar. While this was fine for streaming data to/from tape, the drive was not designed for handling the type of data access patterns at which the Magstar drives excelled. The different types of tape cartridge can be seen in Figure 1. For comparison purposes Table 1 shows the

Technology	Capacity (GB)	Performance (MB/s)
AIT-5	400	24
STK T10000	500	120
IBM TS1120	700	100
LTO-4	800	120

Table 1 Characteristics of modern tape drives and media.

characteristics of some of the latest generation of tape drives and media that are generally available.

The Centre purchased an ADIC (Grau EMASS at the time) AML/J automated tape library, with twelve AIT-1 tape drives. Over the years these were replaced with AIT-2 drives and were later augmented by LTO-1 and later LTO-2 tape drives. “LTO” stands for Linear Tape Open and is an open standard set up by several tape manufacturers (see [www.lto.org](http://www.lto.org) for more information). On an LTO tape data is written in a series of tracks linearly along the tape. The tape itself passes very quickly over the stationary tape heads. LTO has the advantage of transferring data faster than AIT and storing more data per cartridge. In the end LTO was used for secondary copies of data, while AIT was used for other types of backup data. Both the AML/J and its replacement are linear robotic libraries (i.e. a set of cabinets connected in a straight line with internal racking for cartridges and tape drives and a “railway track” along which a robot runs). The robot travels in the x-direction, while the robot’s “hand” moves in the y-direction; in this way it can access any cassette and insert it into any tape drive that is installed in the library. The robotic hand mechanism can also rotate 180° in the z-direction to enable it to access cartridges and drives on both sides of the library. The robot and internal racking can be seen in Figure 2.

In 2005 ADIC informed its customers that the AML/J was coming towards end of life and would not be maintained from 2008 onwards, so in 2006 ECMWF issued an Invitation to Tender (ECMWF/2006/189) for a replacement ATL and tape drives. Tenderers were free to propose any tape technology but it was deemed to be highly desirable that they also equip the ATL with some LTO drives to facilitate the migration of the LTO cartridges in the AML/J. In the event all of the tenderers bid only LTO-3 tape technology, which contrasts with the IBM TS1120 enterprise level tape drives used by the DHS with the IBM 3592 tape cassettes to store the primary data. However none of the robots that were bid could read the barcode labels on our LTO-2 tape cassettes and as a consequence it was necessary to remove all of these labels and replace them with new ones. This manual work extended over a period of several weeks and the methodical and painstaking way this was done is a credit to all of the staff involved.



Figure 2 The IBM TS3500 ATL located in the DRS Building. The internal racking is visible and the robotic “hand” mechanism can be seen at the bottom of the cabinet. LTO tapes are also stacked on the external racking to the right of the ATL.

The new ATL consists of an IBM TS3500 linear robotic library containing twenty LTO-3 tape drives. The LTO-3 drives can read legacy 100 GB native capacity LTO-1 cassettes, read/write the 200 GB LTO-2 tape cassettes from the AML/J, and write new LTO-3 tape cassettes at 400 GB native capacity. At 80 MB/s the performance of the drives is twice that of the old LTO-2 drives. The doubling in capacity comes from three factors.

- ◆ The tape is thinner (8 µm versus 8.9 µm) and hence can be made longer, 680 m as opposed to 609 m.
- ◆ The number of tracks written across the tape has increased from 512 to 704.
- ◆ The linear density has improved from 7,398 bits/mm to 9,638 bits/mm.

LTO-4 tape drives are now making their way onto the market. The LTO-4 tape is even thinner, longer and has a much higher recording density and so is able store 800 GB of data (uncompressed) in a cartridge. These drives will provide an upgrade path for ECMWF in the future.

The library and its drives are controlled by HPSS, the underlying data management software used by ECFS and MARS to store data. A secondary copy of the “operational” MARS and ECFS data is always taken. For the remainder of the data it is left to the data’s owner to decide whether or not a secondary copy is made, the ECFS command “**ecp**” for example has a “**-b**” option to indicate that a secondary (or backup) copy should be created.

The new ATL was installed in the DRS Building on-site in the spring of this year and was run for a short period of time in parallel with the old AML/J. Once ECMWF was satisfied with its performance and reliability the AML/J was switched off and decommissioned. The old ATL provided an excellent service over its eight-year life at ECMWF and so far all indications are that the new one will provide just as good a service, if not better.

## Improving the Regional Meteorological Data Communications Network (RMDCN)

AHMED BENALLEGUE, CARMINE RIZZO,  
SEBASTIEN BARBEREAU, TONY BAKKER, REMY GIRAUD

ANOTHER milestone in the Regional Meteorological Data Communications Network (RMDCN) was reached with the successful migration to a new technology which was completed on 18 June 2007. The migration to an IPVPN (Internet Protocol Virtual Private Network) provides the meteorological community with a state of the art network infrastructure which will give improved service levels and will enable new services to be introduced.

### Background

The RMDCN has been in operation since March 2000. It provides a network infrastructure for both the connections between ECMWF and its Member States and most of the GTS connections for WMO Regional Association VI. Over time it has expanded to encompass the Far East with connections to Japan, China and India. Currently there are 42 User Sites connected to it. Orange Business Services (OBS), formerly known as EQUANT, is the provider of this network. ECMWF manages the project and monitors the network on behalf of the connected User Sites following an agreement with WMO.

The initial network was based on a Frame Relay infrastructure using Permanent Virtual Circuits (PVC) between User Sites. There have been regular reviews of the contract which concentrated on pricing issues and also looked at the technology used for the network infrastructure. It was found that networks using Multi Protocol Label Switching (MPLS) were becoming more and more the norm. The RMDCN Operations Committee (ROC) and the ECMWF Technical Advisory Committee (TAC) were regularly updated on the progress of these types of networks, both in terms of reach and reliability and in terms of commercial viability. In 2004 OBS made an offer for a migration of the RMDCN from Frame Relay to an MPLS-based IPVPN (Internet Protocol Virtual Private Network) solution. The main features of the offer from OBS were as follows.

- ◆ A doubling of the bandwidth for the network connection for the same charge.
- ◆ An improved backup service with the effect that OBS were able to offer improved availability figures (the majority of sites now have 99.9% availability, while Mission Critical sites have 100%). A pre-condition for these improved figures is that the access circuits for both the primary and the backup connection are diversely routed from User Site to OBS Point of Presence.

- ◆ The provision of Class of Service (CoS) to allow traffic prioritization.
- ◆ Any-to-any connectivity.
- ◆ The ability of Sites to choose a reduced service type (Silver service versus Gold).

However some technical trade-offs were made.

- ◆ Frame Relay networks provide site-to-site bandwidth guarantees by default, while MPLS-based networks only provide a bandwidth guarantee on the access into the MPLS network (referred to as the cloud).
- ◆ In a Frame Relay network the traffic is automatically partitioned by the PVC infrastructure, whereas in an MPLS network the infrastructure is a shared resource and therefore allows for better utilization of the available bandwidth.
- ◆ The CoS feature in MPLS networks allows for traffic prioritization and substitutes the end-to-end bandwidth guarantees. Also the network management overhead in a Frame Relay network is quite significant. For an MPLS network this is greatly simplified. Figures 1 and 2 show the differences between the two network infrastructures, before and after the migration to the MPLS infrastructure.

The proposal from OBS for the migration of the network was approved by the ECMWF Council in December 2004 and this was also accepted by the other WMO members connected to the RMDCN. Since the new network infrastructure was significantly different the Service Level Agreement had to be revised. Also the implementation plan required detailed discussion with OBS. In order to guarantee an uninterrupted service on the existing Frame Relay network it was decided to implement the new network in parallel with the old network. Following intense negotiations Supplement 4 to the RMDCN contract was signed on 8 May 2006.

### From Frame-Relay to MPLS, a technical comparison

The MPLS technology used by the new RMDCN network is different from that of the previous Frame Relay technology. We now consider the differences and the improvements that are provided by the new network.

#### *The Frame-Relay technology*

Frame Relay is a relatively old technology which has the following two major characteristics.

- ◆ **Link-based Network:** In order to be able to exchange data, two sites must share a common dedicated point-to-point circuit. This circuit is deployed by the provider and is called a Permanent Virtual Circuit (PVC). Typically, a site shares several PVCs with all the sites with which it needs to exchange traffic.

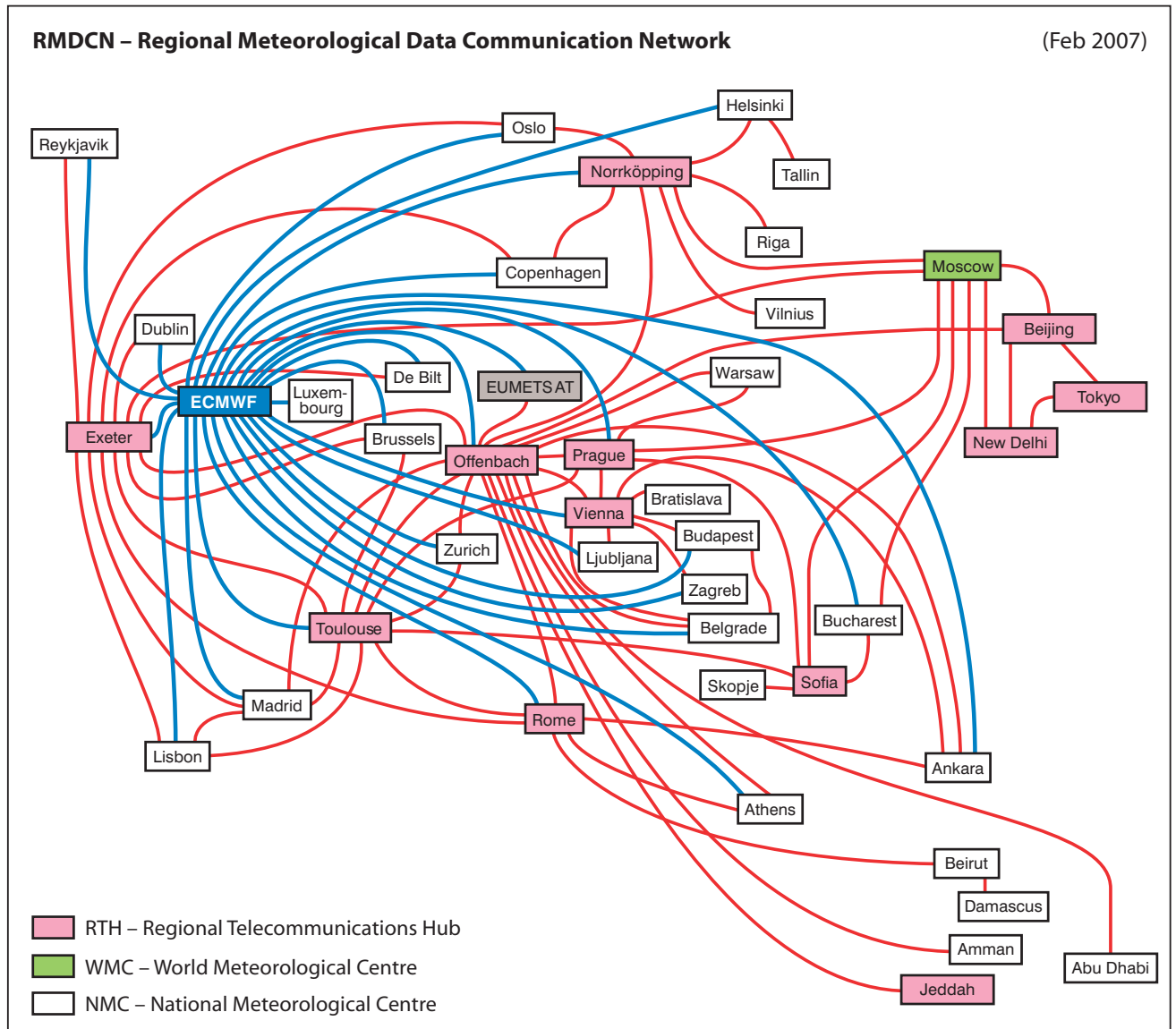


Figure 1 RMDCN Frame Relay network.

◆ **Dedicated bandwidth between two sites:** When a PVC is deployed between two sites, it provides a dedicated bandwidth. This also highlights a limitation, as unused PVC bandwidth can not be (re)used by other PVCs. For example Figure 3 shows a simplified Frame Relay network. Note that sites B and D cannot exchange data as they do not share a PVC.

**The MPLS technology (Multi-Protocol Label Switching)**

MPLS is an IP-centric solution that includes significant new features such as CoS (Class of Service) and VPN (Virtual Private Network). It is “Multi Protocol” as it can utilise different network technologies (FR, Ethernet etc.). It performs “Label Switching” since the data packets are switched through the network by virtue of an attached label. The following features characterize an MPLS-based solution.

◆ **One access circuit per site:** In order to exchange data with any of the other sites that are connected to the

network, a site needs only one access circuit to the MPLS “cloud”.

◆ **Dedicated bandwidth to the network:** The bandwidth value of the access circuit is the only guaranteed bandwidth for a site.

◆ **Traffic prioritisation and CoS (Class of Service):** Through its traffic engineering mechanisms, MPLS provides a granular way of distinguishing the different traffic flows that cross the network and assign them the appropriate priority. Critical traffic can therefore be allocated a higher bandwidth.

Typically with MPLS a site can exchange data with all of the sites that are connected to the network. In essence, the network acts as a private Internet-like topology. This is known as any-to-any setup (see Figure 4). The lack of dedicated bandwidth between sites is compensated by the CoS configuration that allocates a higher priority the more critical the traffic is.

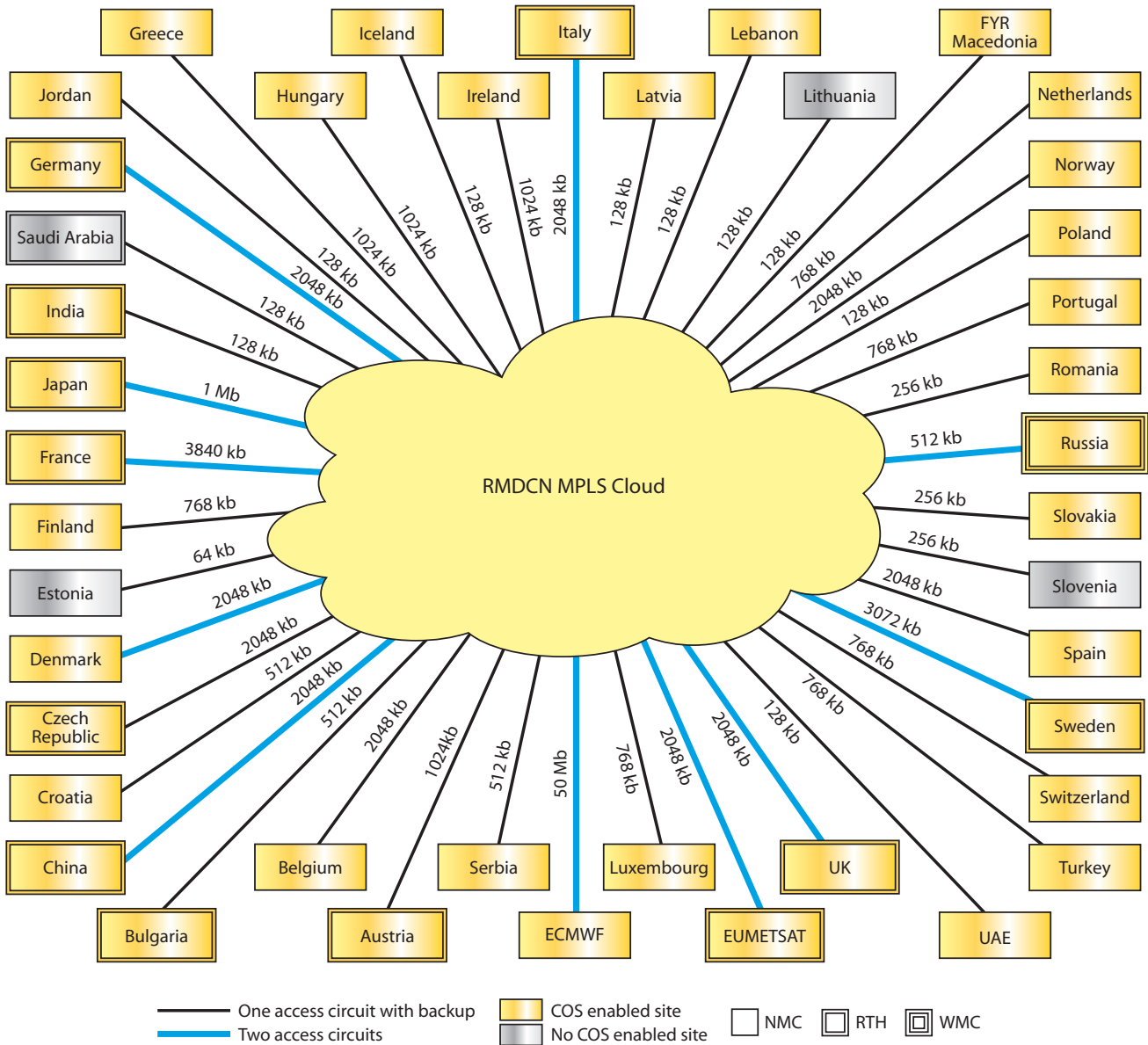


Figure 2 RMDCN MPLS IPVPN network – June 2007.

**The new MPLS-based RMDCN network**

For the RMDCN community, the two main benefits of an MPLS-based RMDCN network over one based on Frame Relay are the following.

- ◆ **Any-to-any connectivity:** Without further changes to the existing network, any pair of RMDCN sites can exchange data as soon as they have implemented

the necessary routing changes locally.

- ◆ **Class of Service:** Taking into account that there is no dedicated bandwidth between the different RMDCN sites, the emphasis is on the traffic prioritisation and CoS. It is important that each RMDCN site classifies its traffic properly.

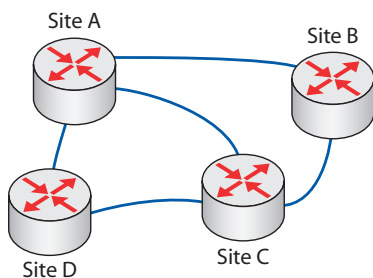


Figure 3 A network based on Frame Relay.

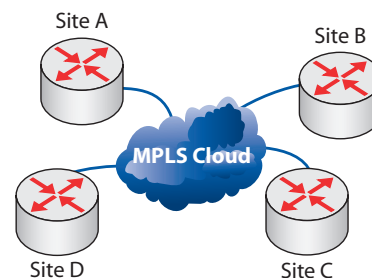


Figure 4 A network based on MPLS.

Date	Task
8 May 2006	Signature of Supplement 4 of the RMDCN contract
11 September 2006	Start of installation – roll-out
16 April 2006	Ready for Trial Date – OBS handed over the network
	Start of the User Site Acceptance Tests
19 May 2007	Start of the Reliability Acceptance Test
4 June 2007	Start of the migration of all operational traffic
18 June 2007	Final acceptance of the new network

**Table 1** The major milestones during the migration project.

### The Implementation

The actual migration project commenced following the signature of Supplement 4 of the RMDCN contract on 8 May 2006. Table 1 outlines the major milestones during the migration project. The following phases for the implementation were identified.

#### *Specification of the configuration for each User Site*

During this period the final configuration details such as access speed, mission critical setup, backup method, etc. were agreed with all RMDCN Members and the information was passed on to OBS.

#### *Installation of the network*

OBS rolled out the new MPLS-based network in parallel with the existing Frame Relay network. ECMWF gathered from all of the RMDCN members the detailed technical information (CoS classification, IP network addresses etc.) which OBS required to configure the network equipment.

#### *Validation of the new network*

In order to be confident that the new network was able to meet the operational requirements it had to be validated. This validation was split into two parts.

Firstly there would be a two week User Site Acceptance period during which tests were run to identify any configuration or deployment issues for each User Site on the network. This phase was also used to validate whether or not the traffic on the network was properly classified according to the CoS specifications and that the expected performance levels could be attained. To achieve this, all User Sites were provided with a common set of test software that had been developed by ECMWF.

The second phase of the validation was the Reliability Acceptance Test. Before running any real operational traffic on the network it was necessary to validate the service provided by OBS. During this phase ECMWF duplicated its dissemination traffic that was using the operational network and transmitted this duplicated data over the new network to systems that had been set up for testing by some member sites. Some Regional Telecommunications Hubs did similar tests by transmitting a copy of their operational GTS traffic over the new network to some of their partner sites.

#### *Migration of operational traffic*

In order to migrate the 91 PVCs in a controlled manner a detailed time schedule for migrating the operational traffic flows was agreed by all RMDCN Members.

### Conclusion and perspectives

After a process lasting almost three years, the RMDCN has been significantly improved. The new MPLS technology provides a state of the art solution for RMDCN's Managed Virtual Private Network. The network is now ready to face the upcoming challenges:

- ◆ Increased traffic flow.
  - ◆ More versatile exchanges of data between sites.
  - ◆ The ability of new sites easily to join the network.
- Although the backup solution in the new network is a significant improvement compared the one used for the network based on Frame Relay, the limitation in speed is seen as a severe constraint.

In the coming months ECMWF and some volunteer Member States will be testing secure VPN connections over the Internet. This type of connection can be used as a backup connection for the RMDCN with ECMWF acting as a gateway to the RMDCN. A backup of this type will enable faster transfers to take place, as the limit will be the Internet access speed of the User Site. Diverse access of the Internet connection and reliability of the VPN connection are areas that will be part of the investigation. With the improved bandwidth, the current backup solution used by most countries could then be replaced by this new secure Internet VPN based backup solution.

With the migration to the MPLS technology, another major step in the development of the RMDCN has been made. The further evolution of the network, which has been running operationally since March 2000, will have to be addressed by the Steering Committee of the RMDCN in the near future. ECMWF Member States and more generally the WMO community (i.e. the GTS and very soon the WMO Information System (WIS)) will continue to need an improved, managed and reliable network. The MPLS RMDCN is ready to face these new requirements.

## ECMWF publications

(see <http://www.ecmwf.int/publications/>)

### Technical Memoranda

- 538 **Morcrette, J.-J., G. Mozdzyński & M. Leutbecher:** A reduced radiation grid for the ECMWF Integrated Forecasting System. *September 2007*
- 537 **Tan, D.G.H., E. Andersson, J. de Kloe, G.-J. Marseille, A. Stoffelen, P. Poli, M.-L. Denneulin, A. Dabas, D. Huber, O. Reitebuch, P. Flamant, O. Le Rille & H. Nett:** The ADM-Aeolus wind retrieval algorithms. *August 2007*
- 535 **Geer, A.J., P. Bauer & P. Lopez:** Lessons learnt from the 1D-Var assimilation of rain and cloud affected SSM/I observations at ECMWF. *September 2007.*
- 533 **Kelly, G., P. Bauer, A. Geer, P. Lopez & J.-N. Thépaut:** Impact of SSM/I observations related to moisture, clouds and precipitation on global NWP forecast skill. *August 2007*
- 532 **Collard, A.D.:** Selection of IASI channels for use in numerical weather prediction. *July 2007*
- 531 **Janssen, P.A.E.M.:** Detection of extreme events from a SAR image spectrum. *July 2007*

### Workshop Proceedings

- ECMWF Workshop on Flow-dependent Aspects of Data Assimilation. *11 to 13 June 2007*
- ECMWF Workshop on Parametrization of Clouds in Large-scale Models. *13 to 15 November 2006.*

## Index of past newsletter articles

This is a selection of articles published in the ECMWF Newsletter series during the last five years. Articles are arranged in date order within each subject category. Articles can be accessed on the ECMWF public web site – [www.ecmwf.int/publications/newsletter/index.html](http://www.ecmwf.int/publications/newsletter/index.html)

	No.	Date	Page		No.	Date	Page
<b>NEWS</b>				<b>NEWS</b>			
Dr Anthony (Tony) Hollingsworth (1943 – 2007)	113	Autumn 2007	2	ECMWF's plan for 2007	110	Winter 2006/07	3
ENSEMBLES public data dissemination	113	Autumn 2007	4	66th Council session on 7–8 December 2006	110	Winter 2006/07	4
New items on the ECMWF web site	113	Autumn 2007	4	ECMWF workshops and scientific meetings 2007	110	Winter 2006/07	5
Changes to the operational forecasting system	113	Autumn 2007	5	Opening of the new office block at ECMWF	110	Winter 2006/07	6
Third EUMETCAL Workshop at ECMWF	113	Autumn 2007	5	Workshop on the parametrization of clouds in large-scale models	110	Winter 2006/07	6
Replacement of the Automated Tape Library for the Disaster Recovery System	113	Autumn 2007	6	David Anderson awarded the Sverdrup Gold Medal	110	Winter 2006/07	8
Management changes in the Research Department	112	Summer 2007	3	Applying for resources for a "Special Project"	110	Winter 2006/07	8
67 <sup>th</sup> Council session on 28–29 June 2007	112	Summer 2007	3	Co-operation Agreement signed with Morocco	110	Winter 2006/07	9
Forecast Products Users' Meeting, June 2007	112	Summer 2007	3	Celebration of the career of Clive Temperton	110	Winter 2006/07	10
Inauguration of ECMWF's new office block	112	Summer 2007	5	Gerbier-Mumm Award used for a project on the impacts of climate variability on malaria in Tanzania	110	Winter 2006/07	11
ECMWF Annual Report for 2006	112	Summer 2007	6	ECMWF education and training programme for 2007	109	Autumn 2006	3
Workshop on "Flow-dependent Aspects of Data Assimilation"	112	Summer 2007	7	The new IBM Phase 4 HPC facility	109	Autumn 2006	5
Access to TIGGE database	112	Summer 2007	7	CTBTO: "Synergies with Science"	109	Autumn 2006	7
German State Secretary visits ECMWF	112	Summer 2007	8	Co-operation Agreement with Estonia	106	Winter 2005/06	8
IASI radiance data operationally assimilated	112	Summer 2007	8	Long-term co-operation established with ESA	104	Summer 2005	3
Moroccan Secretary of State visits ECMWF	111	Spring 2007	3	Collaboration with the Executive Body of the Convention on Long-Range Transboundary Air Pollution	103	Spring 2005	24
Meteosat-9: The new prime satellite at 0° longitude	111	Spring 2007	3	Co-operation Agreement with Lithuania	103	Spring 2005	24
Monitoring of SSMIS from DMSP-16 at ECMWF	111	Spring 2007	4	25 years since the first operational forecast	102	Winter 2004/05	36
Update on ERA-Interim	111	Spring 2007	5				

	No.	Date	Page		No.	Date	Page
<b>COMPUTING</b>				<b>OBSERVATIONS AND ASSIMILATION</b>			
<b>ARCHIVING, DATA PROVISION AND VISUALISATION</b>				An atlas describing the ERA-40 climate during 1979–2001			
New Automated Tape Library for the Disaster Recovery System	113	Autumn 2007	34		103	Spring 2005	20
The next generation of ECMWF's meteorological graphics library – Magics++	110	Winter 2006/07	36	Planning of adaptive observations during the Atlantic THORPEX Regional Campaign 2003	102	Winter 2004/05	16
A simple false-colour scheme for the representation of multi-layer clouds	101	Sum/Aut 2004	30	ERA-40: ECMWF's 45-year reanalysis of the global atmosphere and surface conditions 1957-2002	101	Sum/Aut 2004	2
The ECMWF public data server	99	Aut/Win 2003	19	Assimilation of high-resolution satellite data	97	Spring 2003	6
<b>COMPUTERS, NETWORKS, PROGRAMMING, SYSTEMS FACILITIES AND WEB</b>				<b>ENSEMBLE PREDICTION</b>			
Improving the Regional Meteorological Data Communications Network (RMDCN)	113	Autumn 2007	36	The ECMWF Variable Resolution Ensemble Prediction System (VAREPS)	108	Summer 2006	14
New features of the Phase 4 HPC facility	109	Autumn 2006	32	Limited area ensemble forecasting in Norway using targeted EPS	107	Spring 2006	23
Developing and validating Grid Technology for the solution of complex meteorological problems	104	Summer 2005	22	Ensemble prediction: A pedagogical perspective	106	Winter 2005/06	10
Migration of ECFS data from TSM to HPSS ("Back-archive")	103	Spring 2005	22	Comparing and combining deterministic and ensemble forecasts: How to predict rainfall occurrence better	106	Winter 2005/06	17
New ECaccess features	98	Summer 2003	31	EPS skill improvements between 1994 and 2005	104	Summer 2005	10
Migration of the high-performance computing service to the new IBM supercomputers	97	Spring 2003	20	Ensembles-based predictions of climate change and their impacts (ENSEMBLES Project)	103	Spring 2005	16
ECaccess: A portal to ECMWF	96	Winter 2002/03	28	Operational limited-area ensemble forecasts based on 'Lokal Modell'	98	Summer 2003	2
<b>METEOROLOGY</b>				Ensemble forecasts: can they provide useful early warnings?			
<b>OBSERVATIONS AND ASSIMILATION</b>				<b>ENVIRONMENTAL MONITORING</b>			
Operational assimilation of surface wind data from the Metop ASCAT scatterometer at ECMWF	113	Autumn 2007	6	Progress with the GEMS project	107	Spring 2006	5
Evaluation of the impact of the space component of the Global Observing System through Observing System Experiments	113	Autumn 2007	16	A preliminary survey of ERA-40 users developing applications of relevance to GEO (Group on Earth Observations)	104	Summer 2005	5
Data assimilation in the polar regions	112	Summer 2007	10	The GEMS project – making a contribution to the environmental monitoring mission of ECMWF	103	Spring 2005	17
Operational assimilation of GPS radio occultation measurements at ECMWF	111	Spring 2007	6	Environmental activities at ECMWF	99	Aut/Win 2003	18
The value of targeted observations	111	Spring 2007	11	<b>FORECAST MODEL</b>			
Assimilation of cloud and rain observations from space	110	Winter 2006/07	12	A new radiation package: McRad	112	Summer 2007	22
ERA-Interim: New ECMWF reanalysis products from 1989 onwards	110	Winter 2006/07	25	Ice supersaturation in ECMWF's Integrated Forecast System	109	Autumn 2006	26
Analysis and forecast impact of humidity observations	109	Autumn 2006	11	Towards a global meso-scale model: The high-resolution system T799L91 and T399L62 EPS	108	Summer 2006	6
Surface pressure bias correction in data assimilation	108	Summer 2006	20	The local and global impact of the recent change in model aerosol climatology	105	Autumn 2005	17
A variational approach to satellite bias correction	107	Spring 2006	18	Improved prediction of boundary layer clouds	104	Summer 2005	18
"Wavelet" $J_b$ – A new way to model the statistics of background errors	106	Winter 2005/06	23	Two new cycles of the IFS: 26r3 and 28r1	102	Winter 2004/05	15
New observations in the ECMWF assimilation system: satellite limb measurements	105	Autumn 2005	13	Early delivery suite	101	Sum/Aut 2004	21
CO <sub>2</sub> from space: estimating atmospheric CO <sub>2</sub> within the ECMWF data assimilation system	104	Summer 2005	14	Systematic errors in the ECMWF forecasting system	100	Spring 2004	14
Sea ice analyses for the Baltic Sea	103	Spring 2005	6	A major new cycle of the IFS: Cycle 25r4	97	Spring 2003	12
The ADM-Aeolus satellite to measure wind profiles from space	103	Spring 2005	11	<b>METEOROLOGICAL APPLICATIONS</b>			
				Ensemble streamflow forecasts over France	111	Spring 2007	21
				Recent developments in extreme weather forecasting	107	Spring 2006	8
				Early medium-range forecasts of tropical cyclones	102	Winter 2004/05	7
				European Flood Alert System	101	Sum/Aut 2004	30

	<b>No.</b>	<b>Date</b>	<b>Page</b>		<b>No.</b>	<b>Date</b>	<b>Page</b>
<b>METEOROLOGICAL STUDIES</b>				<b>OCEAN AND WAVE MODELLING</b>			
Model predictions of the floods in the Czech Republic during August 2002: The forecaster's perspective	97	Spring 2003	2	Progress in wave forecasts at ECMWF	106	Winter 2005/06	28
Impact of airborne Doppler lidar observations on ECMWF forecasts	113	Autumn 2007	28	Ocean analysis at ECMWF: From real-time ocean initial conditions to historical ocean analysis	105	Autumn 2005	24
Hindcasts of historic storms with the DWD models GME, LMQ and LMK using ERA-40 reanalyses	109	Autumn 2006	16	High-precision gravimetry and ECMWF forcing for ocean tide models	105	Autumn 2005	6
Hurricane Jim over New Caledonia: a remarkable numerical prediction of its genesis and track	109	Autumn 2006	21	MERSEA – a project to develop ocean and marine applications	103	Spring 2005	21
Starting-up medium-range forecasting for New Caledonia in the South-West Pacific Ocean – a not so boring tropical climate	102	Winter 2004/05	2	Towards freak-wave prediction over the global oceans	100	Spring 2004	24
A snowstorm in North-Western Turkey 12–13 February 2004 – Forecasts, public warnings and lessons learned	102	Winter 2004/05	7	<b>MONTHLY AND SEASONAL FORECASTING</b>			
Exceptional warm anomalies of summer 2003	99	Aut/Win 2003	2	Seasonal forecasting of tropical storm frequency	112	Summer 2007	16
Record-breaking warm sea surface temperatures of the Mediterranean Sea	98	Summer 2003	30	New web products for the ECMWF Seasonal Forecast System-3	111	Spring 2007	28
Breakdown of the stratospheric winter polar vortex	96	Winter 2002/03	2	Seasonal Forecast System 3	110	Winter 2006/07	19
Central European floods during summer 2002	96	Winter 2002/03	18	Monthly forecasting	100	Spring 2004	3
<b>OCEAN AND WAVE MODELLING</b>				DEMETER: Development of a European multi-model ensemble system for seasonal to interannual prediction	99	Aut/Win 2003	8
Climate variability from the new System 3 ocean reanalysis	113	Autumn 2007	8	The ECMWF seasonal forecasting system	98	Summer 2003	17
				Did the ECMWF seasonal forecasting model outperform a statistical model over the last 15 years?	98	Summer 2003	26

## Useful names and telephone numbers within ECMWF

### Telephone

Telephone number of an individual at the Centre is:  
 International: +44 118 949 9 + three digit extension  
 UK: (0118) 949 9 + three digit extension  
 Internal: 2 + three digit extension  
 e.g. the Director's number is:  
 +44 118 949 9001 (international),  
 (0118) 949 9001 (UK) and 2001 (internal).

### E-mail

The e-mail address of an individual at the Centre is:  
 firstinitial.lastname@ecmwf.int  
 e.g. the Director's address is: D.Marbouty@ecmwf.int  
 For double-barrelled names use a hyphen  
 e.g. J-N.Name-Name@ecmwf.int

### Internet web site

ECMWF's public web site is: <http://www.ecmwf.int>

	<b>Ext</b>		<b>Ext</b>
<b>Director</b>		<b>Meteorological Division</b>	
Dominique Marbouty	001	<i>Division Head</i>	
<b>Deputy Director &amp; Head of Research Department</b>		Horst Böttger	060
Philippe Bougeault	005	<i>Meteorological Applications Section Head</i>	
<b>Head of Operations Department</b>		Alfred Hofstadler	400
Walter Zwielfhofer	003	<i>Data and Services Section Head</i>	
<b>Head of Administration Department</b>		Baudouin Raoult	404
Ute Dahremöller	007	<i>Graphics Section Head</i>	
		Stephan Siemen	375
<b>Switchboard</b>		<i>Meteorological Operations Section Head</i>	
ECMWF switchboard	000	David Richardson	420
<b>Advisory</b>		<i>Meteorological Analysts</i>	
Internet mail addressed to <a href="mailto:Advisory@ecmwf.int">Advisory@ecmwf.int</a>		Antonio Garcia-Mendez	424
Telefax (+44 118 986 9450, marked User Support)		Anna Ghelli	425
<b>Computer Division</b>		Claude Gibert (web products)	111
<i>Division Head</i>		Fernando Prates	421
Isabella Weger	050	Meteorological Operations Room	426
<i>Computer Operations Section Head</i>		<b>Data Division</b>	
Sylvia Baylis	301	<i>Division Head</i>	
<i>Networking and Computer Security Section Head</i>		Jean-Noël Thépaut	030
Rémy Giraud	356	<i>Data Assimilation Section Head</i>	
<i>Servers and Desktops Section Head</i>		Erik Andersson	627
Richard Fisker	355	<i>Satellite Data Section Head</i>	
<i>Systems Software Section Head</i>		Peter Bauer	080
Neil Storer	353	<i>Re-Analysis Project (ERA) Head</i>	
<i>User Support Section Head</i>		Saki Uppala	366
Umberto Modigliani	382	<b>Probabilistic Forecasting &amp; Diagnostics Division</b>	
<i>User Support Staff</i>		<i>Division Head</i>	
Paul Dando	381	Tim Palmer	600
Anne Fouilloux	380	<i>Seasonal Forecasting Section Head</i>	
Dominique Lucas	386	Franco Molteni	108
Carsten Maaß	389	<b>Model Division</b>	
Pam Prior	384	<i>Division Head</i>	
<b>Computer Operations</b>		Martin Miller	070
<i>Call Desk</i>		<i>Numerical Aspects Section Head</i>	
<i>Call Desk email: <a href="mailto:calldesk@ecmwf.int">calldesk@ecmwf.int</a></i>	303	Agathe Untch	704
<i>Console – Shift Leaders</i>	803	<i>Physical Aspects Section Head</i>	
<i>Console fax number +44 118 949 9840</i>		Anton Beljaars	035
<i>Console email: <a href="mailto:newops@ecmwf.int">newops@ecmwf.int</a></i>		<i>Ocean Waves Section Head</i>	
<i>Fault reporting – Call Desk</i>	303	Peter Janssen	116
<i>Registration – Call Desk</i>	303	<b>GMES Coordinator</b>	
<i>Service queries – Call Desk</i>	303	Adrian Simmons	700
<i>Tape Requests – Tape Librarian</i>	315	<b>Education &amp; Training</b>	
		Renate Hagedorn	257
		<b>ECMWF library &amp; documentation distribution</b>	
		Els Kooij-Connally	751